PROTEIN KINASE C – DELTA (PKCδ): A CRITICAL HUB FOR IMMUNOMODULATORY FUNCTIONS IN MACROPHAGES DURING *MYCOBACTERIUM TUBERCULOSIS* INFECTION

Submitted by

Rudranil Hazra

HZRRUD001

Thesis Presented for the Degree of ***Ph.D. (Clinical Sciences and Immunology)*** *in the Department of Pathology, Faculty of Health Science, University of Cape Town*

September 2022

Supervisor: Associate Prof. Suraj P. Parihar

Co-supervisors: Prof. Frank Brombacher & Dr. Nashied Peton

Wellcome Centre for Infectious Diseases Research in Africa (CIDRI-Africa),
International Centre for Genetic Engineering and Biotechnology (ICGEB), Cape Town,
Institute of Infectious Diseases and Molecular Medicine (IDM),
Department of Pathology, Faculty of Health Sciences, University of Cape Town,
Cape Town, South Africa.

CONTENTS

DECLARATION

I, ***Rudranil Hazra***, hereby declare that this dissertation or thesis is constructed is entirely original work of mine, with the exception of instances where it is noted in the acknowledgments, and that neither the entire work nor any portion of it has ever been, is currently being, or will ever be submitted for another degree in this university or any other university.

I grant permission to the university to reproduce the purpose of research either the whole or any portion of the contents in any manner whatsoever.

Signature:

Date: 14th September 2022

ACKNOWLEDGEMENTS

I would like to avail this great opportunity to express my sincere gratitude to **A/Prof. Suraj P. Parihar** for his immense guidance during my journey toward Ph.D. in an esteemed research environment. I was very fortunate to work under his observation. His critical supervision, patience, and support were incredible. The freedom he gave me for excelling in the scientific field and developing critical thinking during the project is well appreciated. I will always remain desirous of his blessings in the future.

I would like to show my greatest appreciation to **Prof. Frank Brombacher** and **Prof. Robert J. Wilkinson** for their vital guidance, encouragement, and considering me as a potential Ph.D. aspirant, and for providing prestigious funding support through CIDRI-Africa. I offer my sincerest thanks to my colleagues and mentors **Dr. Nashied Peton, Dr. Abhimanyu Abhimanyu**, **Raymond Moseki, Mthawelanga Ndengane, Avuyonke Balfour, Dr. Hygon Mutavhatsindi, Robyn Waters, Dr. Caron Jacobs** for their experimental and emotional support for the completion of my degree. I would also like to thank **Kathryn Wood** for her tremendous administrative support throughout my project.

I extend my gratitude to **Dr. Mumin Ozturk** and **Dr. Shelby-Sara Jones** who helped me a lot in the lab and shared their valuable experiences with me. Their knowledgeable guidance, innovative ideas, and scientific discussions were the true reason behind the work being a success. I am indebted to them, as without their encouragement and guidance this project would not have materialized.

Last but certainly not least, I am thankful to my friends and fellow trainees **Sibongiseni K L Poswayo, Robert Rousseau, Saiyukthi Naidoo,** and **Dr. Shandre Pillay** as they were the silent helpers who assisted me during my research work and always encouraged me. Without them, my journey during Ph.D. would not be fruitful.

In the end, I would like to thank my parents **Debaprasad Hazra** and **Seuli Hazra** for keeping my spirits alive and for encouragement during the thesis work. I would like to thank almighty for allowing me to work with such intelligent, helpful, and friendly people. I remain indebted to the unseen people across the world wide web, for providing the resources through the internet.

PUBLICATIONS

1. Jones S, Ozturk M, Kieswetter NS, Poswayo S, **Hazra R**, Tamgue O, Parihar SP, Suzuki H, Brombacher F and Guler R (2022) "**Lyl-1-deficiency promotes inflammatory response and increases mycobacterial burden in response to Mycobacterium tuberculosis infection in mice.**" Front Immunol. 13:948047. IF: 8.786

2. Ozturk M, Chia JE, **Hazra R**, Saqib M, Maine RA, Guler R, Suzuki H, Mishra BB, Brombacher F and Parihar SP (2021) "**Evaluation of Berberine as an Adjunct to TB treatment.**" Front. Immunol. 12:656419. IF: 6.429

3. Sen P, Ghosal S, **Hazra R**, Mohanty R, Arega S, Sahu B and Ganguly N (2020) "**CRISPR-Mediated Knockdown of miR-214 Modulates Cell Fate in Response to Anti-Cancer Drugs in HPV negative and HPV positive Cervical Cancer Cells.**" J Biosci 45. IF: 1.826

4. Sen P, Ghosal S, **Hazra R**, Arega S, Mohanty R, Kulkarni KK, Budhwar R and Ganguly N (2019) "**Transcriptomic Analyses of Gene Expression by CRISPR Knockout of miR-214 in Cervical Cancer Cells.**" Genomics 112, no. 2: 1490-99. IF: 5.736

5. **Hazra R**, Ozturk M, Peton N, Jones S, Poswayo S, Rousseau R, Naidoo S, Savulescu A, Moseki R, Brombacher F, Wilkinson R and Parihar SP. "**Protein Kinase C – delta (PKCδ): a critical hub for immunoregulatory functions in macrophages during Mycobacterium tuberculosis infection.**" (Manuscript in preparation)

6. Savulescu A, Peton N, Oosthuizen D, **Hazra R**, Mhlanga M and Coussens AK. "**Mycobacterium tuberculosis infection of primary human monocyte-derived macrophages on microfabricated patterns.**" (Manuscript in preparation)

ABBREVIATIONS

AIDS	Acquired Immunodeficiency Syndrome
AIM	Apoptosis Inhibitor of Macrophages
AM	Alveolar Macrophages
APC	Antigen-Presenting Cells
ATG5	Autophagy related 5
ATP	Adenosine Triphosphate
BAD	Bcl-2-associated death promoter
BAL	Bronchoalveolar Lavage
BCG	Bacille Calmette-Guerin
BMDM	Bone-Marrow-Derived Macrophages
BSL	Biosafety Level
CAGE	Cap Analysis of Gene Expression
CCR2	C-C chemokine receptor type 2
CFU	Colony Forming Unit
COX1/2	Cyclooxygenase 1/2
CXCL	Chemokine (C-X-C motif) ligand 1
DAB	Diaminobenzidine
DAG	Diacylglycerol
DC-SIGN	DC-Specific Intercellular Adhesion Molecule-3 Grabbing Nonintegrin
DNA	Deoxyribonucleic Acid
ELISA	Enzyme-Linked Immunosorbent Assay
ENCODE	Encyclopedia of DNA Elements
ERK	Extracellular-signal Regulated Kinase
ESX-1	ESAT-6 secretion system 1
FACS	Fluorescence Activated Cell Sorting
FANTOM	Functional Annotation of Mammalian Genome
FCS	Fetal Calf Serum
GM-CSF	Granulocyte-Macrophage Colony-Stimulating Factor
GTP	Guanosine Triphosphate
HAT	Histone Acetyltransferase
HDT	Host-Directed Therapy

HIV	Human Immunodeficiency Virus
HPV	Human Papillomavirus
HPRT	Hypoxanthine Phosphoribosyltransferase
HSP27	Heat Shock Protein 27
IFN	Interferon
IGF-1	Insulin-like Growth Factor 1
IL	Interleukins
IM	Interstitial Macrophages
IP3	Inositol Triphosphate
JNK	c-Jun N-terminal Kinases
KLRG1	Killer Cell Lectin Like Receptor G1
LAM	Lipoarabinomannan
LAP	LC3 Associated Phagocytosis
LC3	Microtubule-associated protein 1A/1B-Light Chain 3
LDL	Low-Density Lipoprotein
LM	Lipomannan
LPS	Lipopolysaccharide
LTBI	Latent-TB Infection
MAPK	Mitogen-Activated Protein Kinases
MARCKS	Myristoylated Alanine-Rich Protein Kinase C Substrate
MARCO	Macrophage Receptor with Collagenous Structure
MCL	Macrophage C-type Lectin
MDR-TB	Multidrug-Resistant TB
MDSC	Myeloid-Derived Suppressor Cells
MHCII	Major Histocompatibility Complex II
MR	Mannose Receptor
NADH	Nicotinamide Adenine Dinucleotide Hydrogen
NADPH	Nicotinamide Adenine Dinucleotide Phosphate
NF-κB	Nuclear Factor kappa-light-chain enhancer of activated B cells
NK Cells	Natural Killer Cells
NLRP3	NOD-like Receptor Pyrin Domain 3
NO	Nitric Oxide
NOD2	Nucleotide-Binding Oligomerization Domain-Containing Protein 2

NOS2	Nitric Oxide Synthase 2
NOX2	NADPH Oxidase 2
NTC	Non-Template Control
ODN	Oligodeoxynucleotide
PAMP	Pathogen-Associated Molecular Patterns
PAS	Para-Aminosalicylic Acid
PBS	Phosphate-Buffered Saline
PCR	Polymerase Chain Reaction
PD-1	Programmed Cell Death Protein 1
PIM	Mannosyl-Phosphatidyl-Myo-Inositol-based Glycolipids
PIP2	Phospholipid Phosphatidylinositol 4,5-Biphosphate
PKC	Protein Kinase C
PLC	Phospholipase C
PLS3	Phospholipid Scramblase 3
PMCA	Plasma Membrane Calcium ATPase
PPAR-γ	Peroxisome Proliferator-Activated Receptor-γ
PRR	Pathogen-Recognition Receptors
PS	Phosphatidylserine
PTPα	Protein Tyrosine Phosphatase α
RNA	Ribonucleic Acid
RNS	Reactive Nitrogen Species
ROS	Reactive Oxygen Species
SDS-PAGE	Sodium Dodecyl Sulfate-Polyacrylamide Gel Electrophoresis
SFK	Src Family Kinase
SHPTP1	SHP1 Domain-containing Tyrosine phosphatase
SLEC	Short-Lived Effector Cells
SR-A	Scavenger Receptor Class-A
STAT	Signal Transducer and Activator of Transcription
TB	Tuberculosis
TBS	Tris-Hcl Buffered Saline
TCR	T Cell Receptor
TGF-β	Transforming Growth Factor β
TH1/2	T Helper 1/2

TIR	Toll-Interleukin-1 Receptor
TIRAP	TIR domain-containing Adaptor Protein
TLR	Toll-Like Receptors
TNF	Tumor Necrosis Factor
TRAF6	TNF Receptor-Associated Factor 6
TRAM	TRIF-Related Adapter Molecule
TRIF	TIR-domain-containing Adapter-Inducing Interferon-β
TSS	Transcription Start Sites
UV	Ultraviolet
WHO	World Health Organization
WPI	Weeks Post Infection
XDR-TB	Extensive Drug-Resistant TB

FIGURES & TABLES

CHAPTER 1

CHAPTER 2

ABSTRACT

Tuberculosis (TB) has reached epidemic levels and emerged as the second deadliest infectious disease globally after CoVID-19. By evolving the ability to evade host defense via intrinsic mechanisms, *Mycobacterium tuberculosis* (Mtb), the etiological agent of TB has been deleterious to human health and has necessitated novel therapeutic interventions, the primary notion to combat Mtb infection. Hence, the identification of host-modulating candidate genes involved in immune evasion and putative pathogen-killing pathways during Mtb infection is crucial. Additionally, macrophages are the first line of defense against Mtb infection through activating effector genes, which lead to pathogen killing and acquiring long-lasting immunity. One such candidate gene with potential novel therapeutic intervention, Protein Kinase C – δ (PKCδ) has been recognized as a critical marker with clinical and experimental evidence in recent years. An experimental mouse model of global PKCδ knockout ($PKC\delta^{-/-}$) revealed mechanistic alterations enhancing the susceptibility to various infectious diseases including Mtb infection, suggesting a protective phenotype of PKCδ against invading pathogens. However, the macrophage-specific role of PKCδ during Mtb infection remains unknown and has not been delineated yet. Because the pulmonary microenvironment during Mtb infection is majorly governed by macrophages, initiating innate and skewing adaptive immune response, we have exploited the role of PKCδ in macrophages using the macrophage-specific PKCδ knockout mice ($LysM^{cre}PKC\delta^{flox/flox}$). Our success in characterizing this experimental murine strain has resulted in the establishment of an immunologically comparable PKCδ functional study platform, which has been adopted herein to investigate the immunomodulatory effects of Mtb infection in the ablation of PKCδ in macrophages. An early lymphocytic immune response increased neutrophil turnover, and reduced inflammatory macrophages are all accompanied by PKCδ deficiency in macrophages, which was abolished in the chronic stage of infection. Bone-marrow-derived macrophages from $LysM^{cre}PKC\delta^{flox/flox}$ murine model further showed that the disease susceptibility is a consequence of an array of cellular intrinsic mechanisms and dysregulated proteome which are modulated by PKCδ. Furthermore, increased expression in bronchoalveolar lavage (BAL) samples from active TB patients and increased bacterial burden in PKCδ silenced human monocyte-derived macrophages with decreased pro-inflammatory cytokine response strongly signify PKCδ as a key hub for immunomodulatory functions during Mtb infection and a potential host-directed therapeutic (HDT) target against TB.

CHAPTER 1: Literature review

1.1. Tuberculosis

A deadly infectious bacterial disease, Tuberculosis (TB) ranks 13th on the global toll of deaths[1]. Before the Coronavirus pandemic, TB outranked human immunodeficiency virus/ acquired immunodeficiency syndrome (HIV/AIDS) as the largest global infectious disease-related cause of mortality. Insufficient vaccine efficacy, emerging drug resistance, and lack of new therapeutic approaches are the major contributors to the success of TB disease. Moreover, reduced TB diagnosis and treatment access due to CoVID-19 has increased TB deaths[1, 2]. Several initiatives have been conducted to better understand complex TB pathogenesis and implement stringent diagnostics and effective therapy. These advancements have not been able to stop the worldwide TB pandemic, and fatality rates are still rising, due to the multidimensional nature of this disease. The evolution of genetic alterations in bacterial strains to aid in their survival, antibiotic resistance, and ineffective therapies are only a few of the difficulties in controlling this disease. Hence, more insights into understanding the biology of the disease are necessary actions to mitigate and reverse these impacts.

1.1.1. Tuberculosis – throughout human history

The causative agent of Tuberculosis (TB), *Mycobacterium tuberculosis* (Mtb), has existed for about 70,000 years[3] and with around 10 million cases each year it presently infects worldwide nearly 2 billion people[1]. The TB bacillus is carried by one-third of the world's population, putting them at risk of developing active TB illness[1]. Studies have hypothesized that *Mycobacterium* have originated more than 150 million years ago[3] and an early predecessor of Mtb might have infected early humanoid creatures in East Africa approximately three million years ago[4]. In 1679, detailed pathological and anatomical descriptions of the disease were given by Francis Sylvius through his work “Opera Medica”, where tubercles, abscesses, cavities, and empyema are described in the lungs and other sites of consumptive patients. During the 17th and 18th centuries, TB was characterized using the terms – “consumption” and “phthisis” respectively, before Johann Lukas Schönlein devised the term “Tuberculosis” in the mid-19th century[5]. Understanding the complexities of this disease condition, which absorbed and damaged many individuals' lives in earlier times, became increasingly difficult as a result of its unexpected, challenging, unseen, long-tenure, and often lifetime nature. As a result, numerous researchers have been acknowledged and praised for

their work in making significant discoveries regarding the illness we are still battling in the 21st century, now known as Tuberculosis (TB). An English physician, Benjamin Marten, first speculated on the infectious origin of this infectious disease in 1720 with his publication, "A new theory of Consumption"[6]. Later in the 17th century, Matthew Baille physiologically described tubercles in his publication "A Morbid Anatomy of the Human Body." TB had become an epidemic in the western region of Europe by the 18th century, with 900 fatalities per 100,000 inhabitants each year, particularly among young people[3]. Also, industrialization during the 18th century caused the diffusion of social conditions that were particularly problematic, including poor ventilation and overcrowding in residential properties, primitive and poor sanitation systems, malnourishment, and other risk factors that were solely associated with the disease manifestation[7]. Due to its epidemic progress in Europe and North America, TB was considered "Captain of All These Men of Death" a century later[3]. Different theories concerning the etiopathological origin of this disease were debated at the beginning of the 19th century, claiming whether TB might be considered as an infectious disease – which was generally assumed in Southern Europe – as a hereditary disease – as was asserted in Northern Europe – a form of cancer[7]. In 1865, Jean-Antoine Villemin, a French military surgeon, demonstrated the contagious nature of TB, by injecting a rabbit with the fluid obtained from the tuberculous cavity of an individual who had died of the disease[4]. It was not until 1867 that Theodor Albrecht Edwin Klebs became one of the first scientists to isolate the TB bacteria by implanting tuberculous material into sterile flasks filled with egg white[8]. In 1882, Robert Koch contributed the most to the evolution of the medical and scientific understanding of TB complexities[9]. The TB bacillus was demonstrated by Koch as he presented his findings to the "Berlin Physiological Society", where he went into depth about his renowned postulates, which have since become the global standard for identifying infectious organisms[10]. Later in 1890, he reported his research on a substance that he isolated from Mtb[10]. He asserted that the substance, "Tuberculin", was the first anti-TB therapy for the treatment of TB since it could eradicate the TB bacteria from human bodies. However, Koch claimed that "Tuberculin" may eventually play a role in diagnostics, even though the substance was found to be ineffective against TB[9]. Another interesting finding of Pirquet's study in the same year was that children exposed to "Tuberculin" showed a confined immune response parallel to active TB patients but did not develop the disease themselves. Pirquet referred to these children as "latently infected"—a phrase still in use and still the subject of discussion today. The "Tuberculin Skin Test (TST)" by Pirquet and Mantoux in 1908[3], the first Mycobacterium vaccine employing *Mycobacterium bovis* known as "Bacille Calmette-Guerin (BCG)" by Albert Calmette and

Camille Guerin in the early 20th century[11], and the discovery of numerous therapeutic agents were all made possible by Robert Koch's breakthrough. These included the discovery of "Streptomycin" by Albert Schatz and Selman Waksman in 1944[12], "para-aminosalicylic acid (PAS)" by Jorgen Lehmann in 1949[13], "TB chemotherapy" by Sir John Crofton in 1952[14], the introduction of "Rifampicin" in 1957[15], and the discovery of ethambutol in 1961[16]. At the Pasteur Institute of Lille, Albert Calmette and Camille Guerin developed a TB vaccine in 1921 while attempting to attenuate Mycobacterium Bovis. The only commercially available TB vaccine for almost the next 100 years was this attenuated mycobacterium vaccine, also known as BCG[11, 17]. A child from TB positive mother, who was given into the care of a TB-positive grandmother, was the first to benefit from BCG's protective effects against TB. By 1966, Rifampicin entered the TB drug line and has since grown to be a crucial part of TB treatment regimens[18]. According to a study conducted in 2019, "M72/ASO1$_E$", a promising vaccine candidate, provides approximately 3 years of protection against TB disease progression in HIV-negative individuals after two dosages[19]. Even though the pathogenesis and etiology of TB are increasingly understood, the disease continues to be a global health concern. We have been dealing with a particularly difficult microbe in recent years because it keeps evolving drug resistance and infects people who are immunocompromised, leading to the TB-HIV epidemic. The "TB crisis" thus persists into the 21st century and continues to be a persistent problem throughout human history, in addition to having various social ramifications if not cured[3].

Table 1. Timeline of historical landmarks in Tuberculosis research

Timeline	Landmarks
1854	First sanatorium for the treatment of TB by Hermann Brehmer
1869	Jean Antoine Villemin proved the contagious and infectious nature of TB
1882	The pathogenic origin of TB was described by Robert Koch
1894	The first TB research center - Edward Livingston Trudeau was established in New York
1906	Development of BCG vaccine by Albert Calmette and Camille Guerin
1944	Anti-TB effective drug - Streptomycin invention by Albert Schatz and Selman Waksman
1946	Discovery of para-aminosalicylic acid (PAS)
1951	Several research groups reported a drug with anti-TB effects known as Isoniazid
1952	Inclusion of Streptomycin, PAS, and Isoniazid in TB drug regimen
1961	Ethambutol was introduced

1966	First usage of Rifampicin as an anti-TB treatment
1993	Isoniazid and Rifampicin became the first-line TB treatment drugs
2000's	Observation of increasing number of MDR/XDR TB patients
2019	Development of M72/ASO1E vaccine with 50% success rate

1.1.2. Tuberculosis – a modern-day epidemic

Years of advancement in the provision of crucial TB services and the reduction of the burden of TB disease have been halted by the COVID-19 pandemic[1]. Following centuries of efforts to tackle TB, the World Health Organization (WHO) launched "The End TB Strategy" in 2016 to eliminate the worldwide tuberculosis pandemic by creating a world free of TB-related illness, suffering, and fatalities by 2035[2]. According to WHO, the drop in TB incidence has slowed, with an expected 9.9 million individuals becoming infected with TB in 2020[1, 2]. One explanation is that delays in diagnosis and treatment services disproportionately impact those who already have TB, leading to an increase in the number of fatalities. Due to the relatively long gap between contracting an infection and the onset of disease (which can last anywhere from weeks to decades), the influence on the incidence of the

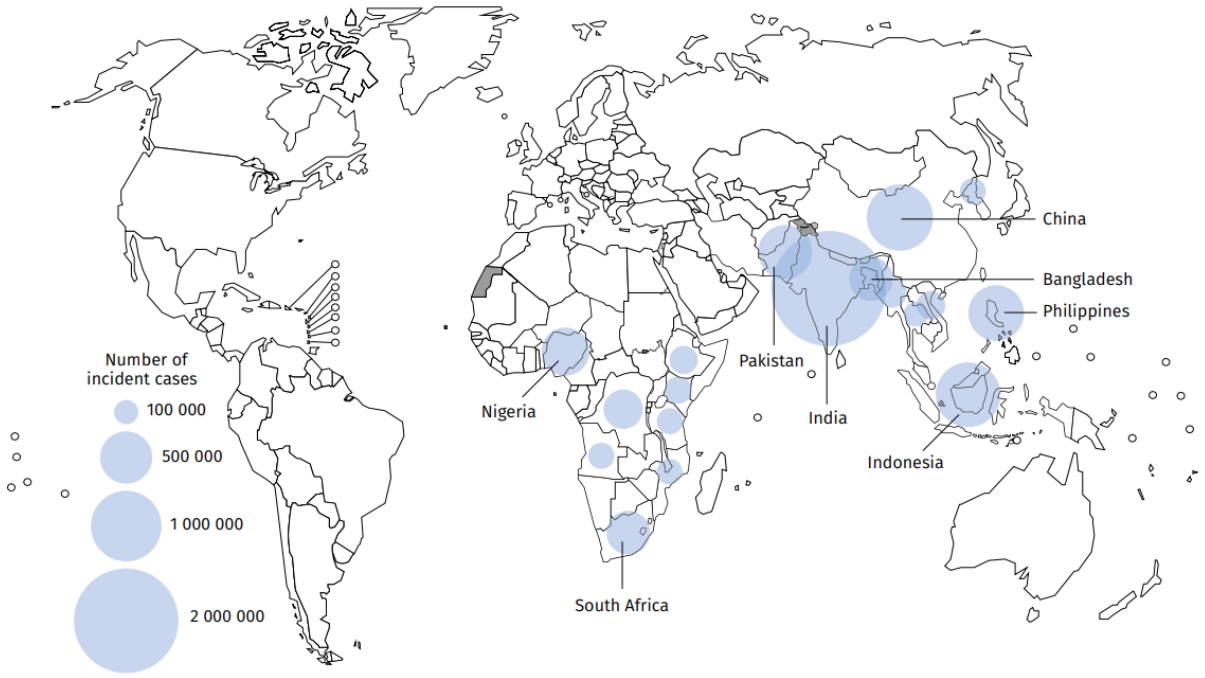

Figure 1. Estimated TB cases with at least 100 000 incidents in 2020. (Adapted from WHO Global Tuberculosis Report 2021[1]).

larger pool of patients not diagnosed and treated is delayed[1]. Globally, an estimated 10 million TB cases were documented in 2020, with a frightening mortality rate of 1.5 million individuals, making TB one of the top ten causes of death[1]. Age and gender-based breakdown of TB incidence further revealed an increase in men with 5.6 million cases than women with 3.3 million cases in 2020. Children under the age of 15 years were included in the remaining 1.1 million cases as adults (above the age of 15) are more likely to develop tuberculosis[1]. In 2020, the 30 high-TB-burdened nations including the regions of South-East Asia and Sub-Saharan Africa reported 85% of infected patients of global TB incidence[1]. Nevertheless, only eight nations accounted for 60% of all occurrences, with South Africa being one of them with 3% of the total occurrence of TB incidence worldwide (**Figure 1**). TB disease outcome and increased burden strongly rely on an individual's socio-economic status, recognizing TB as a destitution-influenced disease leading to the suffering of most third-world countries which are majorly afflicted by low income [20]. Besides, individuals with a weakened immune system are more likely to develop active tuberculosis. Studies depicted that the susceptibility of TB increased 3 times more in an individual with malnutrition and 18 times more with co-morbidities including HIV/AIDS[1, 2]. Total estimation of deaths in HIV-negative individuals raised from 1.2 million (2019) to 1.3 million (2020) with a slight increase in HIV-positive individuals from 209 000 (2019) to 214 000 (2020)[1]. With the high prevalence of HIV cases, South Africa accounts for 59% of HIV-associated TB incidence, being the major contributor to the HIV/AIDS-associated deaths worldwide[1]. Indeed, the CoVID-19 pandemic brutally impacted TB mortality more than HIV/AIDS in 2020 according to WHO[1]. Impacts of COVID-19 are estimated to be a significant increase in TB mortality in South Africa among other 16 countries by 2021 (including HIV incidence) and projected to be much higher in coming years (**Figure 2**)[1]. Reports also stated that the set benchmark by "The End TB Strategy" for TB disease reduction by 35% and TB incidence drop by 20% in contrast to 2015 levels was not achieved[1, 2]. Apart from socioeconomic obstacles, drug resistance by TB bacilli has always been a crucial threat to public health and successful in opposing recent developments in research. Currently, rifampicin and isoniazid are the first-line drugs, and individuals developing resistance against both drugs are known as "Multidrug-Resistant TB (MDR-TB) patients." Also, "Extensive Drug-Resistant TB (XDR-TB) patients" do not exhibit positive disease outcomes by the regimen of both the first-line and second-line anti-TB drugs with either bedaquiline or linezolid[21]. Globally, rifampicin resistance (MDR-TB) was assessed in 2.1 million of those with bacteriologically proven pulmonary TB in 2020. There were 157 903 patients altogether, of which 132 222 instances of MDR-TB and 25 681 cases of

XDR-TB were found[1]. Hence, understanding and encountering deleterious disease determinants with progressive research is necessary to alter the worsening epidemiology of TB in the modern day.

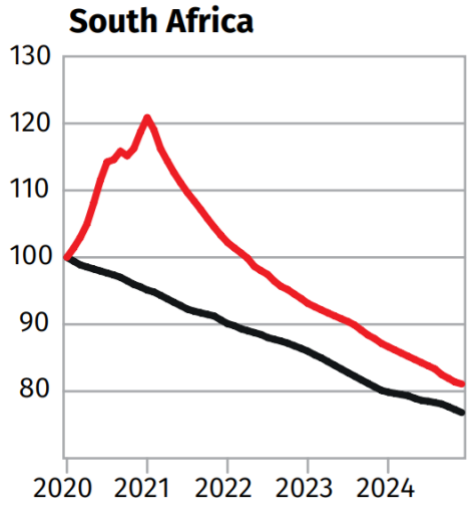

Figure 2. Estimated effect of COVID-19 pandemic on TB mortality in South Africa in the upcoming years. Data shown in percentage of TB incidence and baseline (black solid line) is a scenario of no COVID-19 disruptions. (Adapted from WHO Global Tuberculosis Report 2021[1]).

1.1.3. Impeding host-defense by *Mycobacterium tuberculosis* – a causative agent for Tuberculosis

A broad set of bacteria under the Mycobacteriaceae family that display varying pathogenic features in animals and humans also exhibit distinct morphologic and phenotypic dynamics in the host[22]. One such member of the Mycobacteriaceae family, the rod-shaped, acid-fast bacillus *Mycobacterium tuberculosis* (Mtb) causes TB disease and possesses protection by a wax-rich cell wall[22, 23]. The unique three-layer cell wall characteristics specific to bacteria under the *Mycobacterium* genus provide a clear difference from other fast-growing non-pathogenic bacteria[24]. The outmost layer of the cell wall is comprised of polysaccharides and free proteins whereas the inner membrane (also known as “phospholipid bilayer”) consists of glycolipids linking them to the periplasmic region. The fundamental core between the inner and outer membrane is made up of long-chain mycolic acids and densely

branched arabinogalactan polysaccharides (**Figure 3**) essential for Mtb survival and persistency in the host[24].

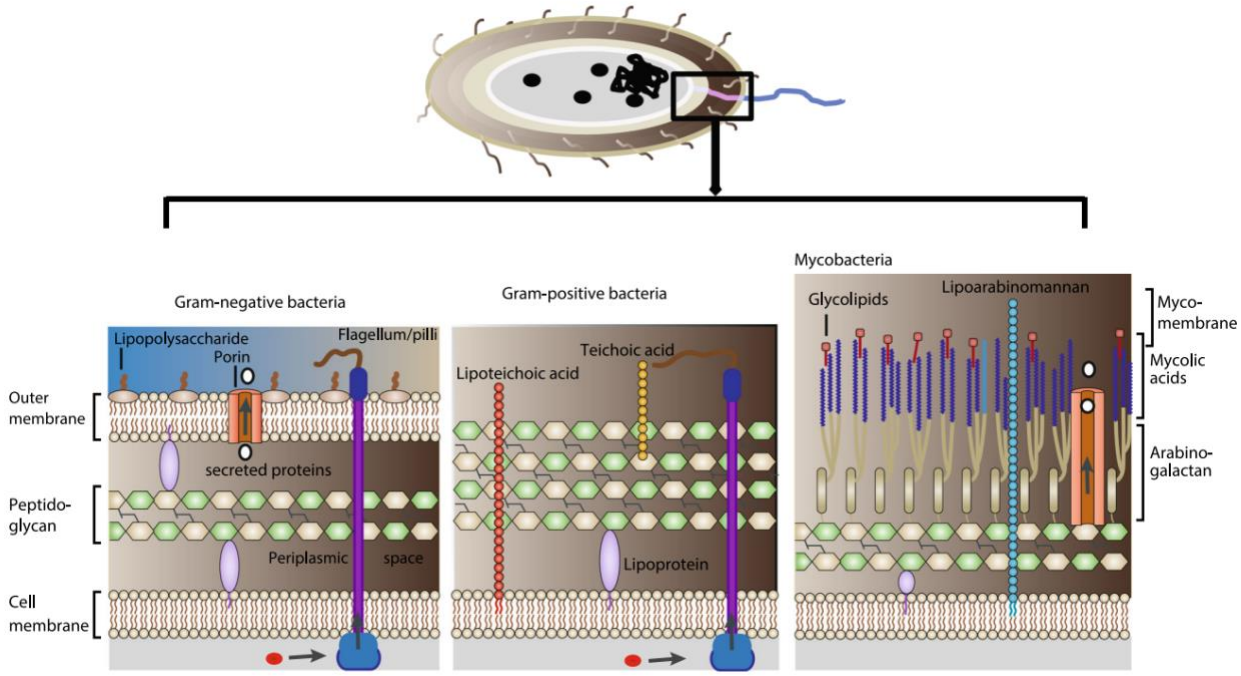

Figure 3. Schematic diagram of the architecture of different bacterial cell walls and their components. Left to Right: Gram +ve, Gram -ve, and Mycobacteria. (Adapted from Awuh et. al. [25]).

The Mtb bacteria does not grow in any other species or abiotic habitats since humans are the only reservoir for it. However, non-human primates (Macaques) and mammals (mice, rabbits, etc.) have been used to induce TB disease and conduct numerous studies understanding the pathogenesis of Mtb bacterium[26]. Despite having limited knowledge of TB immunology, several authors have adequately summarized the host immunity response influencing TB pathogenesis[22, 27]. At first, Mtb from an active TB patient is inhaled through airborne droplets including Mtb-nuclei, following translocation to the lower respiratory tract, where it encounters terminal alveolar macrophages and begins with adverse pathophysiological mechanisms for survival[22, 27]. Receptor-mediated internalization known as “phagocytosis” of Mtb by tissue-resident alveolar macrophages and other myeloid cells facilitates a replicative niche favorable for Mtb, leading to a latent form of TB[28]. Upon completion of internalization, Mtb actively blocks the maturation of phagosome by utilizing the “ESX-1 secretion system”,

causing the release of Mtb-DNA into the cytosol of the macrophages[29, 30]. This phenomenon by Mtb promotes intracellular growth through a type I IFN response mediated cytosolic pathway[31-33]. In addition, the Mtb pathogen is eventually dispersed within the pulmonary interstitium, lymph nodes, and adjacent extrapulmonary tissues before the initiation of adaptive immune responses[22]. Inflammatory macrophages and dendritic cells (DCs) govern the transportation of Mtb pathogen to initiate CD4+ T cell priming following trafficking to the lungs[34, 35]. Following transportation, CD4+ T cells undergo T_H1 clonal expansion via MHCII-mediated signaling by infected DCs resulting in increased secretion of "interferon-gamma (IFN-γ)" and "interleukin-2 (IL-2)" in the draining lymph nodes[36]. However, it has been shown that the Mtb pathogen delays this process to facilitate host defense evasion and survival[34, 36]. IFN-γ secreting CD4+ T cells skewed towards the periphery of the granuloma and maintains the integrity, whereas blockade of IFN-γ showed increased susceptibility to Mtb infection with high neutrophil recruitment, inflammation, and defective granuloma development, causal for bacterial dissemination in both mice and humans[36-38].

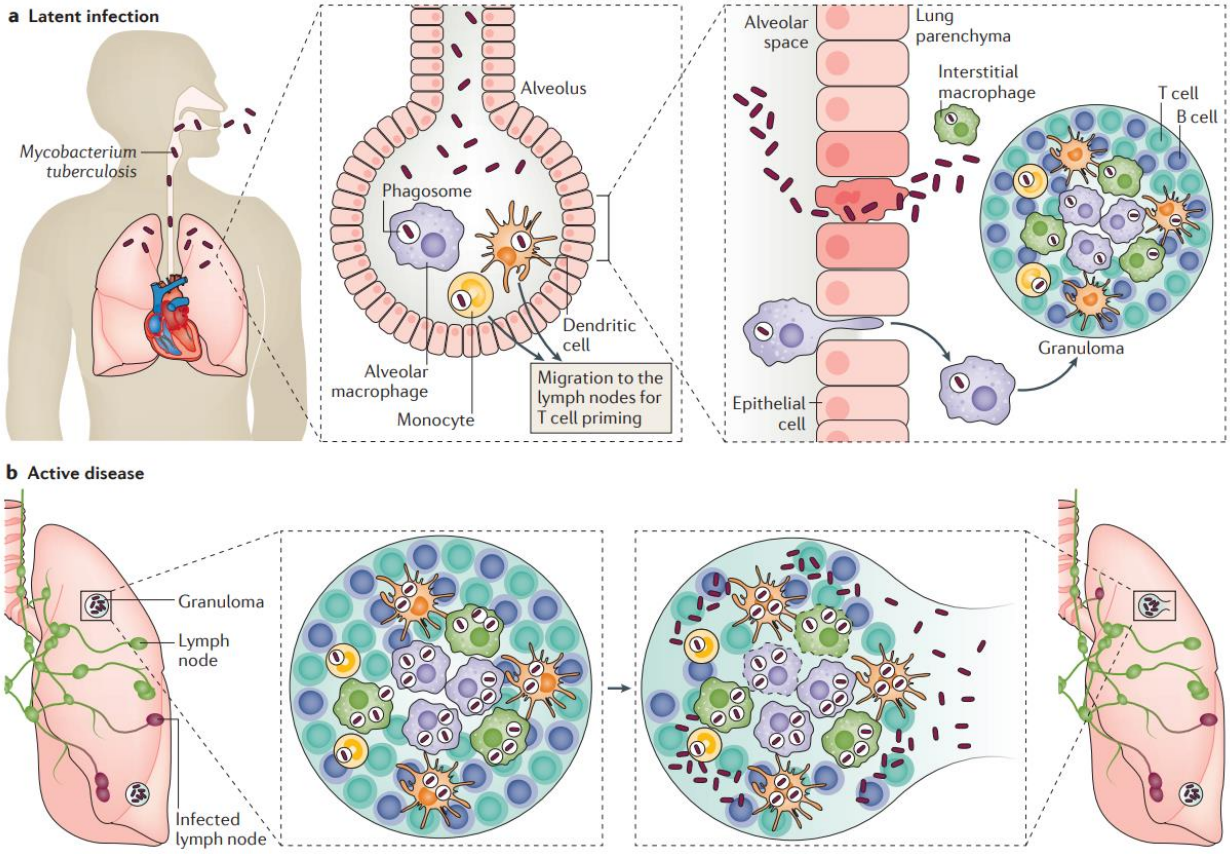

Figure 4. TB pathogenesis from latent infection to active disease. (Adapted from Pai et. al. [27]).

Pulmonary TB is distinguished by granuloma development surrounded by an influx of macrophages and other antigen-presenting cells (APCs) that occurs early after infection[22]. Histopathological analysis revealed that granulomas contain diverse immune cells including "foamy macrophages", "epithelioid cells", and "multinucleated giant cells". Moreover, the extreme boundary of granuloma develops a "lymphatic cuff" composed of conventional lymphocytes (CD4+/CD8+) and B cells which limits bacterial dissemination[22]. Failure to limit the bacterial replication in the granulomatous region by host inflammatory responses may cause the release of Mtb bacilli in the extracellular milieu leading to active Mtb replication and secretion of pathogenic lipids and proteins[39]. The duality of TB disease state depends on either a pulmonary microenvironment devoid of significant inflammation by modulating Mtb replication in immunocompetent hosts, leading to latent-TB infection (LTBI), or excessive inflammatory response mediated Mtb restriction and host tissue damage, promoting active-TB disease[40] (**Figure 4**).

1.1.4. *Mycobacterium tuberculosis* survival in macrophages – a molecular basis

Disease progression uniquely depends on the pathogen's ability to survive within the host by regulating combat strategies. The pathogen in the intracellular milieu is protected from humoral immunity but exposed to cellular immunity during Mtb infection[25]. Also, the pulmonary environment known to be pervaded by macrophages originated from multiple ontogenies. Studies have shown that before the occurrence of Mtb infection, diverse phagocytes like macrophages modulate the microenvironment to facilitate or restrict the infection[41]. Upon Mtb infection, Alveolar macrophages (AMs) trap the bacterium and initiate an early cascade for innate inflammatory responses leading to the recruitment of other myeloid cells, which forms the "granuloma." During phagocytosis, macrophages, dendritic cells (DCs), and other granulocytes confront and internalize Mtb pathogen through extracellular "pathogen-recognition receptors (PRRs) recognizing pathogen-associated molecular patterns (PAMPs)" of Mtb (**Figure 5**)[25, 42]. Depending on the pathogenic architecture covered by specific soluble PRRs and antibodies, opsonic and non-opsonic phagocytosis begins with expressing extracellular receptors. Various integrins, complement receptors (CR), and Fc receptors mediate the opsonic phagocytosis cascade, whereas receptors such as "CD169 and CD33" (microbial recognition); "Dectin-1, -2, mannose receptor (MR), DC-specific intercellular adhesion molecule-3 grabbing nonintegrin (DC-SIGN), MCL, and

Mincle (carbohydrate moieties recognition)"; and "CD36, AIM, SR-A, and MARCO (Scavenger receptors)" mediate non-opsonic phagocytosis[42, 43]. Other receptors such as "CD14 and CR3" are known to be directly involved in PRRs-PAMPs interactions[44-46]. A family of PRRs known as "Toll-like receptors (TLRs)" facilitates Mtb uptake and is considered to be a key sensor of pathogen invasion[43]. Major activities during Mtb infection are regulated by "TLR2, TLR4, and TLR9", and their ability to recognize various Mtb-associated PAMPs. Knowingly, TLR2 has been shown as the most decisive responder to Mtb among all TLRs, and its potential to recognize cell wall elements such as "mannosyl-phosphatidyl-*myo*-inositol-based glycolipids (PIM), lipoarabinomannan (LAM), and lipomannan (LM)" has been illustrated previously[25]. Besides, TLR4 has been shown as a potent TLR for bacterial lipopolysaccharide (LPS) recognition whereas TLR9 was shown to detect oligodeoxynucleotide (ODN) motifs of Mtb deoxyribonucleic acid (DNA)[47].

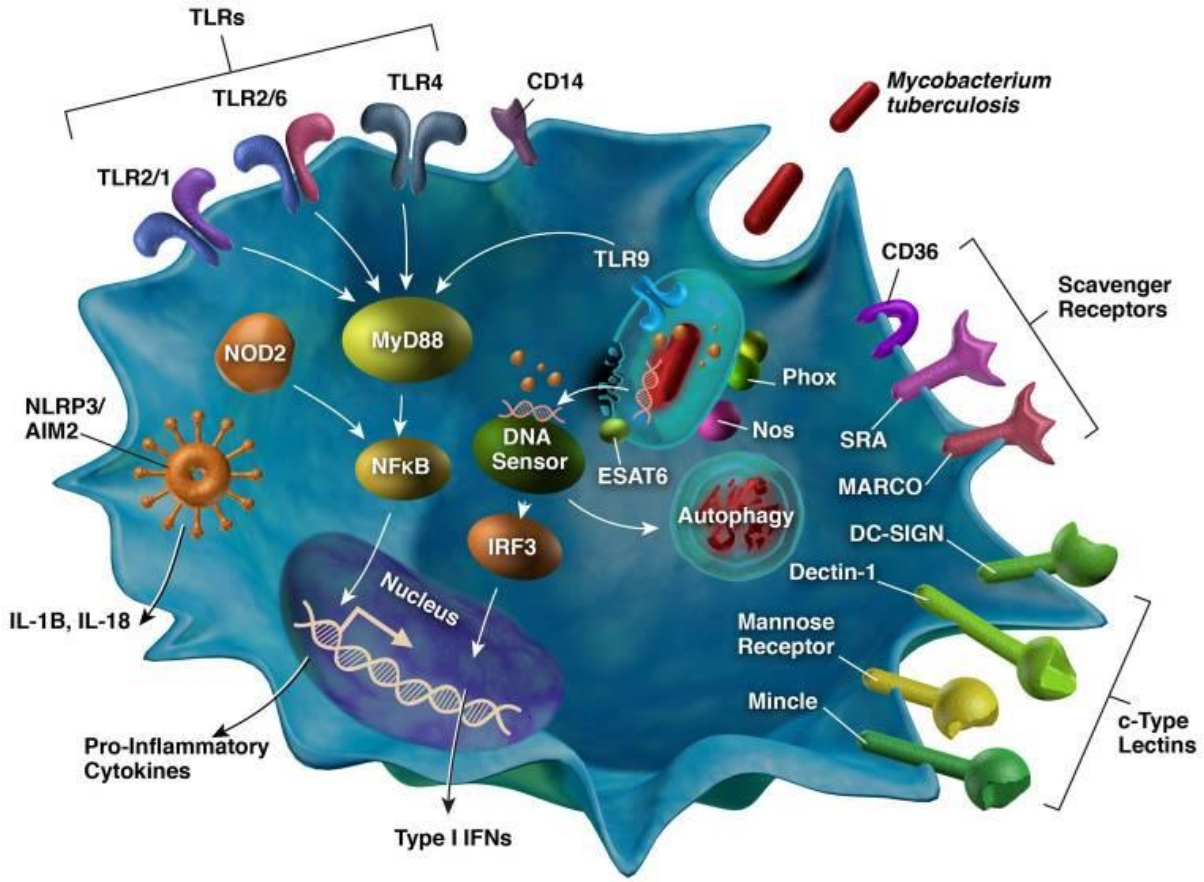

Figure 5. The interplay between Mtb PAMP and potential host PRRs. (Adapted from Stamm et. al.).

Furthermore, various “Toll-interleukin-1 receptor (TIR)” dependent signaling pathway activation attributed to the recruitment of adaptor molecules such as “myeloid differentiation primary response protein 88 (MyD88)”, “TIR-domain-containing adapter-inducing interferon-β (TRIF)”, “TIR domain-containing adaptor protein (TIRAP)”, and “TRIF-related adapter molecule (TRAM)”[48]. “Interleukin-1 receptor 1 (IL-1R1) - associated protein kinases (IRAKs)” form a complex with MyD88 known as “myddosome” which interacts with “TNF receptor-associated factor 6 (TRAF6)” leading to the activation of “nuclear factor kappa-light-chain enhancer of activated B cells (NF-κB)” and release of pro-inflammatory cytokines during Mtb pathogenesis[25]. NF-κB-mediated release of proinflammatory cytokines such as “interleukin-1β (IL-1β), IL-18”, and activation of different caspases also regulated by “nucleotide binding and oligomerization domain (NOD2)” and “NOD-like receptor pyrin domain (NLRP3)” which leads to inflammasome pathway activation and induction of “pyroptosis”, a programmed cell-death mechanism[49]. Macrophage activation during Mtb infection often depends on several antimicrobial capacities such as “Reactive Oxygen Species (ROS)” or “Reactive Nitrogen Species (RNS)” production which occurs during early phagocytic events. These early pathogen-responsive antimicrobial capacities are strongly regulated by the “nitric oxide synthase 2 (NOS2)”, “NADPH oxidase (NOX2)”, and their enzymatic activities[50]. ROS and Nitric Oxide (NO) can dynamically combine to produce strong oxidizing intermediates against Mtb-DNA, membrane lipids, and pathogenic enzymes. Although, Mtb has evolved the capacity to diminish the effects of ROS by utilizing an “enhanced intracellular survival (Eis)” gene expression. Deletion of the Eis gene from the Mtb strain revealed a host dominating protection against Mtb infection with increased ROS levels [51]. Previously, an inducible form of NOS (NOS2 or iNOS) production by Mtb pathogen-directed signaling has been considered the prime host defense mechanism during Mtb infection[52]. However, activated macrophage-mediated production of NOX2 and its inhibition by “nucleoside diphosphate kinase (Ndk)” protein of Mtb blocks the translocation of NOX2 into the phagolysosomal fusion leading to intracellular survival[53]. Progressive phagosomal maturation depends on sequential events including “vacuolar-adenosine triphosphatases (V-ATPases)” mediated acidification, NOS2, and NADPH assembly, and the activity of various cathepsins, “rat sarcoma virus (Ras)-associated binding (Rab) guanine triphosphatases (Rab-GTPases)”, and kinases[25]. The circumvention of phagolysosomal degradation by Mtb pathogen with sustained pH at 6-6.5 and constant nutrient uptake is well evident at an early endosomal event in macrophages during Mtb infection[54, 55]. Moreover, prevention of phagolysosomal acidification by the “tyrosine phosphatase (PtpA)” protein of

Mtb has been also shown to display similar strategies of maintaining the pH at 6.2-6.5 leading to Mtb survival[56]. Mtb also blocks the sequential conversion of Rab5 to Rab7 which is conducive to the inhibition of phagosomal maturation during Mtb infection[55]. Inhibition of Rab7 modulates the subsequent "autophagic progression" favorable for intracellular Mtb persistency, a well-known host cell-death program. An "autophagy-related gene (Atg5)" has shown to be crucial for bacterial control as Atg5 deficient mice showed increased susceptibility to Mtb infection and loss of "microtubule-associated protein 1A/1B-light chain 3 (LC3) associated phagocytosis (LAP)"[57, 58]. Another "autophagy-related gene (Atg7)" significantly induces the autophagic pathway by activation of "c-Jun N-terminal kinases (JNK)" which is a target for the Eis gene of Mtb[51]. Thus, Mtb-directed host immune modulation is favorable for the survival of the pathogen in the macrophages despite having several cell-autonomous defense mechanisms including phagocytosis, acidification, lysosomal disruption, programmed cell-death – apoptosis, necrosis, autophagy, and adaptive immune responses through surface antigen presentation[59]. There is no doubt that new insight and understanding are required of these pathogen-evasive mechanisms to implement host-directed therapies that target an array of potential host-directed targets (HDTs) against tuberculosis.

1.1.5. An alternative approach – Host-Directed Therapy for Tuberculosis

Tuberculosis (TB), one of the oldest recorded human afflictions, is still one of the biggest killers among infectious diseases and an alarming problem led to deaths globally. To reduce the increasing incidence of TB, it is important to understand the host-pathogen interaction to learn how these bacteria circumvent host defense and cause disease[60]. Mtb is a rod-shaped, acid-fast bacillus that can develop resistance to existing treatments. The chronic nature of Mtb relies on its impeccable cell wall as well as the ability to manipulate antibiotics by altering their structure or cleaving them, thus rendering them ineffective [61, 62]. Unfortunately, the first TB vaccination, known as "Bacille Calmette-Guerin (BCG)", only protects against childhood manifestations such as TB meningitis, and not against the most prevalent form of TB, pulmonary tuberculosis[63]. This phenotypical barrier of TB causes difficulties in the diagnosis and requires long-term treatment[23]. Moreover, based on a large-scale animal experiment, although a significant level of protective immunity to Mtb challenge was observed through immunization with environmental mycobacteria and highly variable and reduced effects of BCG were detected, indicating a complex and debatable platform against

BCG vaccination strategy[64, 65]. Additionally, second-line treatment leads to serious side effects which result in severe lung damage. Thus, a novel, effective and strategic therapy against pulmonary TB has become a research priority. As more knowledge is gathered about the host components involved in pathogenic infection and death, targeting the host-pathogen interaction has emerged as a critical strategy. For instance, Mtb has infected a massive population by acquiring a significant ability to exploit cellular host factors for its survival and persistence. Mtb has an evolutionary effect that makes them "multidrug-resistant (MDR)" and "extensively drug-resistant (XDR)"[62]. In recent years, a new approach has been raised i.e., "Host-Directed Therapy (HDT)" to develop novel interventions against these drug-resistant Mtb strains by reducing pathology, mycobacterial burden, and possible dormancy[60]. As a strategic therapy, it reduces prolonged treatment duration by targeting various host-mediated pathways such as Mtb antigen processing and presentation, innate signaling pathways, phagosomal maturation, bactericidal mechanism, autophagy and also pathogen binding and uptake, phagosomal escape, and/or detoxification to reduce lung inflammation during Mtb infection (**Figure 6)**[60, 66].

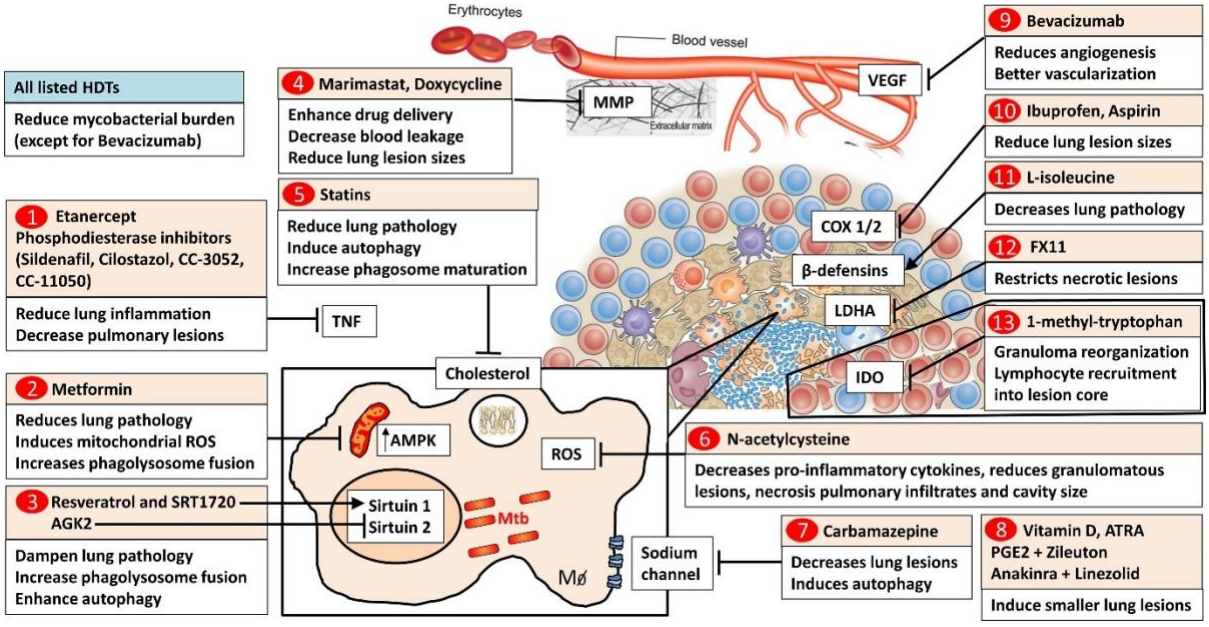

Figure 6. Host-Directed Therapy (HDT) strategies against Tuberculosis. (Adapted from Guler et. al. [66]).

One such HDT, "Statins" (HMG-CoA inhibitor), showed promising outcomes in decreasing the Mtb burden in a murine model and human macrophages[67]. Additionally, Statin administration with first-line TB drugs reduced the duration of TB treatment in a murine model

and has been shown to have a protective role against active TB in humans by reducing "low-density lipoprotein (LDL)" cholesterol in serum[68-70]. By modulating "peroxisome proliferator-activated receptor-gamma (PPAR-γ)" and "transforming growth factor beta (TGF-β)", statins also exhibit pleiotropic inflammatory responses[71]. Another promising HDT, "Gefitinib" (growth factor inhibitor) has revealed a potential role in the autophagic progression in murine macrophages by the "p38 mitogen-activated protein kinases (MAPK)" signaling pathway[72]. Moreover, "Ibuprofen" has been proved as a standalone drug improving TB disease outcomes in mice by its inhibitory effects on "prostaglandin H2" and "cyclooxygenase 1/2 (COX1/2)"[73]. Furthermore, numerous studies have revealed that a potent immunomodulator, "Vitamin-D" also possesses abilities to protect against Mtb infection in macrophages by skewing innate immunity[74]. Antimicrobial capacities such as ROS production and phagosome maturation are diminished by a biguanide HDT candidate - Metformin has also been widely studied in the advancement of diabetes mellitus in adults[75]. An "anti-Lipoarabinomannan (LAM)" antibody as HDT has shown a unique method of augmenting bacterial inactivity through conventional CD3+ T cell recruitment and phagolysosomal progression[76]. More recent findings demonstrated a significant role of "Berberine" (DAXX2 inhibitor) in the improvement of Mtb infection outcome, as adjunctive therapy with existing anti-Mtb drugs[77]. However, safe administration of all these drug candidates has not been clinically proven and limited success has been achieved in the inclusion of these drugs in the existing TB drug regimen. Also, lung resident macrophages are the primary target for Mtb to establish the infection by actively evading host defenses through modulating host transcription and translation. As macrophages are the most active immune cells during Mtb infection, research priority is inclined towards investigating the macrophage effector-killing pathways. To gain long-lasting immunity, macrophages can activate different effector genes to combat invader pathogens. It is necessary to characterize these novel effector-killing genes to develop rational HDTs or prophylactic drug design to increase the host's protective immunity against Mtb infection.

1.1.6. FANTOM5: A functional genomics approach to identify Mtb targeted gene

Microarray, RNA sequencing, proteomics, metabolomics, and other technologies have contributed to the unwinding of complex biological interactions at the cellular level. The fundamental approach for investigating the molecular concept of biological systems and gene

regulation is the quantification of transcript abundance. Whole "transcriptome microarrays" and "RNA-Sequencing (RNA-Seq)" are widely used tools to exploit distinct transcriptome profiles of Mtb-infected macrophages[78, 79]. Also, host cell determinants during Mtb infection and disease progression have been identified with the advancements in RNA-seq known as "single-cell RNA-Sequencing (scRNA-Seq)"[79]. For instance, "granulocyte-macrophage colony-stimulating factor (GM-CSF)" has been found by scRNA-Seq and shown as a potent modulator to induce inflammatory response against Mtb infection by pushing the macrophages towards their activation state[80]. In recent years, innate immunity responsive alveolar and interstitial macrophages revealed a unique host-pathogen interplay and molecular dynamics through a transcriptome dataset using a dual RNA-Seq approach[79, 81]. Such large transcriptome datasets have been accumulated over the years by numerous research groups in different consortiums known as "Functional Annotation of Mammalian Genome (FANTOM)" and "Encyclopedia of DNA Elements (ENCODE)"[82, 83]. Moreover, exploitation of comprehensive and quantitative transcriptome abundance in various mammalian cells using "Cap Analysis of Gene Expression (CAGE)" technology allows the discovery of activated genes, transcription factors, and noncoding RNAs during Mtb infection by mapping transcription start sites (TSSs) and core promoters [83]. This extensive profiling of the transcriptome dataset in a project known as the "FANTOM5 CAGE" atlas led to the identification of many immune candidates during Mtb infection in murine macrophages[84]. These large transcriptomics data have been used by several research groups to identify genes potentially contributing to host immune evasion during Mtb infection. Murine bone-marrow-derived macrophages are the most crucial cells maintaining pulmonary immune homeostasis during Mtb infection[85]. In FANTOM5 murine CAGE studies, different activation states of these macrophages and their response during Mtb infection through time-kinetics manner were detected by polarizing them using IFN-γ (caMPh: classically activated macrophages), interleukin-4 (IL-4), interleukin-13 (IL-13) and combination of IL-4/IL-13 (aaMph: alternatively activated macrophages)[84]. A total of 158966 tags were found to be relevant by CAGE transcriptome analysis and mapped to the mouse genome[84]. This revealed a cluster of protein-coding and non-coding transcripts among which only two protein kinases TSSs were found to be yielded significant alteration in alternatively activated macrophages – "cGMP-dependent protein kinase 1 (Prkg1)" and "protein kinase C delta (PKCδ)" [84]. However, PKCδ has been widely studied in different infectious diseases and established as a marker of inflammation during Mtb infection[86-88]. Hence, based on FANTOM5 CAGE transcriptome

profiling and previous literature findings, PKCδ plays an extensive role and has the potential to be exploited as a therapeutic target against TB.

1.1.7. Protein kinase C delta (PKCδ) – a novel kinase among protein kinase C superfamily

The phospholipid-dependent serine/threonine kinase, protein kinase C (PKC), was first described in 1977 by Nishizuka and colleagues, demonstrating a vital role in intracellular signal transduction[89]. PKCs can both positively and negatively regulate signaling pathways depending on their context-sensitive activity[90-92]. Classification of PKC isoforms has been divulged based on their structural elements and cofactor requirements necessary for activation. The Mammalian PKC family comprises three distinct categories known as "classical PKCs (α, β, and γ)", "novel PKCs (δ, ε, η, and θ)", and "atypical PKCs (ι and ζ)"[89]. Classical PKCs activate utilizing secondary messenger "diacylglycerol (DAG)" and "calcium (Ca^{2+})", whereas novel PKCs rely only on DAG for their activation. However, the activation of atypical PKCs mediates by a secondary messenger known as phosphatidylserine (PS)[89]. The broad spectrum of PKC isoforms shares similar conformation and catalytic activation patterns[93]. The architecture of PKC isoforms includes three major domains – "catalytic, hinge, and a regulatory domain". In brief, ATP and substrate binding sites are located in the catalytic domain at the C-terminus. The regulatory domain at N-terminus facilitates the activation or inactivation of the kinase utilizing the pseudosubstrate region, the binding site for various cofactors. A hinge domain separates the catalytic domain from the regulatory domain (**Figure 8**)[89, 90]. C1 region (including cysteine-rich C1A and C1B region) at the regulatory domain is the binding site for PS and DAG. When "phospholipase C (PLC)" hydrolyzes the "phospholipid phosphatidylinositol 4,5-biphosphate (PIP2)", it generates "inositol triphosphate (IP3)" - activates classical PKCs and DAG - activates novel PKCs[89]. Also, IP3 elevates the levels of cytosolic Ca^{2+} which binds to the C2 region at the regulatory domain leading to the activation of classical PKCs. However, the lack of an aspartate residue in the C2-like region at the regulatory domain allows the activation of novel PKCs without Ca^{2+} binding. [90, 94]. Besides, atypical PKCs lack the C2 region and have an irregular C1 region which restricts the binding of both cofactors such as DAG and Ca^{2+}. Moreover, C3 and C4 regions mediate the binding of ATP and substrate or pseudosubstrate respectively[89]. In recent years, the novel isoform PKCδ has been implicated in various diseases including cancer, diabetes,

neurodegenerative diseases, ischemic heart diseases, and infectious diseases such as listeriosis, cutaneous leishmaniasis, and tuberculosis[86-89].

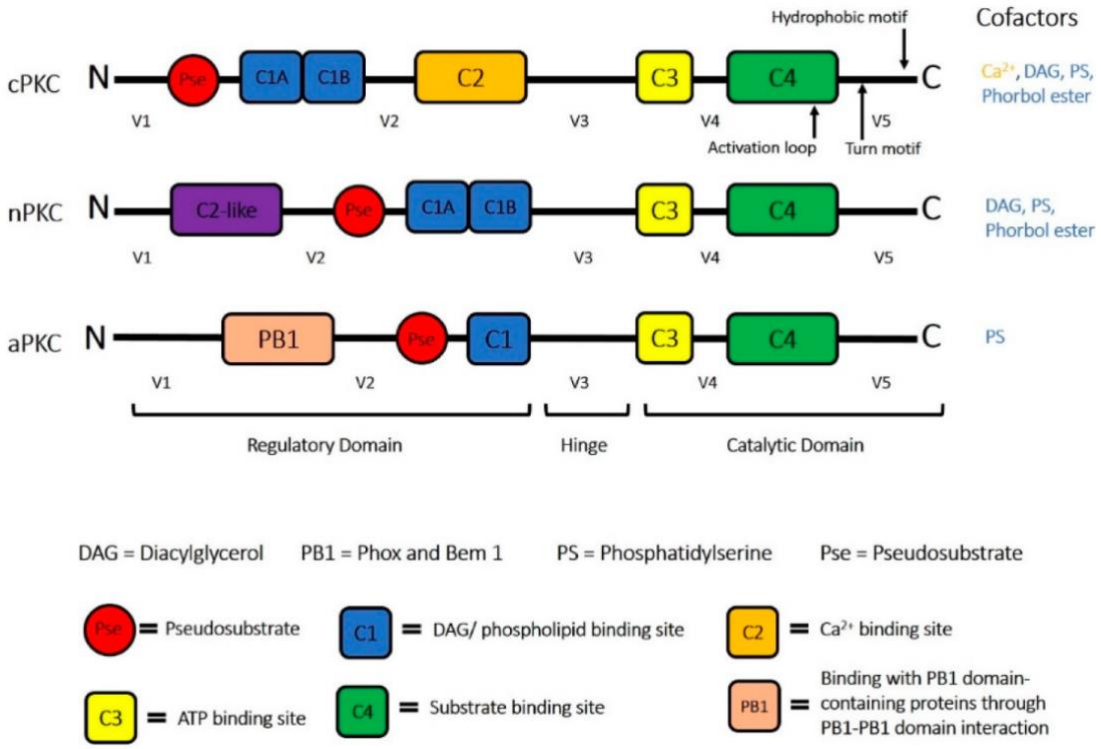

Figure 7. Structural construction of various classes of PKC. (Adapted from Yang et. al.[89])

Unlike other isoforms, PKCδ is unique in its regulation by tyrosine phosphorylation leading to its activation state, specificity to the substrate, and localization. The activity of PKCδ depends on the phosphorylation of three major conserved serine and threonine sites which are the activation loop: Threonine-505 (T-505), hydrophobic motif: Serine-662 (S-662) and turn motif: Serine-643 (S-643). The phosphorylation of these sites is crucial for catalytic activity and enzyme stability regulated by PKCδ[89, 95]. More recent studies have demonstrated that PKCδ-mediated cellular intrinsic proinflammatory signaling, programmed cell-death triggering pathways, nuclear translocation, and enzymatic activation are the consequences of two vital tyrosine phosphorylation sites – Tyrosine-155 (Y-155) and Tyrosine-311 (Y-311)[89]. The apoptosis mediator, Y-155 locates in the middle of the C1A region at the catalytic domain and the regulatory domain, whereas Y-311 locates in the hinge domain mediating caspase-3 proteolytic cleavage[90]. These unique tyrosine phosphorylation sites of

novel PKCδ have also been shown to play a major role in endothelium-neutrophil interplay and lung injury caused by sepsis. Significantly, another important phosphorylation site of PKCδ, Tyrosine-52 (Y-52) residing in the C2 region at the regulatory domain, has been described as a potent regulator for substrate recognition by initiating a docking site for binding of substrates[96]. In addition, Tyrosine-512 (Y-512) and Tyrosine-332 (Y-332) have also been found as crucial as other tyrosine phosphorylation sites enriching activation of PKCδ and localization (**Figure 9**)[89, 90, 96].

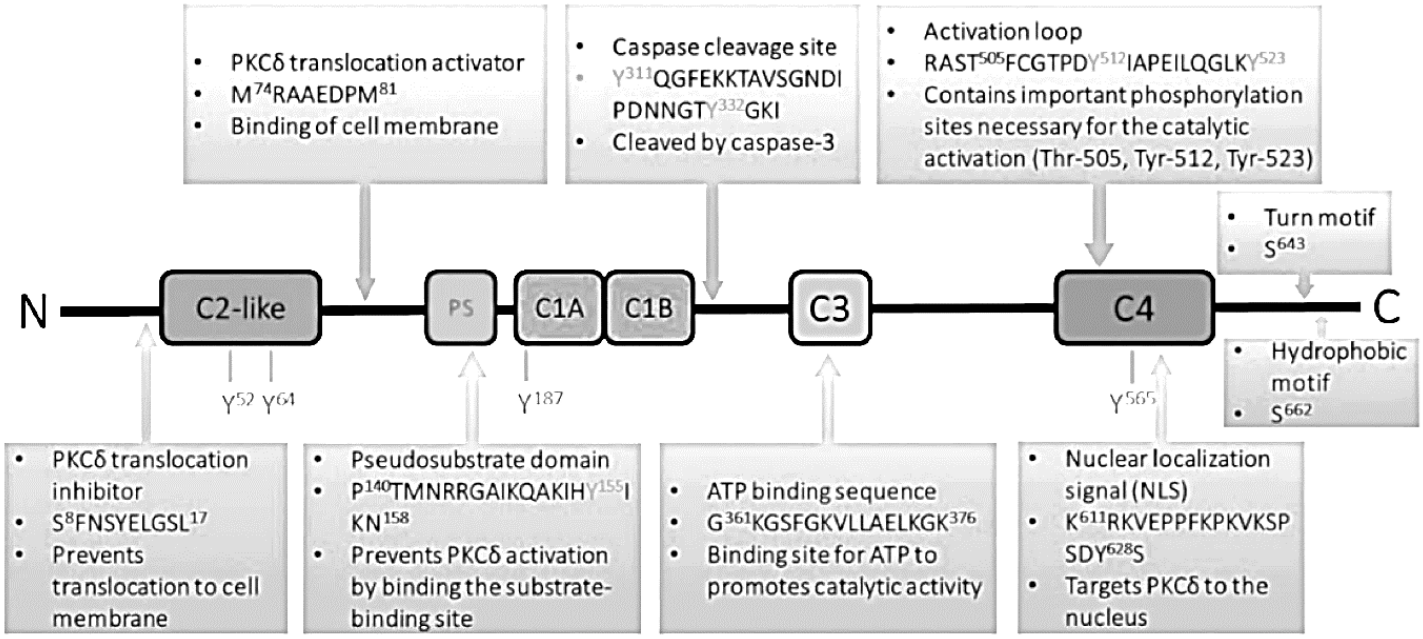

Figure 8. Major Tyrosine phosphorylation sites of PKCδ and various regulators (amino acid sequences). (Adapted from Yang et. al. [89]).

Moreover, kinase activity and subsequent cellular function certainly depend on the binding of the specific substrate at the regulatory domain of PKCδ. Previous literature has compiled various substrates of PKCδ and their role in diverse cellular intrinsic functions which is shown below (**Table 2.).**

Table 2. Various substrates of PKCδ and identified functions. (Adapted from Yang et. al. and Steinberg et. al.[89, 90]).

Substrates	Functions
14-3-3	Interference with 14-3-3 polymerization and interactions
Bcl-2-associated death promoter (BAD)	Initiate apoptosis post cardiac ischemia
c-Abl	Enhanced activity
Caspase-3	Caspase-3 mediated proteolytic cleavage in monocytes
DNA-dependent protein kinase	p53 phosphorylation restriction
DNA-PK	DNA damage
Dynamin-related protein 1 (Drp1)	Mitochondrial fission following cardiac ischemia
Glyceraldehyde-3-phosphate dehydrogenase (GADPH)	Injured mitochondria removal following ischemic damage
gp130	Increased gp130 interaction with STAT3
Heat Shock Protein 25	Restriction of apoptosis
Heat Shock Protein 27 (HSP27)	Antioxidants, chaperone, apoptosis restriction
hRad4	Increased hRad9 interaction with Bcl-2
Lamin B	Apoptosis
M2 Pyruvate Kinase	Involvement in tumor metabolism
MARCKS	Cell attachment in skeletal muscle cell
p300	Decreased transcriptional function and reduced HAT activity
p47(pbox) unit of NADPH	Increased activity
p52Shc protein	Positively modulates activation of H2O2-induced ERK signaling
p66Shc protein	Negatively modulates activation of H2O2-induced ERK signaling
p73β(Ser-289)	Apoptosis
PKCε (hydrophobic motif)	Elevates release from membranes

Plasma membrane calcium ATPase (PMCA)	Increased calcium levels in the skin
PLS3	Increased phospholipid translocation
Protein tyrosine phosphatase PTPα	Phosphatase activity
Pyruvate Dehydrogenase Kinase	Necrosis and blocking ATP production
RasGRP	Uncertain
SFKs	Variable
SHPTP1 (protein tyrosine phosphatase) (SHP1)	Reduced phosphatase activity
STAT1 (Ser-727)	Expression of Interferon gene
STAT3 (Ser-727)	Decreased DNA binding and transcription
Troponin	Reduced Calcium sensitivity of actomyosin
β4-integrin	Decreased cell-laminin attachment

PKCδ activity appears to be significantly influenced by its localization. Previously, leukemia cells showed TNF and Fas-receptor mediated release of "Ceramide" induces the phosphorylation of PKCδ via Src kinase and translocation of PKCδ from the plasma membrane to the cytosol[97]. Also, PKCδ phosphorylates the "Immunoglobulin E (IgE)" receptor during mast cell activation, which aids in endocytosis[98]. Phosphorylation of PKCδ is also shown to be mediated by several tyrosine kinases such as "Src (Sarcoma), Fyn, Lyn (v-yes-1 Yamaguchi sarcoma viral related oncogene homolog), PDK1 (Phosphoinositide dependent kinase 1), PYK2 (Protein tyrosine kinase 2)"[99]. A unique "epidermal growth factor (EGF)" receptor, has been shown to be transactivated by PKCδ which in turn activates ERK1/2 and ATF-1, upregulates the expression of NOX1 in the vascular smooth muscle cells (VMSC)[100]. Also, proteolytic cleavage of PKCδ by caspase-3 renders apoptosis and translocation of PKCδ catalytic fragments to the nucleus for downstream events[101]. This apoptotic activity has been shown to be inhibited by a "heat shock protein (Hsp25/27)" through its binding to the catalytic region of PKCδ[99]. The role of PKCδ in maintaining cellular homeostasis and membrane excitability through Ca^{2+} efflux regulators and K^{+} channels has been extensively studied which shows a prime function of DAG and IP3 mediated activation of PKCδ[99]. In the context of transcription factors regulation, PKCδ has been shown to effectively and sufficiently activated JNK via RelA phosphorylation leading to cell death[102]. Studies also demonstrated the requirement of PKCδ in the activation of NF-κB, inhibition of histone acetyltransferase (p300),

and regulation of Stat1 via MHCII receptors [102-104]. Moreover, as a "redox-sensitive kinase", PKCδ activates via ROS-mediated release of DAG and membrane translocation and regulates the role of NF-κB as redox-sensitive manner[105]. When considered collectively, the role of PKCδ by utilizing its substrates reveals the crucial function of this kinase in facilitating diverse biological process (**Figure 9**).

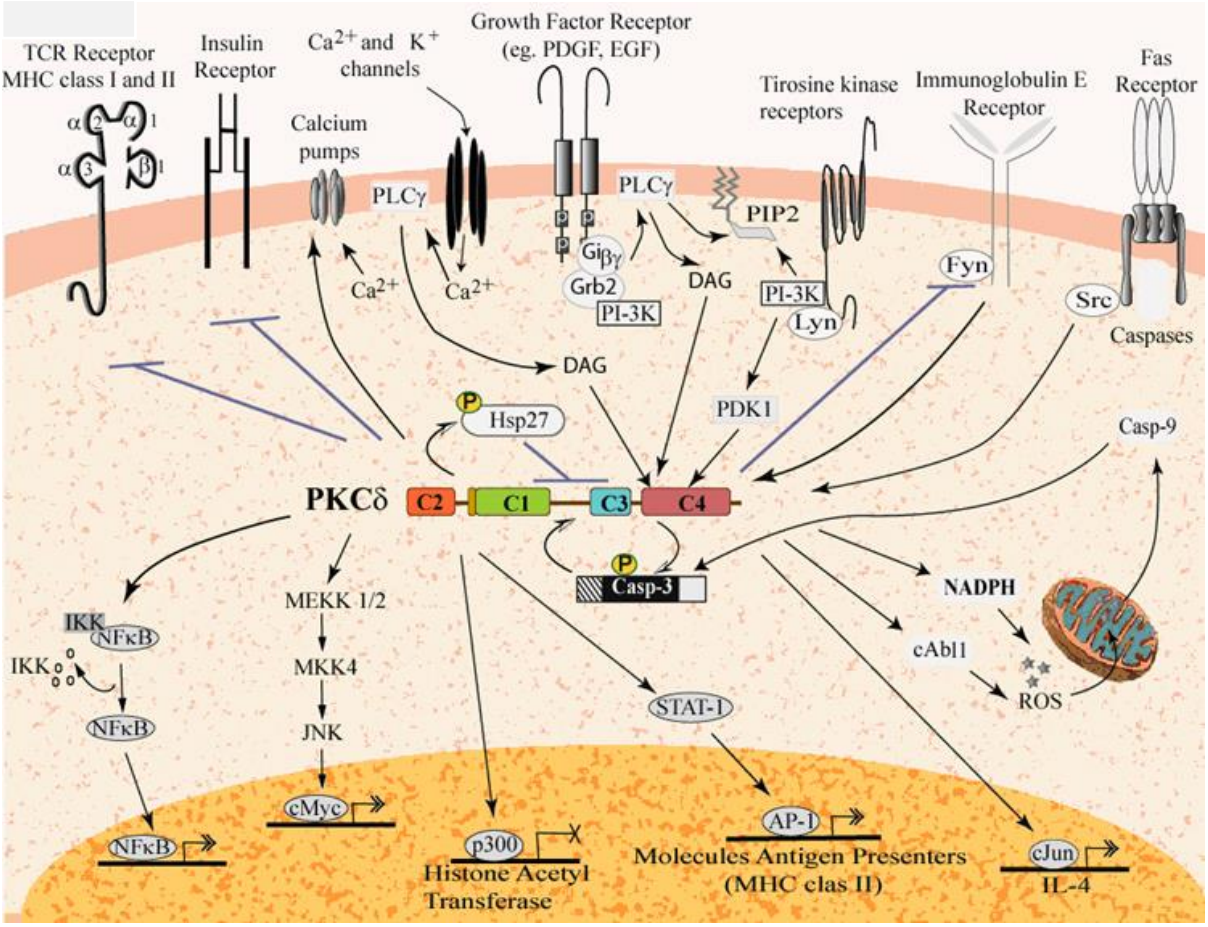

Figure 9. Cellular intrinsic mechanisms mediated by PKCδ. (Adapted from Malavez et. al.[99]).

1.1.8. *In vivo* and *in vitro* role of PKCδ in inflammation

Results from studies exploited over the last years have identified the role of PKCδ as a potent signal transducer of various signaling pathways. Studies with germ-line PKCδ deficient murine model and PKCδ inhibition *in vitro* revealed a multitude of physiological roles involving various cellular processes[88]. PKCδ activation during inflammatory response illustrates the involvement of various proinflammatory cytokines (IL-1 and TNF), PAMPs such

as bacterial peptide "N-formylmethionyl-leucyl-phenylalanine (fMPL)", and LPS[89]. Utilizing a chemical inhibitor Rottlerin, blocking PKCδ has shown to have major effects on reducing enzymatic activity in the pancreas[106]. Also, human monocyte-derived macrophages infected with HIV-1 were shown to have lower viral burdens when treated with rottlerin[107]. In hamster kidney cells and the murine macrophage cell line RAW264.7, silencing PKCδ with anti- PKCδ "small interfering RNA (siRNA)" increased cholesterol efflux[108]. Rottlerin-mediated inhibition of PKCδ also showed a repressive effect on the activation of NF-κB, subsequent NO, and proinflammatory cytokine production during innate immunity[109]. Besides, a PKCδ-specific peptide inhibitor, TatVδ1.1 showed improved outcomes during sepsis by reduced lung injury and better gaseous exchange[110]. Knowingly, PKCδ ablation is directly involved in reduced kinase activity with TIRAP through TLR-mediated signaling[109]. Moreover, the PKCδ global knockout murine model ($PKC\delta^{-/-}$) unveiled the role of PKCδ in the migration of neutrophils at the site of infection during bacterial sepsis, acute lung inflammation, and acute pancreatitis[89]. More recently, a functional role of PKCδ modulating the immune response in various infectious diseases has been found by conducted *in vivo* studies. $PKC\delta^{-/-}$ mice were shown to play a crucial role in the phagosomal clearance of *Listeria monocytogenes* by macrophages[86]. An animal model of cutaneous leishmaniasis indicates that PKCδ also regulates the production of interleukin-12 (IL-12) in macrophages and dendritic cells necessary for T helper cell type I protective immune responses[87]. Furthermore, Card9-mediated antifungal immunity of mice that lack PKCδ renders them susceptible to *Candida albicans* infection[111]. In recent studies, Parihar and colleagues investigated the functional significance of PKCδ in humans and mice in tuberculosis immunity, along with how it influences lipid homeostasis[88]. These studies also showed that PKCδ holds a possibility as a novel candidate gene for therapeutic interventions against infectious diseases. However, these studies were performed in mice deficient for PKCδ in all cell types. To develop host-directed interventions for the correlates of host protection or susceptibility, it is essential to understand the cell-specific role of PKCδ in infectious diseases.

1.1.9. Project Rationale

Mycobacterium tuberculosis (Mtb) remains one of the deadliest infectious diseases worldwide, where dormant Mtb bacilli do not respond to existing anti-Tuberculosis (TB) drugs and turned out to be a crucial threat to human beings. Insufficient vaccine efficacy, budding

drug resistance by Mtb pathogen, and lack of new therapeutic approaches are the major contributors to the success of TB disease after CoVID-19. Mtb is latently present in one-third of the human population, yet only a small percentage develops active TB disease over time, suggesting host immune responses play a protective role. A thorough understanding of the dynamic interaction between the pathogen and the host is essential to the identification of alternative HDT targets and control of TB. The outcome of TB disease is primarily determined by myeloid-mediated manipulation of the pulmonary microenvironment. Also, the intracellular augmentation of the Mtb burden is mostly caused by the modulation of several killing effector

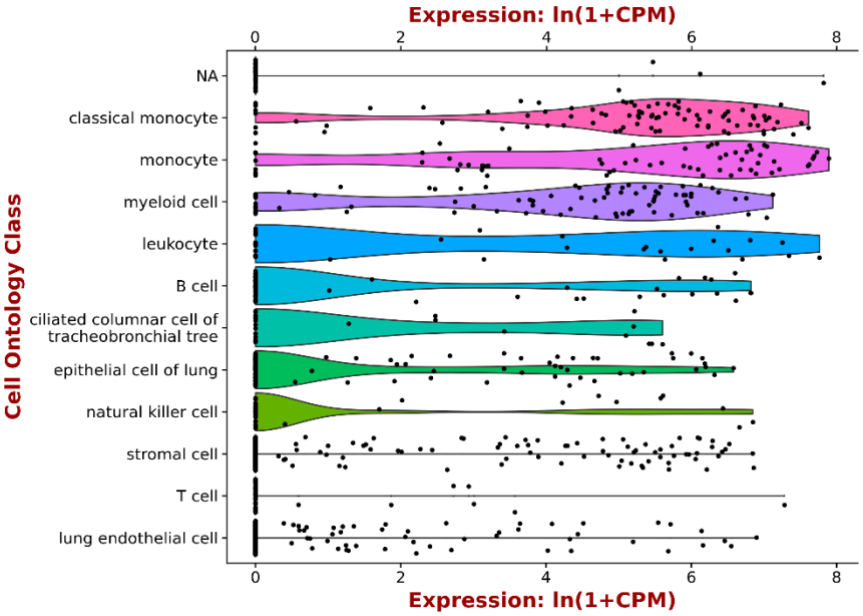

Figure 10. Tabula Muris database of single-cell transcriptomics of murine lungs demonstrating PKCδ expression in different lung cell types. (Adapted from Tabula Muris Consortium[112]).

functions in the hostile environment of macrophages. Previously, PKCδ$^{-/-}$ mice showed a significant decline in different myeloid cell populations along with reduced macrophage killing effector functions leading to the increased mycobacterial burden, worsened lung pathology, and exaggerated inflammatory response. PKCδ is ubiquitously expressed in most of the murine tissues with abundance in the lung myeloid subset including monocytes and classical

monocytes (**Figure 10**)[112]. In addition, the germline deficient PKCδ murine model (PKCδ-/-) failed to illustrate the myeloid inclusive role of PKCδ during Mtb infection. Based on the inadequacy in a myeloid comprehensive knowledge of PKCδ and the dominancy of macrophages during Mtb infection, we hypothesize that ablation of PKCδ specifically in macrophages will reveal insight into immune response regulated by PKCδ in macrophages during Mtb infection which has not been delineated yet. Our systemic study involves the generation of a functional macrophage-specific PKCδ deficient murine model ($LysM^{cre}PKC\delta^{flox/flox}$) that divulges the immunomodulatory functions of PKCδ *in vivo* and *in vitro* during Mtb infection.

1.1.10. Aim and Objectives of the study

This study aims to investigate the macrophage-specific role of PKCδ and its pathogen pathogen-killing functions, with the aim that it will eventually serve as a target for host-directed therapy against TB. To achieve this aim, we have executed the following objectives:

1. The characterization of a macrophage-specific PKCδ deficient murine model ($LysM^{cre}PKC\delta^{flox/flox}$).
2. Investigating the immunomodulatory effects of macrophage-specific PKCδ deficiency during Mtb infection *in vivo.*
3. Investigating the immunomodulatory effects of macrophage-specific PKCδ deficiency during Mtb infection *in vitro.*

CHAPTER 2: Manuscript in preparation

LysM^{cre}PKCδ$^{flox/flox}$ mice are indistinguishable from PKCδ$^{flox/flox}$ littermate control at the naive state

Rudranil Hazra[1,2], Shelby-Sara Jones[1,3], Mumin Ozturk[3,4], Sibongiseni K.L. Poswayo[3], Saiyukthi Naidoo[3], Robert Rousseau[3], Nashied Peton[5], C. Ronald Kahn[6], Frank Brombacher[1,3], Robert J. Wilkinson[1,7], Suraj P. Parihar[1,2,3*]

[1] Wellcome Centre for Infectious Diseases Research in Africa (CIDRI-Africa), Institute of Infectious Diseases and Molecular Medicine (IDM), Faculty of Health Sciences, University of Cape Town, Cape Town 7925, South Africa.

[2] Division of Medical Microbiology, Institute of Infectious Diseases and Molecular Medicine (IDM), Department of Pathology, Faculty of Health Sciences, University of Cape Town, Cape Town 7925, South Africa.

[3] Division of Immunology, South African Medical Research Council (SAMRC) Immunology of Infectious Diseases, and International Centre for Genetic Engineering and Biotechnology (ICGEB), Cape Town Component, Institute of Infectious Diseases and Molecular Medicine (IDM), Department of Pathology, Faculty of Health Sciences, University of Cape Town, Cape Town 7925, South Africa.

[4] Epigenomics & Single Cell Biophysics Group, Department of Cell Biology FNWI, Radboud University, Nijmegen, Netherlands

[5] Drug Discovery and Development Centre (H3D), University of Cape Town, Cape Town 7925, South Africa.

[6] Section of Integrative Physiology and Metabolism, Joslin Diabetes Center, Harvard Medical School, Boston, MA, USA

[7] The Francis Crick Institute and Department of Infectious Diseases, Imperial College London, London, UK.

[*] Correspondence: A/Prof. Suraj P. Parihar, suraj.parihar@uct.ac.za

Keywords: LysM^{cre}PKCδ$^{flox/flox}$, naive state, characterization

2.1. Abstract

Protein Kinase C – δ (PKCδ) has previously been shown to play a vital role in a wide range of infectious diseases using global knockout ($PKC\delta^{-/-}$) mice models. The protective role of PKCδ has been demonstrated using the global knockout ($PKC\delta^{-/-}$) mouse model during *Mycobacterium tuberculosis* (Mtb) infection. However, macrophages are the first line of host defense against Mtb infection, hence, we developed a myeloid-specific knockout mouse model ($LysM^{cre}PKC\delta^{flox/flox}$) on C57BL/6 background using a Cre/loxP recombination system to investigate the role of PKCδ in macrophages during Mtb infection. To ensure accurate interpretation of macrophage-specific studies related to PKCδ and ruling out any possible immunological anomalies at a naive state, we have characterized this strain by investigating lymphoid and myeloid cells recruitment via flow cytometry and cytokines/chemokines level by ELISA. Our data reveal no noticeable differences in the immune cell population except impaired lung B lymphocytes in $LysM^{cre}PKC\delta^{flox/flox}$ mice model as compared to the littermate control ($PKC\delta^{flox/flox}$). Furthermore, the cytokine/chemokine profile in lung homogenates of $LysM^{cre}PKC\delta^{flox/flox}$ mice was invariable from littermate control ($PKC\delta^{flox/flox}$) mice. Overall, the $LysM^{cre}PKC\delta^{flox/flox}$ mice model provides a valuable platform for further PKCδ functional studies during Mtb infection and is established as an immunologically comparable and indistinguishable strain to its littermate control ($PKC\delta^{flox/flox}$).

2.2. Introduction

Protein kinase C - δ (PKCδ) is a phospholipid-dependent serine/threonine kinase first described in 1977 by Nishizuka and colleagues, and it plays a critical role in intracellular signal transduction[90, 113, 114]. As a result of its ability to phosphorylate a variety of target proteins necessary for cellular functions such as signal transduction[115], apoptosis[101], proliferation and survival[96], transcription[116], hormonal regulation[117], and immunological responses[86-88] - PKCδ is considered as a key hub for immunoregulatory functions among other Protein Kinase C (PKC) isoforms. The development of the PKCδ null mouse ($PKC\delta^{-/-}$) model on a 129/SV background was first generated by replacing the first two exons of the PKCδ gene with PGK-neo-poly(A) cassette in mouse embryonic stem cells which exhibited B-cell accumulation[118] and systemic autoimmunity[119]. The absence of the PKCδ gene in mice results in the infiltration of B cells, leading to severe humoral autoimmunity, characterized by immune complex regulated glomerulonephritis, lymphadenopathy, and splenomegaly[119]. Similar physiological abnormalities and clinical manifestations are also

evident in PKCδ deficient individuals in a study published by Anna-Lena et.al.[120]. PKCδ$^{-/-}$ mice also revealed increased T cell activation in reduced ERK signaling pathway with compromised methylation-sensitive genes[121]. Negative interference of PKCδ on autocrine IL-6 driven B cell proliferation is also well defined in the PKCδ null mouse (PKCδ$^{-/-}$) model[119]. Additionally, PKCδ$^{-/-}$ mice that were generated by deleting only the second exon had increased lesions in vein grafts compared to wild-type controls[122]. In a recent study, authors also evidenced that the deletion of all shared exons of PKCδ causes abnormal effects on fetal development along with pulmonary and cardiac dysfunction[123].

PKCδ is ubiquitously expressed in lymphocytes and most mammalian tissue and cell types, including myeloid populations such as DC and Macrophages[124, 125]. However, the characterization of the PKCδ$^{-/-}$ mouse was limited to progenitor development in which only B cells functionality was emphasized along with the recruitment of T lymphocytes and bone marrow cells in the spleen, lymph nodes, and thymus[119]. Although the development of PKCδ knockout mice on 129/SV background was normal and fertile with no apparent issues[119, 122], there are very few studies have been conducted using conditional knockout of PKCδ[126]. Previous studies using the PKCδ deficient mouse model (PKCδ$^{-/-}$) indicated an immune evasion mechanism[86, 87] and protective role[88] against different infectious diseases. Given the role of PKCδ specific to optimal macrophage killing effector functions against bacterial diseases, we aimed to generate a macrophage-specific PKCδ knockout model (LysM^{cre}PKCδ$^{flox/flox}$) by crossing lysozyme M – Cre (LysM^{cre}) mice with loxP flanked PKCδ mice[127, 128]. LysM^{cre} mice enable both specific and efficient Cre-mediated deletion of lox-P flanked target genes in myelomonocytic cells including granulocytes, monocytes, and macrophages[129]. In this study, we have demonstrated the impact of macrophage-specific PKCδ conditional knockout on various immune cell populations across organs, lung cytokine profile, and chemokine levels compared to murine PKCδ comprehensive immune system for establishing an immunologically comparable mice model to better understand the macrophage-specific role of PKCδ.

2.3. Methods

2.3.1. Mouse Strains

To generate the macrophage-specific PKCδ knockout mice model we have crossed loxP flanked PKCδ mice of C57BL/6 strain [127, 128] with in-house LysM^{cre} mice of C57BL/6 strain for three generations to achieve homozygous knockout model LysM^{cre}PKCδ$^{flox/flox}$. LoxP flanked PKCδ (PKCδ$^{flox/flox}$) mice were gifted from Prof. C Ronald Kahn at the Joslin Diabetes Center and considered as a littermate control for all downstream experiments[127]. All mice were generated and maintained under specified pathogen-free conditions by the Animal Research Facility under strict guidelines of approved protocols by the University of Cape Town Research Ethics Committee and South African Veterinary Council (SAVC). Experimental mice were matched for age (8-12 weeks) and sex. All procedures were conducted in the Research Animal Facility (RAF) Biosafety Level 2 (BSL2).

2.3.2. Mouse genotyping

Genomic DNA was extracted from both PKCδ$^{flox/flox}$ and LysM^{cre}PKCδ$^{flox/flox}$ mice tails to confirm the genotype[130, 131]. Multiplex PCR on T100™ Thermal Cycler (Bio-Rad) was performed to amplify the transcripts using the following primers: PKCδ: Forward sequence: 5'- CTG GGT AAC TTA ACA AGA CC-3'; Reverse sequence: 5'- CTG CTA AAT AAC ATG TTC GGT CC-3'; LysM^{cre}: Forward sequence: 5'-CCC AGA AAT GCC AGA TTA CG-3', Reverse sequence: 5'-CTT GGG CTG CCA GAA TTT CTC-3'. Optimal PCR conditions include an initial denaturation (94°C for 3 min), denaturation (35 cycles; 94°C for 30 sec), annealing (60°C for 30 sec), extension (72°C for 30 sec) and final extension (72°C for 5 min) were conducted. The PCR product was separated on 1.6% Agarose gel (SYBR Safe DNA gel stain, Thermofisher) and visualized under UV light on Syngene G: Box and analyzed on GeneSnap (Syngene, Cambridge). Expected PCR amplicon sizes: Wildtype(n/n): 350bp; floxed PKCδ (fl/fl): 425bp; LysM^{cre}PKCδ$^{flox/flox}$ (LysM^{cre+}): 700bp.

2.3.3. Ethical consideration

All experimental animals were operated following the Animal Research Facility approved protocols (Permit No: 019/023 and 019/031) and regulations under the South African

National Standard (SANS 10386:2008) at the Faculty of Health Sciences, University of Cape Town.

2.3.4. Generation of Bone-marrow derived macrophages

As previously described, bone-marrow-derived macrophages (BMDM) were generated from 8-12 weeks old PKC$\delta^{flox/flox}$ and LysMcrePKC$\delta^{flox/flox}$ mice [132]. Briefly, bone marrow cells were flushed out from femurs and cultured for 10 days at 37°C under 5% CO_2 in sterile tissue culture grade Petri dishes (140mm x 20mm Petri dish, Nunc, Denmark) consisting of PLUTZNIK media (DMEM containing 30% L929 cell-conditioned medium, 10% fetal calf serum, 5% horse serum, 1 mM sodium pyruvate, 2 mM L-glutamine, 0.1 mM β-mercaptoethanol, 100 U/ml penicillin G, and 100 µg/ml streptomycin). BMDMs were harvested and plated in desired culture plates in complete media (DMEM containing 10% fetal calf serum) to proceed with the downstream experimental procedure.

2.3.5. Quantitative real-time polymerase chain reaction (qRT-PCR)

RNA was extracted using the RNeasy Mini Kit (Qiagen, cat# 74106) from stored RNA samples in 350 µl of RLT lysis buffer with 3.5 µl β-mercaptoethanol. 400ng normalized RNA was reverse transcribed using a High-Capacity cDNA Reverse Transcription Kit (Applied Biosystems, cat# 4368814) with random primers to yield first-strand cDNA following the manufacturer's protocol. Desired gene expressions were amplified using Fast SYBR™ Green Master Mix (Applied Biosystems, cat# 4385612) and analyzed using Quantstudio 7 (Applied Biosystems, USA). The qRT-PCR conditions were as follows: Stage 1 (x1 cycle): Pre-incubation 95°C for 10 min; Stage 2 (x45 cycle): Denaturation 95°C for 15 sec, Annealing 60°C for 10 sec, Extension 72°C for 15 sec, Final acquisition 80°C for 1 sec. Desired gene expressions were normalized using an endogenous housekeeping control Hprt. Primer sequences are listed in *Appendix A* with their respective gene accession number.

2.3.6. Western blot analysis

As previously described, sodium dodecyl sulfate-polyacrylamide gel electrophoresis (SDS-PAGE) and Western Blot analysis were performed [67]. Briefly, bone-marrow-derived

macrophages from both PKCδ$^{flox/flox}$ and LysM^{cre}PKCδ$^{flox/flox}$ (3 x 10^6) were seeded in a 6-well tissue culture graded plate containing complete media (DMEM containing 10% fetal calf serum) for overnight at 37°C under 5% CO_2 incubator. Cells were washed and lysed with ice-cold RIPA buffer containing protease and phosphatase inhibitors for 30 min at 4°C. BCA Protein Assay Kit (Thermofisher Scientific Pierce™, cat# 23225) was used to determine the total protein concentration. An equal amount (20 µg) of protein were boiled at 100°C for 5 min with 1X loading dye (2% SDS, 5% 2-mercaptoethanol, 10% glycerol, 0.002% bromophenol blue, 0.62 M Tris-HCl, pH 6.8). Samples were then electrophoresed on 12% SDS-PAGE gel (Mini-PROTEAN® system, Bio-Rad) and transferred to nitrocellulose membrane (Sigma) using the Mini Trans-Blot® Cell system (Bio-Rad). The membrane blocking was done for 2 hours on a shaker at room temperature with 5% w/v BSA, 1X TBS (20 mM Tris with 150 mM NaCl), and 0.1% Tween20 (blocking buffer). Next, the membrane was probed with recombinant anti-PKC delta antibody (Abcam; ab182126) or GAPDH [Santa Cruz Biotechnology; (sc47724)] primary antibodies (in 5% BSA blocking buffer; 1:1000 dilution) according to the manufacturer's protocol at 4°C overnight and goat anti-rabbit IgG H&L (Abcam; ab97040) secondary antibody (in 5% BSA blocking buffer; 1:10000 dilution) at room temperature for one hour. Immunoblots were developed using the KPL LumiGLO® Reserve Chemiluminescent Substrate Kit (SeraCare Life Sciences; cat# 5430-0042(54-61-02)) on the iBright FL1000 Imaging System (Thermofisher Scientific).

2.3.7. Lung and Spleen immune cell populations

Left lobes of the lung were collected and digested in lung digestion buffer (DNase1, Collagenase type 1, DMEM) at 37°C for one hour to prepare a single-cell suspension. Digested lungs were passed through 100 µm and 70 µm sterile cell strainers (SPL Life Sciences) whereas spleens were mechanically digested through 70 µm and 40 µm sterile cell strainers (SPL Life Sciences). Cells were washed with complete media (DMEM + 10%FCS) following red cell lysis buffer (150 mM NaCl, 10 mM KHCO3 and 0.1mM Na2EDTA) incubation for 5 min at room temperature. Then, cells were washed again with complete media before being counted with CytoSMART (Corning) automated cell counter and seeded approximately 1 x 10^6 cells per well in a 96-well U-bottom (Corning) plate. Seeded cells were washed once with PBS and stained with dead cell marker (575V Viability Dye, BD Biosciences) for 15 min at room temperature. After that cells were washed with FACS buffer (0.5% BSA, 0.5% Sodium azide

(NaN3), 1x PBS) and surface stained for the following lymphoid and myeloid-specific markers: Lymphoid markers (Lung/Spleen) - Gamma delta (γδ) T cells: CD3+gdTCR+; Natural Killer (NK) cells: NK1.1+CD3-; B cells: CD19+CD3-; T cells: CD3+CD19-; CD4 T cells: CD3+CD4+; CD8 T cells: CD3+CD8+; Myeloid markers (Lung) - Neutrophils: Ly6G+CD11b+; Eosinophils: SiglecF+CD11b+CD64-; Dendritic cells (DC): CD11b+CD11c+MHCII+; Monocytes: Ly6G+CD11b+CD64-; Alveolar macrophages: CD64+MerTK+SiglecF+CD11c+; Interstitial macrophages: CD64+MerTK+SiglecF+CD11b+CD11c; Myeloid markers (Spleen) - Neutrophils: Ly6G+CD11b+; Monocytes: CD11b+Ly6C+CD11c-; Marginal zone macrophages: CD11bhighF4/80lowCD11c- ; Red pulp macrophages: F4/80highCD11blowCD11c-; CD11b+ DC = CD11c+MHCII+CD11b+. Surface-stained cells were acquired using BD LSR Fortessa (BD Biosciences Immunohistochemistry Systems) and data was analyzed by FlowJo v10.6.1 software (TreeStar, US). All stained cells positive for specific markers are calculated as a percentage of live cells.

2.3.8. Cytokine, chemokine, and growth factors profiling in lung homogenates

Lung homogenates were spun at 3000 g for 5 min to procure cell-free supernatant analyzed using standard sandwich ELISA assay. Coating, standard, and detection antibodies were obtained from BD Biosciences, Biolegend, and R&D Scientific. The assay was performed to detect different cytokines (TH1: IL-2, IL-6, IL-12p40, IL-12p60, IFN-γ, IFN-β, IL-1α, IL-1β; TH2: IL-4, IL-5, IL-10, IL-13, TGF-β; TH17: IL-17, IL-23), chemokines (CCL3, CCL5, CXCL10, CXCL1, CXCL2, CXCL5) and growth factors (IGF-1, GM-CSF) levels according to manufacturer's dilutions and protocol. TMB microwell peroxidase substrate (KPL International) for streptavidin-HRP conjugates or 1 mg/ml p-nitrophenyl phosphate disodium salt hexahydrate (Sigma, cat# N2765) for streptavidin-AP conjugates. VersaMax™ microplate spectrophotometer (Molecular Devices, Sunnyvale, California) was used to measure optical density.

2.3.9. Statistical analysis

All data represented were mean values and analyzed using GraphPad Prism v9.0. Statistical analyses were performed using unpaired student t-test. Asterisks are defining

significance compared to the control group as: *p < 0.05, **p < 0.01, ***p < 0.001, ****p < 0.0001.

2.4. Results

2.4.1. LysM^{cre}-loxP mediated deletion of PKCδ is specific to macrophages while maintaining the expression in other immune cell populations

To generate a myeloid-specific knockout mice model, we have followed the conventional LysM^{cre}-loxP genetic manipulation technique in mice described with a schematic (**Figure 1A**) collected from Jiayuan Shi and co-authors[133]. Next, we confirmed the integrity of loxP-floxed (fl/fl) PKCδ in the genomic DNA extracted from the tail cuts of PKCδ$^{flox/flox}$ mice compared to wildtype(n/n) mice (**Figure 1B**) before crossing with LysM^{cre} mice. The presence of Cre recombinase transgene (LysM^{cre}) was also confirmed in LysM^{cre}PKCδ$^{flox/flox}$ mice compared to PKCδ$^{flox/flox}$ mice shown as linear DNA bands on the agarose gel represented as LysM^{cre+} and LysM^{cre-} respectively (**Figure 1B**). To determine the specificity and efficiency of LysM^{cre}-loxP mediated cell-specific conditional knockout, we have sorted different immune cell populations by flow cytometry to confirm the deletion of PKCδ specifically in macrophages while the expression of PKCδ maintained in other cell types such as Neutrophils, Dendritic cells, and T cells by qRT-PCR (**Figure 1C**). These results collectively confirm the fidelity of the LysM^{cre}-loxP technique to knockout a gene of interest in plastic and extremely diverse myeloid cell type – macrophages in mice.

Figure 1.

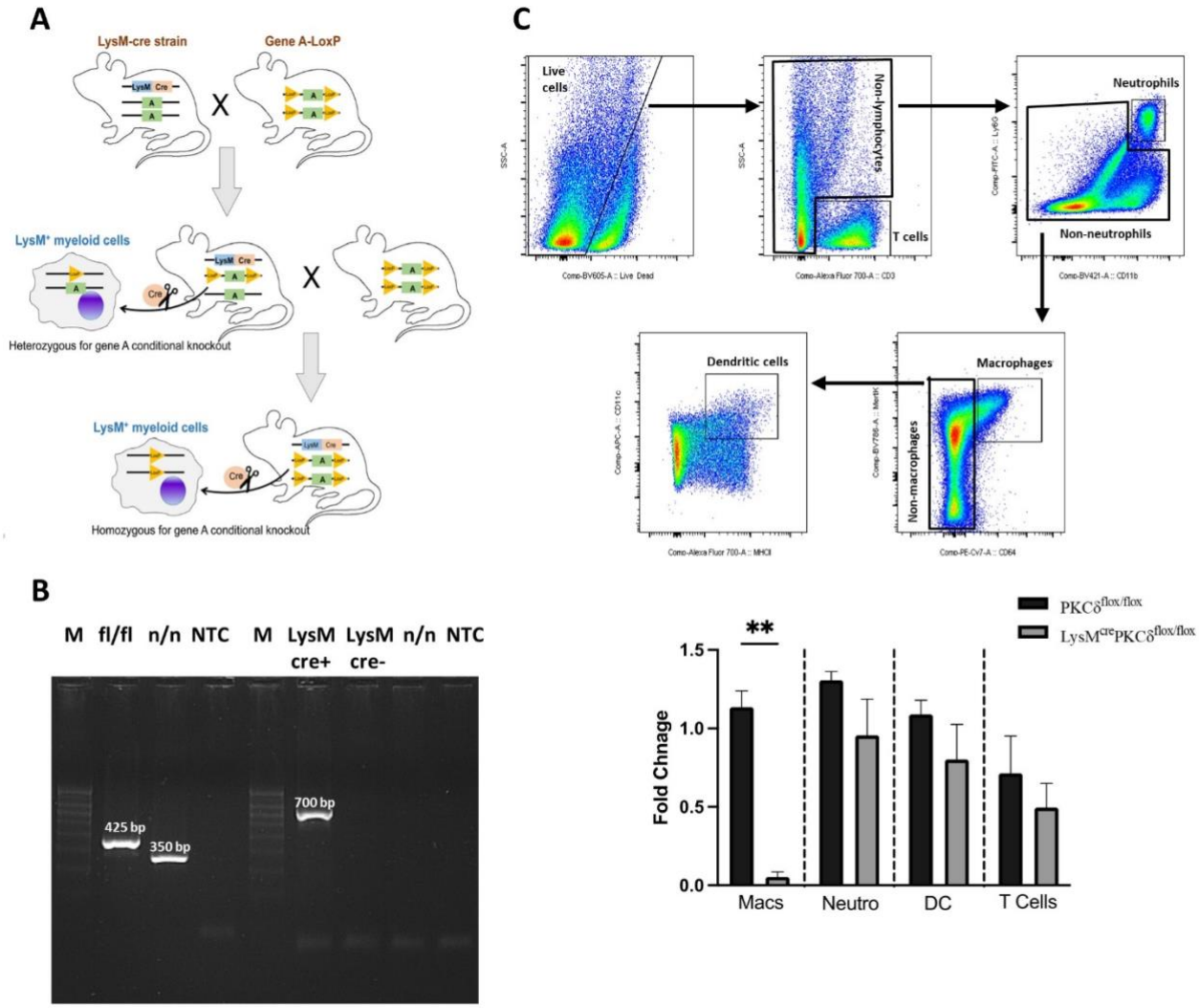

Figure 1. LysM^{cre}-loxP mediated deletion of PKCδ is specific to macrophages while maintaining the expression in other immune cell populations. [A] Schematic representation of LysM^{cre}-loxP mediated conditional knockout technology. (Figure is sourced from Jiayuan Shi and co-authors) [B] Integrity of loxP-floxed PKCδ and presence of LysM^{cre} was confirmed in the genomic DNA extracted from the tail cuts of PKCδ$^{flox/flox}$ and LysM^{cre}PKCδ$^{flox/flox}$ mice. Representative agarose gel demonstrates the marker (m), wild-type (n/n), floxed PKCδ (fl/fl), LysM^{cre}PKCδ$^{flox/flox}$ (LysMcre+), PKCδ$^{flox/flox}$ (LysMcre-), non-template control (NTC). [C] Gating strategy for lung sorted immune cells and confirmation of PKCδ deletion in macrophages by qRT-PCR. Surface markers determining different immune cell populations are as following: T cells SSC-A-CD3+; Neutrophils: CD3-Ly6G+CD11b+; Macrophages: CD3-Ly6G-CD11b-MertK+CD64+; Dendritic cells: CD3-Ly6G-CD11b-MertK-CD64-CD11c+MHCII+. Sorted immune cells were subjected to lysed for RNA collection. PKCδ expression was determined in these immune cell populations by qRT-PCR. Expression levels are normalized to the endogenous housekeeping gene Hprt. Statistical analysis was performed using an unpaired student t-test. Asterisks are defining significance compared to the control group as ***$p < 0.001$.

2.4.2. Confirmed deletion of PKCδ in bone-marrow-derived macrophages has no impact on the expression of other protein kinase C isoforms

The paradigm of macrophage ontogeny from bone-marrow origin including tissue-resident and inflammatory macrophages is well established[134]. As a major contributor to the proliferative and differentiative niche in the macrophage population, bone-marrow-derived macrophages were the primary *in vitro* myeloid target for our study to understand the functional characteristics of PKCδ. Hence, we have assessed the expression of PKCδ in bone-marrow-derived macrophages to confirm the deletion both in mRNA and protein levels. We have found that the PKCδ mRNA transcript was undetectable in bone-marrow-derived macrophages isolated from $LysM^{cre}PKC\delta^{flox/flox}$ mice (**Figure 2A**). Also, reduced protein expression of PKCδ was quantified in bone-marrow-derived macrophages by western blot analysis (**Figure 2B**) which indicates that deleted mRNA transcript has directly reduced the translation of the protein. Additionally, to establish a PKCδ inclusive myeloid knockout setting, we have also determined the effect of PKCδ deletion on different PKC family subsets (cPKC, nPKC, and aPKC) in bone-marrow-derived macrophages through mRNA expression by qRT-PCR (**Figure 2C**)**.** Neither of the PKC isoforms showed significant differences in the mRNA expression in bone-marrow-derived macrophages isolated from $LysM^{cre}PKC\delta^{flox/flox}$ mice compared to $PKC\delta^{flox/flox}$ mice. Collectively, these results suggest the efficiency and specificity of Cre-mediated deletion of PKCδ in bone-marrow-derived macrophages which does not interfere with the configuration of various PKC family subsets at mRNA level at a naive state.

Figure 2.

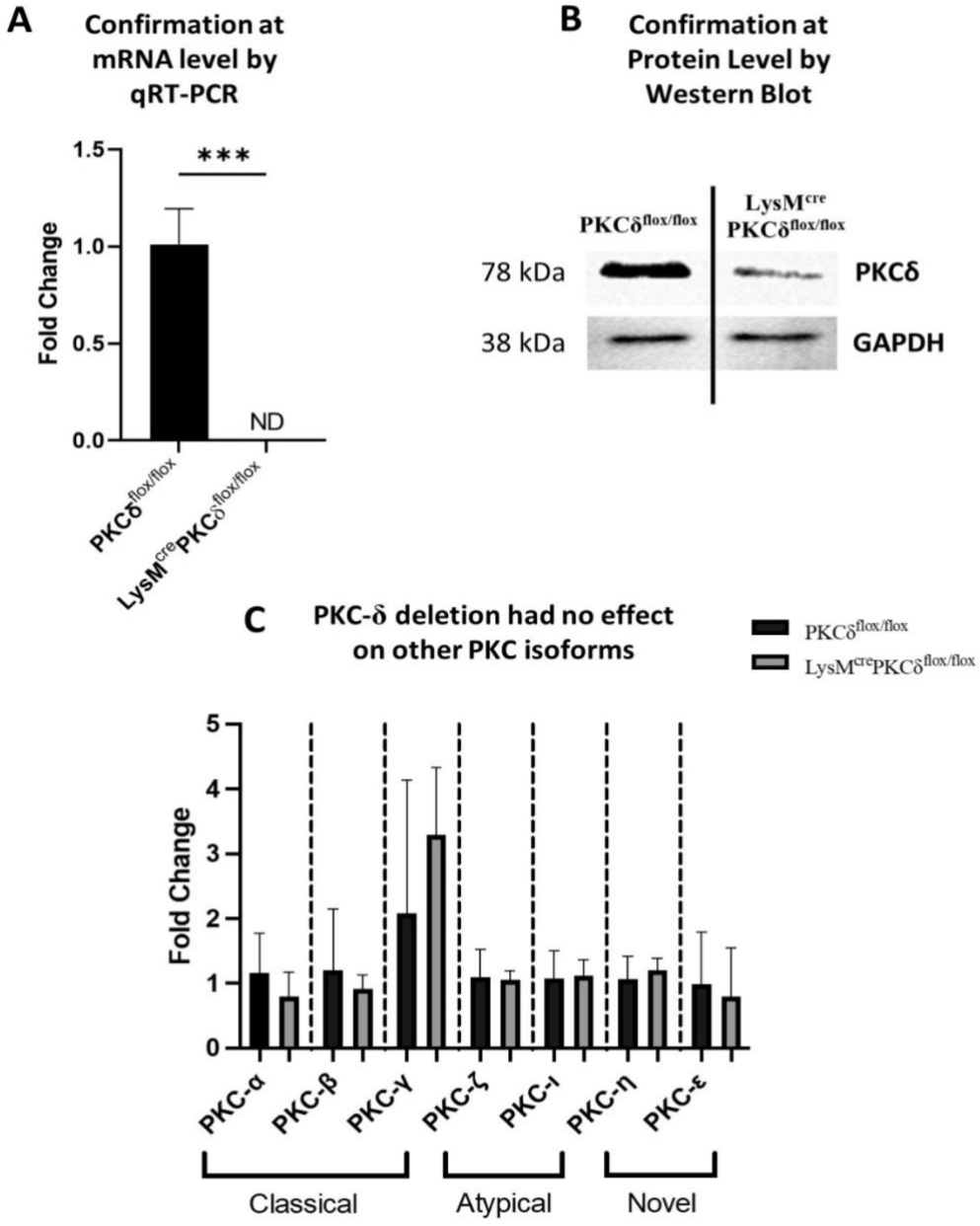

Figure 2. Confirmed deletion of PKCδ in bone-marrow-derived macrophages has no impact on the expression of other protein kinase C isoforms. Bone-marrow-derived macrophages were isolated from $PKC\delta^{flox/flox}$ and $LysM^{cre}PKC\delta^{flox/flox}$ mice following RNA and protein were collected to determine desired gene expressions. [A-B] Deletion of PKCδ in bone-marrow derived macrophages was confirmed by qRT-PCR and western blot analysis. HPRT and GAPDH were used as a normalizing control in qRT-PCR and Western blot respectively. [C] Protein kinase C isoform-specific primers were used for gene expression analysis in PKCδ deficient bone-marrow derived macrophages ($LysM^{cre}PKC\delta^{flox/flox}$) as compared to the control ($PKC\delta^{flox/flox}$) by qRT-PCR. Data represented as the mean of four replicates and representative of two independent experiments. Statistical analysis was performed using an unpaired student t-test. Asterisks are defining significance compared to the control group as ***$p < 0.001$.

2.4.3. Indistinguishable lung physiology, immune cell population with reduced B cell percentage in LysM^{cre}PKCδ$^{flox/flox}$ mice at a naive state

Previously, Miyamoto et. al. developed a PKCδ null mice model that illustrated a strong B-cell hyperproliferative phenotype across different organs with no reported abnormal physiological development of the lungs[119]. To identify any alarming variables in the lung physiology of LysM^{cre}PKCδ$^{flox/flox}$ mice, we have processed single-cell suspension upon collection of the lungs from both LysM^{cre}PKCδ$^{flox/flox}$ and PKCδ$^{flox/flox}$ mice. Total lung cell numbers present in the suspension were counted by an automated cell counter. Neither cell numbers nor the weight of the lungs was different in LysM^{cre}PKCδ$^{flox/flox}$ mice compared to PKCδ$^{flox/flox}$ mice (**Figure 3A-B**). Next, the single-cell suspension was subjected to surface staining for various lymphoid and myeloid immune cell phenotyping. Interestingly, LysM^{cre}PKCδ$^{flox/flox}$ mice showed reduced B-cell percentage among other lymphocytes such as **γ**d T cells, NK cells, and T cells (**Figure 3C, Supplementary Figure 1A**). Also, the T-cell subpopulations CD4+ and CD8+ cell percentages remained unchanged (**Figure 3D, Supplementary Figure 1B**). This diminution in B-cell percentage was suggestive of a strong correlation of PKCδ in B-cell recruitment. Then, we assessed major myeloid cell populations including Neutrophils, Eosinophils, Dendritic cells, and Monocytes (**Figure 3E, Supplementary Figure 1C**), and no strong irregularities were noticed. The percentage of two distinct populations of macrophage subsets – alveolar and interstitial macrophages were identical in LysM^{cre}PKCδ$^{flox/flox}$ mice compared to PKCδ$^{flox/flox}$ mice (**Figure 3F, Supplementary Figure 1D**). Despite having reduced B-cell percentage, these results demonstrate indistinguishable physiologic and phenotypic profiles of the lung of LysM^{cre}PKCδ$^{flox/flox}$ mice, providing a favorable environment for macrophage-specific investigation in the field of respiratory diseases related to PKCδ.

Figure 3.

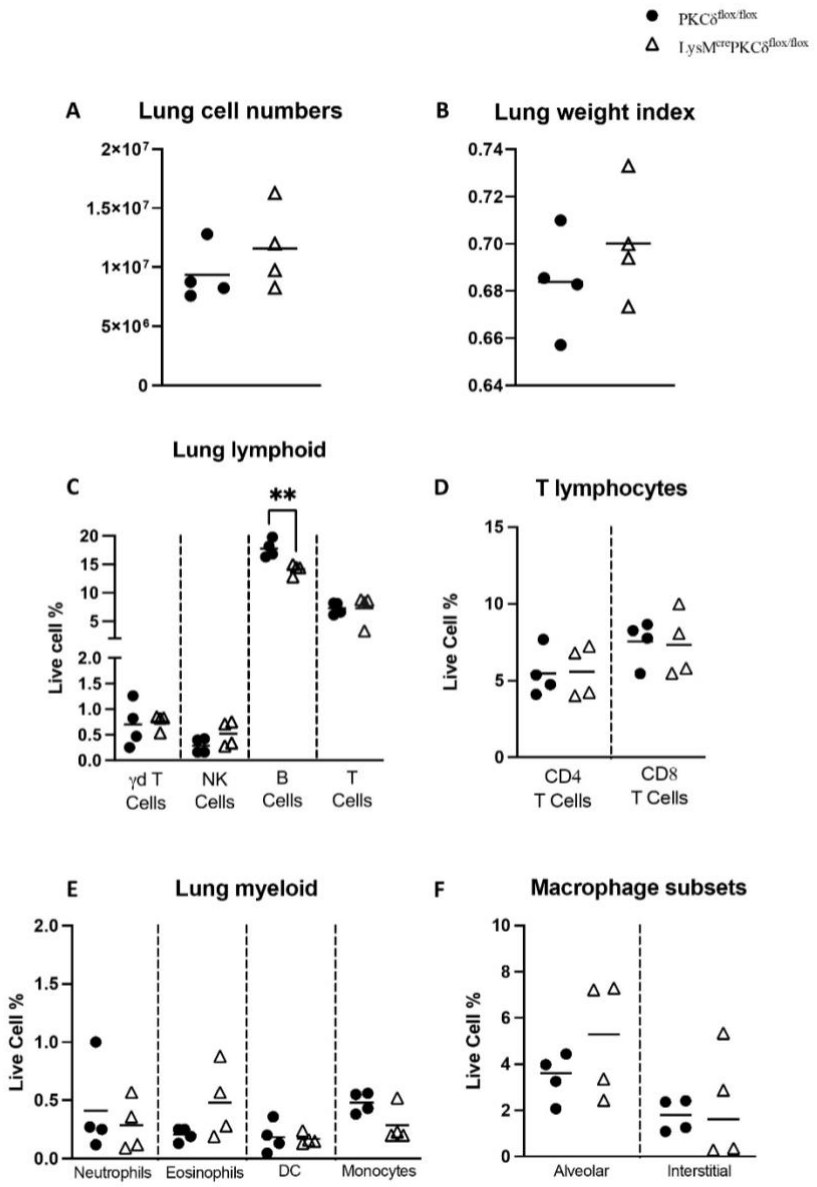

Figure 3. Indistinguishable lung physiology, immune cell population with reduced B cell percentage in LysM^{cre}PKCδ$^{flox/flox}$ mice at a naive state. Lungs were collected, weighed, and processed for single-cell suspension from both PKCδ$^{flox/flox}$ and LysM^{cre}PKCδ$^{flox/flox}$ mice (n=4 mice/group) following surface stained and acquired for different immune cell populations using flow cytometric analysis. Lung [A] cell numbers and [B] weight index were determined in both PKCδ$^{flox/flox}$ and LysM^{cre}PKCδ$^{flox/flox}$ mice. Various [C-D] lymphoid and [E-F] myeloid immune cell populations were detected in the single-cell suspension, processed and surface stained from both PKCδflox/flox and LysM^{cre}PKCδ$^{flox/flox}$ mice. Surface markers determining different immune cell populations are as following: Lymphoid markers - Gamma delta (γδ) T cells: CD3+gdTCR+; Natural Killer (NK) cells: NK1.1+CD3-; B cells: CD19+CD3-; T cells: CD3+CD19-; CD4 T cells: CD3+CD4+; CD8 T cells: CD3+CD8+; Myeloid markers - Neutrophils: Ly6G+CD11b+; Eosinophils: SiglecF+CD11b+CD64-; Dendritic cells (DC): CD11b+CD11c+MHCII+; Monocytes: Ly6G+CD11b+CD64-; Alveolar macrophages: CD64+MerTK+SiglecF+CD11c+; Interstitial macrophages: CD64+MerTK+SiglecF+CD11b+CD11c. All data shown are representative of two independent experiments. Statistical analyses were performed using an unpaired student t-test. Asterisks are defining significance compared to the control group as ***$p < 0.001$.

2.4.4. LysM^{cre}PKCδ$^{flox/flox}$ mice showed similar spleen physiology and immune cell population compared to PKCδ$^{flox/flox}$ mice at a naive state

As a regulator of immune homeostasis, the spleen is a crucial secondary lymphoid organ mounting both innate and adaptive responses[135]. Enlargement of splenic anatomy has been indicated in PKCδ null mice by Miyamoto and colleagues[119]. We have found no anomalies in splenic physiology in LysM^{cre}PKCδ$^{flox/flox}$ mice compared to PKCδ$^{flox/flox}$ mice, represented as total cell numbers and spleen weight index (**Figure 4A-B**). Moreover, immune cell phenotyping of spleen from LysM^{cre}PKCδ$^{flox/flox}$ mice revealed no significant differences in major lymphocytes including γδ T cells, NK cells, B cells, and T cells (**Figure 4C, Supplementary Figure 1E**) compared to PKCδ$^{flox/flox}$ mice. CD4+ and CD8+ T cell percentages were identical in both groups (**Figure 4D, Supplementary Figure 1F**). We have not observed any differences in myeloid cell percentages including Neutrophils, Monocytes, Marginal-zone macrophages, Red-pulp macrophages, and Dendritic cells (**Figure 4E, Supplementary Figure 1G**) in LysM^{cre}PKCδ$^{flox/flox}$ mice compared to PKCδ$^{flox/flox}$ mice. Similar to lungs, these results also explicate that LysM^{cre}PKCδ$^{flox/flox}$ mice showed no physiological differences and immune cell aberration in the spleen compared to PKCδ$^{flox/flox}$ mice.

Figure 4.

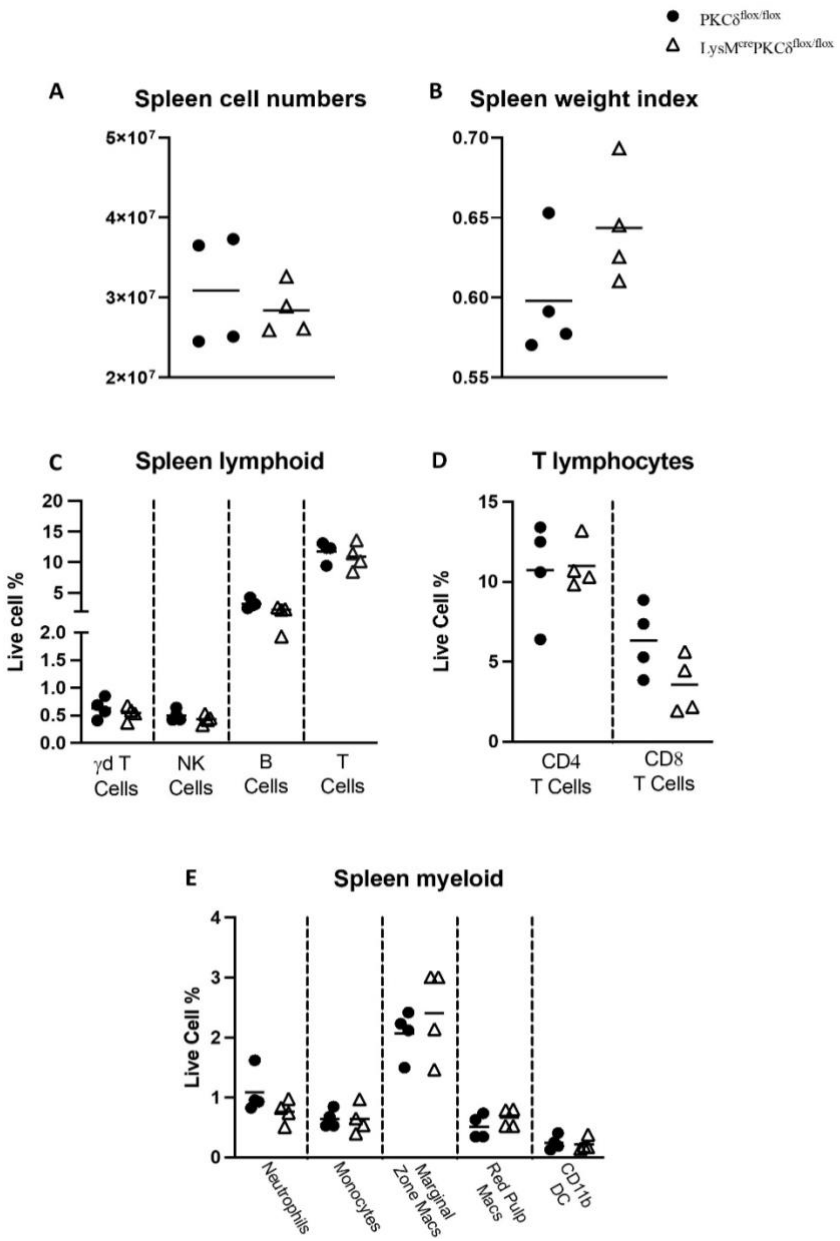

Figure 4. LysM^{cre}PKCδ$^{flox/flox}$ mice showed similar spleen physiology and immune cell population compared to PKCδ$^{flox/flox}$ mice at a naive state. Spleens were collected, weighed, and processed for single-cell suspension from both PKCδ$^{flox/flox}$ and LysM^{cre}PKCδ$^{flox/flox}$ mice (n=4 mice/group) following surface stained and acquired for different immune cell populations using flow cytometric analysis. Spleen [A] cell numbers and [B] weight index were determined in both PKCδ$^{flox/flox}$ and LysM^{cre}PKCδ$^{flox/flox}$ mice. Various [C-D] lymphoid and [E] myeloid immune cell populations were detected in the single-cell suspension, processed and surface stained from both PKCδ$^{flox/flox}$ and LysM^{cre}PKCδ$^{flox/flox}$ mice. Surface markers determining different immune cell populations are as following: Lymphoid markers - Gamma delta (γδ) T cells: CD3+gdTCR+; Natural Killer (NK) cells: NK1.1+CD3-; B cells: CD19+CD3-; T cells: CD3+CD19-; CD4 T cells: CD3+CD4+; CD8 T cells: CD3+CD8+; Myeloid markers - Neutrophils: Ly6G+CD11b+; Monocytes: CD11b+Ly6C+CD11c-; Marginal zone macrophages: CD11bhighF4/80lowCD11c-; Red pulp macrophages: F4/80highCD11blowCD11c-; CD11b+ DC = CD11c+MHCII+CD11b+. All data shown are representative of two independent experiments. Statistical analyses were performed using an unpaired student t-test.

2.4.5. Invariable growth factors, cytokine, and chemokine profile in LysM^{cre}PKCδ$^{flox/flox}$ mice compared to PKCδ$^{flox/flox}$ mice at a naive state

Negative regulation of NF-κB mediated IL-6 production has been stated precisely as a causative molecular mechanism of B cell functions in PKCδ null mice[119]. To assess the consequences of macrophage-specific deletion of PKCδ in the cytokines, chemokines, and growth factor profile, we have determined the protein levels by ELISA assay in collected lung homogenates from both PKCδ$^{flox/flox}$ and LysM^{cre}PKCδ$^{flox/flox}$ mice. As shown (**Figure 5, Supplementary Figure 2**), Cre-mediated deletion of PKCδ did not promote any changes in the basal cytokine levels (**Figure 5A-C**), chemokine levels (**Figure 5D**), and growth factors (**Figure 5E**), indicating no immunological distress in LysM^{cre}PKCδ$^{flox/flox}$ mice compared to PKCδ$^{flox/flox}$ mice.

Figure 5.

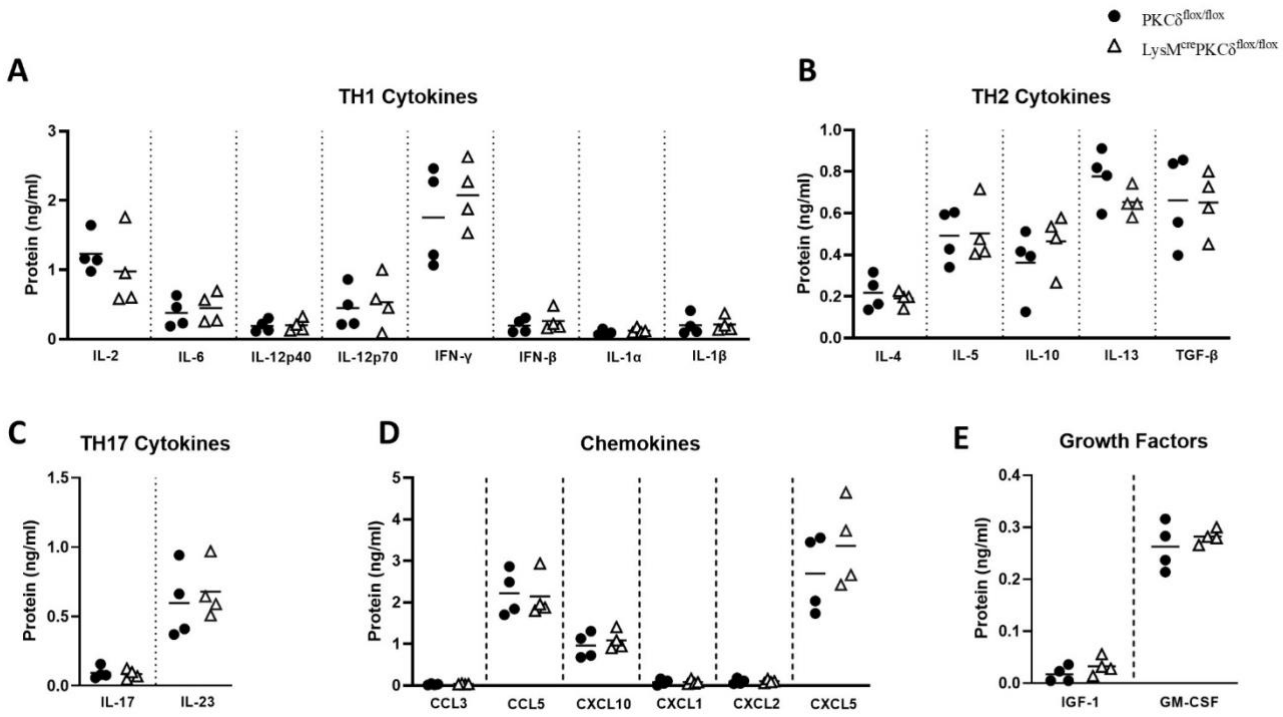

Figure 5. Invariable growth factors, cytokine, and chemokine profile in LysM^{cre}PKCδ$^{flox/flox}$ mice compared to PKCδ$^{flox/flox}$ mice at a naïve state. Lung homogenates were collected from both PKCδ$^{flox/flox}$ and LysM^{cre}PKCδ$^{flox/flox}$ mice (n=4 mice/group) to determine an array of different cytokines [A] TH1: IL-2, IL-6, IL-12p40, IL-12p60, IFN-γ, IFN-β, IL-1α, IL-1β; [B] TH2: IL-4, IL-5, IL-10, IL-13, TGF-β; [C] TH17: IL-17, IL-23) [D] chemokines (CCL3, CCL5, CXCL10, CXCL1, CXCL2, CXCL5) and [E] growth factors (IGF-1, GM-CSF) levels. All data shown are representative of two independent experiments. Statistical analyses were performed using an unpaired student t-test.

2.5. Discussion

Based on findings in PKCδ null mice ($PKC\delta^{-/-}$) and clinically manifested PKCδ deficient individuals in biological and functional studies in different disease settings, it is evident that the role of PKCδ deficiency is a crucial for maintaining immune homeostasis against microbial intruders and various autoimmune disorders[86-88, 120]. Besides, hyperproliferation of B lymphocytes along with anomalous physical properties is also associated with PKCδ deficiency[119, 120, 123]. Although, PKCδ global knockout ($PKC\delta^{-/-}$) mice characterization has revealed strong influences on lymphocytes at naive state[119, 121], very limited studies have been conducted for myeloid-specific deficiency of PKCδ and its immunomodulatory characteristics. As the *in vivo* tissue environment is governed by the development, activation, recruitment, and function of macrophages both in naive and disease states, we have developed a macrophage-specific knockout mice model ($LysM^{cre}PKC\delta^{flox/flox}$) and characterized according to the previous abnormalities found in PKCδ null mice ($PKC\delta^{-/-}$).

$LysM^{cre}$-loxP generated knockout alleles in mice are achieved by crossing the homozygous loxP-floxed strain of interest ($PKC\delta^{flox/flox}$) with $LysM^{cre}$ mice containing macrophages expressing Cre recombinase transgene. Therefore, the excised gene of interest (PKCδ) by Cre recombinase activity will be leading to the generation of the macrophage-specific knockout model ($LysM^{cre}PKC\delta^{flox/flox}$). This method of genetic manipulation is beneficial for understanding the role of a specific gene of interest in given cell types in mice. Although, the existing gene expression overlapping between similar lineages across different cell types such as neutrophils, DC, and other granulocytes is a major concern for the generation of very specific macrophage knockout mice models[133]. Surprisingly, observed loxP-floxed PKCδ integrity, presence of Cre recombinase transgene, and reduced mRNA expression of PKCδ specific to macrophages and not in other myeloid cell populations confirmed the specificity and efficiency of the $LysM^{cre}$-loxP mediated genetic manipulation technique in our $LysM^{cre}PKC\delta^{flox/flox}$ mice model.

In a recent study by Calum et. al, the replenishment of alveolar and interstitial macrophages by bone-marrow-derived macrophages/monocytes from the neonatal period to the adult stage of mice is precisely defined[85]. Longitudinal analysis of $Ms4a3^{cre}$ reporter mice also described the importance of bone-marrow origin for developing a diverse population of granulocyte-monocytes and replenishing alveolar macrophages over time[136]. Thus, bone-marrow derived macrophages are crucial for the development of pulmonary immune

homeostasis during the life course of mice. Hence, we have confirmed the deletion of PKCδ at mRNA and protein levels in bone-marrow derived macrophages from LysM^{cre}PKCδ$^{flox/flox}$ mice for further macrophage-specific functional studies in absence of PKCδ during disease settings. Moreover, the broad spectrum of PKC subsets shares similar conformation and catalytic activation patterns[93], therefore, it is important to determine the effect of PKCδ deletion on other PKC isoforms. We have shown that the deletion of PKCδ has no impact on the expression of other classical, novel, and atypical PKC isoforms. Altogether, LysM^{cre}PKCδ$^{flox/flox}$ mice model provides us a strong macrophage inclusive PKCδ deficient environment which might be beneficial for understanding macrophage biology accompanied by adverse pulmonary inflammation and resolution.

Previously, hyperproliferation of B cells[119] in PKCδ null mice (PKCδ$^{-/-}$) and homozygous mutation of PRKCD in humans led to lymphocyte accumulation[137] is also established. Interestingly, our lung dynamics of the LysM^{cre}PKCδ$^{flox/flox}$ mice model revealed no physiological abnormalities but fewer B cell percentage despite not affecting any other lymphoid cell populations. This consistent regulative characteristic in both global and myeloid-specific PKCδ knockout strongly indicates a critical role for PKCδ in the wiring of B cell proliferation. It will be interesting to further investigate whether macrophages specific deletion triggers an intrinsic mechanism and is directly involved in reduced B cell turnover at a naive state. Moreover, the lung myeloid population including distinct macrophage subsets of LysM^{cre}PKCδ$^{flox/flox}$ mice was unaffected by the macrophage-specific deletion of PKCδ. Furthermore, our characterization did not reveal any abnormalities related to splenic physiology and immune cell populations in LysM^{cre}PKCδ$^{flox/flox}$ mice. Intriguingly, no differences were observed in cytokines, chemokines, and growth factors in the lung homogenates of LysM^{cre}PKCδ$^{flox/flox}$ mice which indicates a steady homeostatic immune environment for future studies related to pulmonary health, lung inflammation, and respiratory diseases.

2.6. Acknowledgements

We are extremely grateful to the UCT Research Animal Facility (RAF) and Mr. Rodney Lucas for providing us the facility to conduct animal research, Ms. Munadia Ansarie for her contribution to animal breeding, genotyping, and maintenance, and Ms. Zarinah Sonday for providing us sterile lab environment. We also express gratitude to the Wellcome Centre for Infectious Diseases Research in Africa (CIDRI-Africa) for supporting this study with WUN

CIDRI Ph.D. Scholarship 2019-2022. The study was carried out using the BSL3 platform with core funding from the Wellcome Trust (203135/Z/16/Z).

2.7. Supplementary Figures

Supplementary Figure 1.

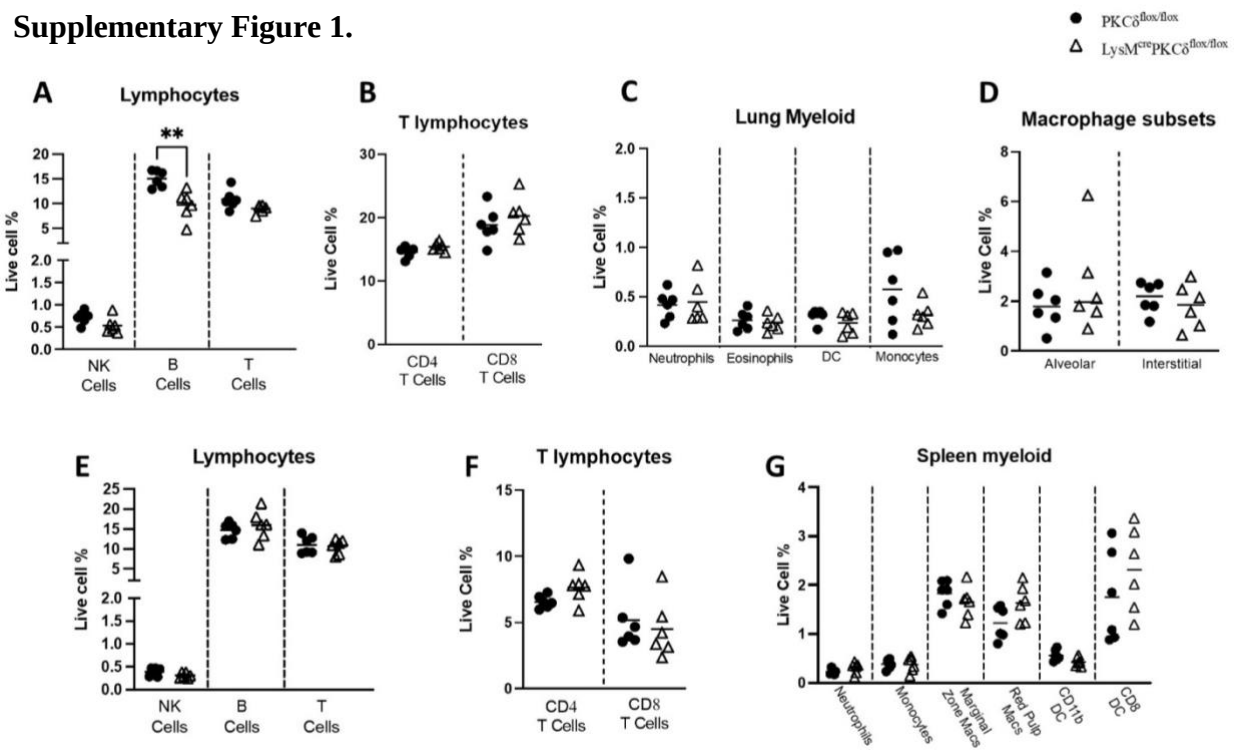

Supplementary Figure 1. Identical immune cell population with reduced lung B cell recruitment in LysM^{cre}PKCδ$^{flox/flox}$ female mice compared to PKCδ$^{flox/flox}$ mice at a naive state. Lungs and spleens were collected and processed for single-cell suspension from both PKCδ$^{flox/flox}$ and LysM^{cre}PKCδ$^{flox/flox}$ mice (n=6 mice/group) following surface stained and acquired for different immune cell populations using flow cytometric analysis. Various lymphoid and myeloid immune cell populations were detected in the single-cell suspension of lungs [A-D] and spleen [E-G] from both PKCδ$^{flox/flox}$ and LysM^{cre}PKCδ$^{flox/flox}$ mice. Surface markers determining different immune cell populations are as following: Lymphoid markers (Lung/Spleen) - Gamma delta (γδ) T cells: CD3+gdTCR+; Natural Killer (NK) cells: NK1.1+CD3-; B cells: CD19+CD3-; T cells: CD3+CD19-; CD4 T cells: CD3+CD4+; CD8 T cells: CD3+CD8+; Myeloid markers (Lung) - Neutrophils: Ly6G+CD11b+; Eosinophils: SiglecF+CD11b+CD64-; Dendritic cells (DC): CD11b+CD11c+MHCII+; Monocytes: Ly6G+CD11b+CD64-; Alveolar macrophages: CD64+MerTK+SiglecF+CD11c+; Interstitial macrophages: CD64+MerTK+SiglecF+CD11b+CD11c; Myeloid markers (Spleen) - Neutrophils: Ly6G+CD11b+; Monocytes: CD11b+Ly6C+CD11c-; Marginal zone macrophages: CD11bhighF4/80lowCD11c- ; Red pulp macrophages: F4/80highCD11blowCD11c-; CD11b+ DC = CD11c+MHCII+CD11b+. All data shown are representative of two independent experiments. Statistical analyses were performed using an unpaired student t-test. Asterisks are defining significance compared to the control group as ***$p < 0.001$.

Supplementary Figure 2.

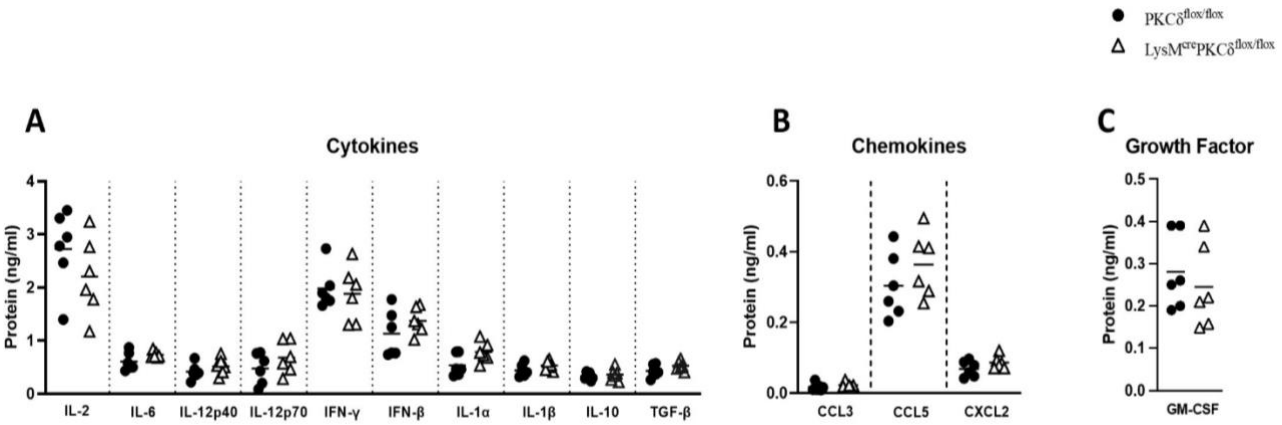

Supplementary Figure 2. Female LysM^{cre}PKCδ$^{flox/flox}$ mice exhibit no effects on growth factors, chemokine, and cytokines profile compared to PKCδ$^{flox/flox}$ mice at a naive state. Lung homogenates were collected from both PKCδ$^{flox/flox}$ and LysM^{cre}PKCδ$^{flox/flox}$ mice (n=4 mice/group) to determine an array of different [A] cytokines (IL-2, IL-6, IL-12p40, IL-12p60, IFN-γ, IFN-β, IL-1α, IL-1β, IL-10, TGF-β) [B] chemokines (CCL3, CCL5, CXCL2) and [C] growth factor (GM-CSF) levels. Statistical analyses were performed using an unpaired student t-test.

Appendix A: Primer pairs for qRT-PCR

PKC Isoforms	Accession number	Forward Primer (5'-3')	Reverse Primer (5'-3')
Mouse PKCα	X52685	TGAATCCTCAGTGGAATGAGT	GGTTGCTTTCTGTCTTCTGAA
Mouse PKCβ	X59274	CCCGAAGGAAGCGAGGGCAATGAAG	AGTTCATCTGTACCCTTCCGCTCTG
Mouse PKCγ	L28035	GCACCTGAGATCATTGCCTATC	CTGTCCTGCCAACATCTCATAC
Mouse PKCδ	M69042	CTGGGTAACTTAACAAGACC	CTGCTAAATAACATGTTCGGTCC
Mouse PKCε	M18331	CATCGATCTCTCGGGATCATCG	CGGTTGTCAAATGACAAGGCC
Mouse PKCη	M62980	AGCTAGCCGTCTTCCACGAGACGC	GGACGACGCAGGTGCACACTTGG
Mouse PKCθ	D11061	AGCTAGCCGTCTTCCACGAGACGC	GGACGACGCAGGTGCACACTTGG
Mouse PKCζ	M94632	CGATGGGGTGGATGGGATCAAAA	GTGTTCATGTCAGGGTTGTCCG
Mouse PKCι	D28577	CGTTGGGAGCTCTGACAATC	ACCTGCTTTTGCTCCATCATG
Mouse HPRT	NM_013556	GTTGGATATGCCCTTGAC	AGGACTAGAACACCTGCT

CHAPTER 3: Manuscript in preparation

Immunomodulatory effects of macrophage-specific PKCδ deficiency during *Mycobacterium tuberculosis* infection in mice

Rudranil Hazra[1,2], Shelby-Sara Jones[1,3], Mumin Ozturk[3,4], Sibongiseni K.L. Poswayo[3], Saiyukthi Naidoo[3], Robert Rousseau[3], Nashied Peton[5], Frank Brombacher[1,3], Robert J. Wilkinson[1,6], Suraj P. Parihar[1,2,3*]

[1] Wellcome Centre for Infectious Diseases Research in Africa (CIDRI-Africa), Institute of Infectious Diseases and Molecular Medicine (IDM), Faculty of Health Sciences, University of Cape Town, Cape Town 7925, South Africa.

[2] Division of Medical Microbiology, Institute of Infectious Diseases and Molecular Medicine (IDM), Department of Pathology, Faculty of Health Sciences, University of Cape Town, Cape Town 7925, South Africa.

[3] Division of Immunology, South African Medical Research Council (SAMRC) Immunology of Infectious Diseases, and International Centre for Genetic Engineering and Biotechnology (ICGEB), Cape Town Component, Institute of Infectious Diseases and Molecular Medicine (IDM), Department of Pathology, Faculty of Health Sciences, University of Cape Town, Cape Town 7925, South Africa.

[4] Epigenomics & Single Cell Biophysics Group, Department of Cell Biology FNWI, Radboud University, Nijmegen, Netherlands

[5] Drug Discovery and Development Centre (H3D), University of Cape Town, Cape Town 7925, South Africa.

[6] The Francis Crick Institute and Department of Infectious Diseases, Imperial College London, London, UK.

[*] Correspondence: A/Prof. Suraj P. Parihar, suraj.parihar@uct.ac.za

Keywords: LysM^{cre}PKCδ$^{flox/flox}$, *Mycobacterium tuberculosis*

3.1. Abstract

Tuberculosis (TB) is caused by a single etiological agent *Mycobacterium tuberculosis* (Mtb), which has emerged as the second deadliest infectious disease worldwide after COVID-19. Among numerous alarming concerns, anti-microbial resistance of the pathogen due to deprived TB drug efficacies is becoming prevalent. Hence, host modulating alternative and innovative therapeutic approaches in combination with existing TB treatment regimens could improve pulmonary function due to Mtb infection. The identification and targeting of candidate genes involved in immune evasion and putative pathogen-killing pathways during Mtb infection have been shown as an effective strategy to confront worsened lung pathology and inflammatory responses. As the first line of defense during Mtb infection, macrophages activate effector genes important for the efficient killing of invader pathogens to gain long-lasting immunity. For instance, one such candidate effector gene - Protein Kinase C – δ (PKCδ) has been demonstrated critical for immunity against *Listeria monocytogenes, Leishmania major, Candida albicans,* and *Mycobacterium tuberculosis* infection. However, these studies have been conducted in germline deficient ($PKC\delta^{-/-}$) mouse model which was unable to address the macrophage-specific functions of PKCδ. In this study, we have investigated the immunomodulatory effects of macrophage-specific PKCδ deficiency *in-vivo* using the $LysM^{cre}PKC\delta^{flox/flox}$ mice compared to the littermate control ($PKC\delta^{flox/flox}$) animals during Mtb infection. Our data reveal a significantly increased mycobacterial burden in the lungs of the male $LysM^{cre}PKC\delta^{flox/flox}$ mice with exacerbated lung pathology and the dissemination in the spleen at the chronic stage similar to germline deficient mice indicating the phenotype was largely driven by the macrophages. Additionally, in the acute phase of Mtb infection, increased conventional (CD4+, CD8+) effector T memory cells and terminal T-cell differentiation (PD1-KLRG1+) with enhanced short-lived effector cells (SLEC) turnover attributed to the macrophage-specific deficiency of PKCδ in $LysM^{cre}PKC\delta^{flox/flox}$ male mice. Interestingly, increased susceptibility to Mtb infection was also accompanied by a steady influx of neutrophil population and reduced restrictive interstitial macrophages (IM) at the acute phase in $LysM^{cre}PKC\delta^{flox/flox}$ male mice model. Furthermore, a consistent reduction of granulocyte-macrophage colony-stimulating factor (GM-CSF) levels in progression with Mtb infection in the lung homogenates of male $LysM^{cre}PKC\delta^{flox/flox}$ mice was observed. Our data suggest that PKCδ is critical for macrophage-specific immunomodulatory effects and exhibits a gender-specific pivotal role in innate immunity during Mtb infection.

3.2. Introduction

Despite BCG vaccination, Tuberculosis (TB) remains a major health concern worldwide. Reduced access to TB diagnosis and treatment due to the COVID-19 pandemic has resulted in a steep increase in TB deaths, according to the Global Tuberculosis Report 2021. However, the emergence of multi-drug resistant (MDR) strains, deprived vaccine efficacy of BCG, prolonged TB treatment regimens, and socio-economic challenges persist as significant factors for failure of TB control[138]. Intensifying virulence and developing resistance of the *Mycobacterium tuberculosis* (Mtb) pathogen prioritize an urgency for the development of adjunctive anti-TB therapies to mitigate the pulmonary pathology caused by TB disease[60, 66]. Exploiting host-pathogen interplay by an alternative approach, host-directed therapies (HDT) have been a widely studied strategy in the field of TB research[60]. These studies aim for an improved mechanism for bacterial killing, strengthening immune and memory responses, disrupting the structural integrity of TB granuloma, and fine-tuning inflammatory responses[60, 139]. Identifying potential HDT targets and understanding their involvement in key immune responses during Mtb infection is a primitive measure of comprehending the innate and adaptive nature of the host defense mechanism[60, 66, 139].

As a critical marker of inflammation, Protein Kinase C – δ (PKCδ) has been recognized as a potential marker employing a multitude of physiological roles and the ability to phosphorylate multiple target proteins involved in the various cellular processes [86-88, 96, 101, 115-117]. High susceptibility to Mtb infection with increased bacterial burden, mortality, weight loss, exaggerated lung inflammation, and unrestrained cytokine response has previously been demonstrated using PKCδ deficient ($PKC\delta^{-/-}$) mice model [88]. Protective immunity to TB is traditionally thought to be a result of a T-cell-dependent immune response, with CD4+ T cells playing a vital role[140, 141]. Although, $PKC\delta^{-/-}$ mice exhibit conventional T-cell-independent susceptibility in response to Mtb infection described by Parihar and colleagues[88]. In recent years, experimental and clinical evidence has increasingly highlighted the importance of innate cells In protective immunity[49, 142]. The initial uptake of Mtb pathogen by macrophages, the primary innate immune cell also possesses T-cell-independent, essential bactericidal activity[143, 144] which is also apparent in $PKC\delta^{-/-}$ mice with increased activated macrophages in the lungs during acute Mtb infection [88]. Besides, reduced alveolar macrophages in the lungs are in line with TB disease progression and increased bacterial burden in the bone-marrow-derived macrophages from $PKC\delta^{-/-}$ mice[88] with oxidative and nitrosative killing functions and dispensable for phagosome maturation also support the fact of

erratic macrophage dynamics and the importance of macrophage-mediated innate immunity in TB disease[145]. Furthermore, increased pro-inflammatory cytokines including IL-6, IFN-γ, IFN-β, TNF, and IL-1β revealed T_H1 governed immune response in PKCδ$^{-/-}$ mice during Mtb infection[88]. However, these findings only emphasized based on global deficiency of PKCδ *in vivo* which also prompted us to investigate the macrophage-specific PKCδ deficiency on the mycobacterial burden, various lung immune cell frequencies, and cytokine responses during TB disease which have not been studied yet. Here, we sought out the immunomodulatory effect of PKCδ deficiency particularly in macrophages using a well-established murine model LysM^{cre}PKCδ$^{flox/flox}$ (Chapter 2) during Tuberculosis. Our results suggest that PKCδ deficiency only in macrophages exhibits a similar increase in mycobacterial burden in the lungs and spleen in the male mice at a later infection stage as shown in the previous global knockout (PKCδ$^{-/-}$) mice model. Surprisingly, the male lung immune cell population revealed an incline towards T-cell-dependent host-defense through increased frequencies of T memory subsets and exhaustion markers during the initial stages of Mtb infection. Also, increased lung cell numbers were associated with infiltration of neutrophils at the acute stage of Mtb infection. In addition, we also anticipate that reduced restrictive interstitial macrophages (IM) may have a strong correlation behind increased bacterial load in the lungs of the male LysM^{cre}PKCδ$^{flox/flox}$ mice. However, permissive alveolar macrophages (AM) frequencies remained unchanged during Mtb infection despite having a significant decrease in GM-CSF levels in the lungs of male LysM^{cre}PKCδ$^{flox/flox}$ mice. Overall, these results indicate a critical role for PKCδ in the macrophage-mediated innate immune response against Mtb infection.

3.3. Methods

3.3.1. Mouse Strains

To generate the macrophage-specific PKCδ knockout mice model we have crossed loxP flanked PKCδ mice of C57BL/6 strain [127, 128] with in-house LysM^{cre} mice of C57BL/6 strain for three generations to achieve homozygous knockout model LysM^{cre}PKCδ$^{flox/flox}$. LoxP flanked PKCδ (PKCδ$^{flox/flox}$) mice were gifted by Professor C Ronal Kahn at the Joslin Diabetes Center, USA, and considered as a littermate control for all downstream experiments[127]. All mice were generated and maintained under specified pathogen-free conditions by the Animal Research Facility under strict guidelines of approved protocols by the University of Cape Town

Research Ethics Committee and South African Veterinary Council (SAVC). Experimental mice were matched for age (8-12 weeks) and sex. All procedures were conducted in the Research Animal Facility (RAF) Biosafety Level 3 (BSL3).

3.3.2. Ethical consideration

All experimental animals were operated following the Animal Research Facility approved protocols (Permit No: 019/023 and 019/031) and regulations under the South African National Standard (SANS 10386:2008) at the Faculty of Health Sciences, University of Cape Town.

3.3.3. Mtb infection and determination of mycobacterial burden in lungs and spleen

A virulent strain of Mtb (HN878) was grown in complete 7H9 media to log phase and glycerol stocks were made for infection of the mice by an intranasal administration procedure as previously described[67]. Stock solutions of Mtb were thawed and washed once with phosphate-buffered saline to get rid of glycerol before infection. The inoculum was prepared in sterile saline containing 0.05% Tween-80. Anesthetized mice were challenged with 50 µl of Mtb inoculum (25 µl/nostril). Inoculum dose uptake was also confirmed one day post-infection by determining the mycobacterial burden in the lungs of 4-5 infected mice. Mycobacterial load in the lungs and spleen of Mtb infected mice was determined at the indicated time points. Briefly, organs were aseptically collected and weighed from euthanized mice and homogenized in 0.04% Tween-80. Organ homogenates were subjected to plated as 10-fold dilution for CFU growth on Middlebrook 7H10 (BD Biosciences) agar plates supplemented with 10% OADC and 0.5% glycerol. Agar plates were incubated for 14-21 days at 37°C before colonies were counted.

3.3.4. Lung histopathology and immunohistochemistry

The right superior lobe of the lung from Mtb infected mice was collected in formalin solution (10% formaldehyde in 1X PBS) and processed for cryo-sectioning with the Leica TP 1020 benchtop processor following embedded in paraffin wax. Processed sections were cut using Leica Sliding Microtome 2000R in four 3 µm thick sections for H&E staining and two 3

μm sections for iNOS staining. Stained sections were subjected to be scanned at 40X in the Olympus VS120 virtual microscope for image acquisition. Alveolar space and iNOS+ areas were measured using Qupath v3.0.2 open-source software. Total alveolar spaces were quantified by subtracting the H&E positive area from the total lung tissue area. Similarly, the iNOS+ area was calculated as the area positively stained with diaminobenzidine (DAB) stain.

3.3.5. Immune cell population in lungs and lymph nodes by fluorescence-activated cell sorting

Left lobes of the lung were collected and digested in lung digestion buffer (DNase1, Collagenase type 1, DMEM) at 37°C for one hour to prepare a single-cell suspension. Digested lungs were passed through 100 μm and 70 μm sterile cell strainers (SPL Life Sciences) whereas lymph nodes were mechanically digested through 70 μm and 40 μm sterile cell strainers (SPL Life Sciences). Cells were washed with complete media (DMEM + 10%FCS) following red cell lysis buffer (150 mM NaCl, 10 mM KHCO3 and 0.1mM Na2EDTA) incubation for 5 min at room temperature. Then, cells were washed again with complete media before being counted with CytoSMART (Corning) automated cell counter and seeded approximately 1 x 10^6 cells per well in a 96-well U-bottom (Corning) plate. Seeded cells were washed once with PBS and stained with dead cell marker (575V Viability Dye, BD Biosciences) for 15 min at room temperature. After that cells were washed with FACS buffer (0.5% BSA, 0.5% Sodium azide (NaN3), 1x PBS) and surface stained for the following lymphoid and myeloid-specific markers: Lymphoid markers (lung/lymph node) - Gamma delta (γδ) T cells: CD3+gdTCR+; Natural Killer (NK) cells: NK1.1+CD3-; B cells: CD19+CD3-; T cells: CD3+CD19-; CD4 T cells: CD3+CD4+; CD8 T cells: CD3+CD8+; CD4+ Naive: CD3+CD4+CD62L+CD44-; CD4+ Central Memory: CD3+CD4+CD62L+CD44+; CD4+ Effector/Effector Memory: CD3+CD4+CD44+CD62L-; CD4+ Double Negative: CD3+CD4+CD44-CD62L-; CD8+ Naive = CD3+CD8+CD62L+CD44- ; CD8+ Central Memory = CD3+CD8+CD62L+CD44+ ; CD8+ Effector/Effector Memory = CD3+CD8+CD44+ CD62L-; CD8+ Double Negative: CD3+CD4+CD44-CD62L-; CD4+ Exhaustion Memory (lung): CD3+CD4+PD1-KLRG1+; CD8+ Exhaustion Memory (lung): CD3+CD8+PD1-KLRG1+; CD8+ Tissue Resident Memory: CD3+CD8+CD103+CD69+; CD8+ Memory Precursor: CD3+CD8+KLRG1-CD127+; CD8+ Short-lived Effector: CD3+CD8+KLRG1+CD127-; Myeloid markers (Lung)

- Neutrophils: Ly6G+CD11b+; Eosinophils: SiglecF+CD11b+CD64-; Dendritic cells (DC): CD11b+CD11c+MHCII+; Monocytes: Ly6G+CD11b+CD64-; Alveolar Macrophages: CD64+MerTK+SiglecF+CD11c+; Interstitial Macrophages: CD64+MerTK+SiglecF+CD11b+CD11c; Myeloid markers (lymph node): Neutrophils: Ly6G+CD11b+; Migratory DC: CD11c+MHCIIhigh; CD11b+ Migratory DC: CD11c+MHCIIhighCD11b+CD103-; CD103+ Migratory DC: CD11c+MHCIIhighCD103+CD11b-; Resident DC: CD11c+MHCIIlow; CD8+ Resident DC: CD11c+MHCIIlowCD8+CD11b-; CD11b+ Resident DC: CD11c+MHCIIlowCD11b+CD8-; Medullary Cord Macrophages: CD11b+F4/80+CD169-; Medullary Sinus Macrophages: CD11b+F4/80-CD169+; Subcapsular Sinus Macrophages: CD11b+F4/80+CD169+; MHCII- Monocytes: Ly6C+MHCIIlow; MHCII+ Monocytes: Ly6C+MHCIIhigh. Surface-stained cells were acquired using BD LSR Fortessa (BD Biosciences Immunohistochemistry Systems) and data was analyzed by FlowJo v10.6.1 software (TreeStar, US). All stained cells positive for specific markers are calculated as a percentage/frequency of live cells.

3.3.6. Cytokine, chemokine, and growth factors in lung homogenates

Lung homogenates were spun at 3000 g for 5 min and passed through a 0.2 μm filter twice to obtain cell-free supernatant analyzed using standard sandwich ELISA assay. Coating, standard, and detection antibodies were obtained from BD Biosciences, Biolegend, and R&D Scientific. The assay was performed to detect different cytokines (TH1: IL-2, IL-6, IL-12p40, IL-12p60, IFN-γ, IFN-β, IL-1α, IL-1β; TH2: IL-4, IL-10, IL-13, TGF-β; TH17: IL-17, IL-23), chemokines (CCL3, CXCL10, CXCL1, CXCL2, CXCL5, CCL2) and growth factors (IGF-1, GM-CSF) levels according to manufacturer's dilutions and protocol. TMB microwell peroxidase substrate (KPL International) for streptavidin-HRP conjugates or 1 mg/ml p-nitrophenyl phosphate disodium salt hexahydrate (Sigma, cat# N2765) for streptavidin-AP conjugates. VersaMax™ microplate spectrophotometer (Molecular Devices, Sunnyvale, California) was used to measure optical density.

3.3.7. Statistical analysis

All data represented were mean values and analyzed using GraphPad Prism v9.0. Statistical analyses were performed using an unpaired student t-test. Asterisks are defining significance compared to the control group as: *$p < 0.05$, **$p < 0.01$, ***$p < 0.001$, ****$p < 0.0001$.

3.4. Results

3.4.1. Male LysM^{cre}PKCδ$^{flox/flox}$ mice displayed high mycobacterial burden during Mtb infection

Previous findings by Parihar and colleagues indicated a greater susceptibility and inflammation to Mtb infection in the lungs of PKCδ$^{-/-}$ mice through high pulmonary cell recruitment, lung/spleen weight index, and enumerated Mtb colonies[88]. Hence, we determined mycobacterial growth in the absence of PKCδ in macrophages. We found significantly increased Mtb burden in the lungs of LysM^{cre}PKCδ$^{flox/flox}$ mice with increased cell recruitment despite unchanged lung weight index in the acute stage (**4 WPI**) of Mtb infection compared to PKCδ$^{flox/flox}$ mice (**Figure 1A-C**). Furthermore, a similar increase in Mtb burden in the lungs and dissemination in the spleen of LysM^{cre}PKCδ$^{flox/flox}$ mice was also observed in the chronic stage (**12 WPI**) of Mtb infection (**Figure 1D-F**). To our surprise, we found that macrophage-specific PKCδ knockout does not impact the mycobacterial burden in the female LysM^{cre}PKCδ$^{flox/flox}$ mice compared to PKCδ$^{flox/flox}$ mice (**Supplementary Figure 1A-D**) suggesting a potential gender-biased role of PKCδ during Mtb infection. Taken together, these results revealed a pathogen-influenced inflammation depicted as an increased and dispersed mycobacterial burden during Mtb infection *in vivo*.

Figure 1.

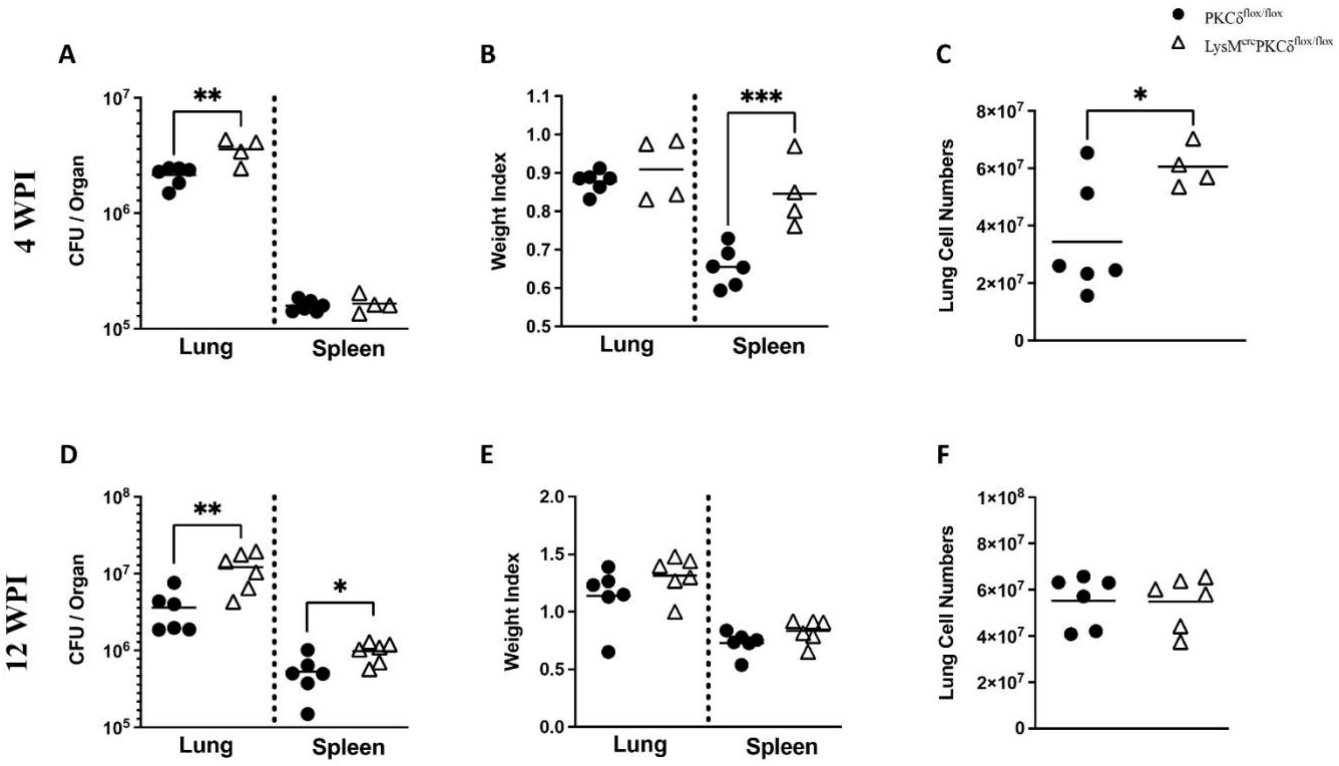

Figure 1. Male LysM^{cre}PKCδ$^{flox/flox}$ mice displayed high mycobacterial burden in the lungs and spleen during Mtb infection. HN878 Mtb strain was challenged intranasally to LysM^{cre}PKCδ$^{flox/flox}$ and PKCδ$^{flox/flox}$ mice at 150 CFU/mouse (n=4-6 mice/group). Animals were euthanized to determine lung/spleen CFU burden, lung/spleen weight index, and lung cell numbers at [A-C] acute stage (4 wpi) and [D-F] chronic stage (12 wpi) of Mtb infection. All data are shown as mean and are representative of two independent experiments (n=6 mice/group). Statistical analyses were performed using an unpaired student t-test. Asterisks are defining significance compared to the control group as: *p < 0.05, **p < 0.01, ***p < 0.001.

3.4.2. Elevated lung pathology in the male LysM^{cre}PKCδ$^{flox/flox}$ mice at the acute and chronic stages of Mtb infection

Pulmonary pathology often correlates with mycobacterial growth and indicates the association of tissue morphology in response to infection. Hence, we asked the question of whether an increased mycobacterial burden elevates the lung inflammation in the male LysM^{cre}PKCδ$^{flox/flox}$ mice by histopathology analysis compared to littermate control mice. Predictably, we found an increased pathology defined as less alveolar space in the lungs at the acute and chronic stages of Mtb infection in the male LysM^{cre}PKCδ$^{flox/flox}$ mice (**Figure 2A-B**). Besides, we have found a significant decrease in the iNOS^{+} area in the lung sections of

male LysM^{cre}PKCδ$^{flox/flox}$ mice during acute Mtb infection compared to the littermate control (**Figure 2C-D**), depicting less nitric oxide (NO) production by the host, indicating an inducive inflammatory environment for pathogen growth and persistence. In addition, we did not notice any changes in the pathology of the lungs of female LysM^{cre}PKCδ$^{flox/flox}$ mice compared to PKCδ$^{flox/flox}$ mice **(Supplementary Figure 1E).**

Figure 2.

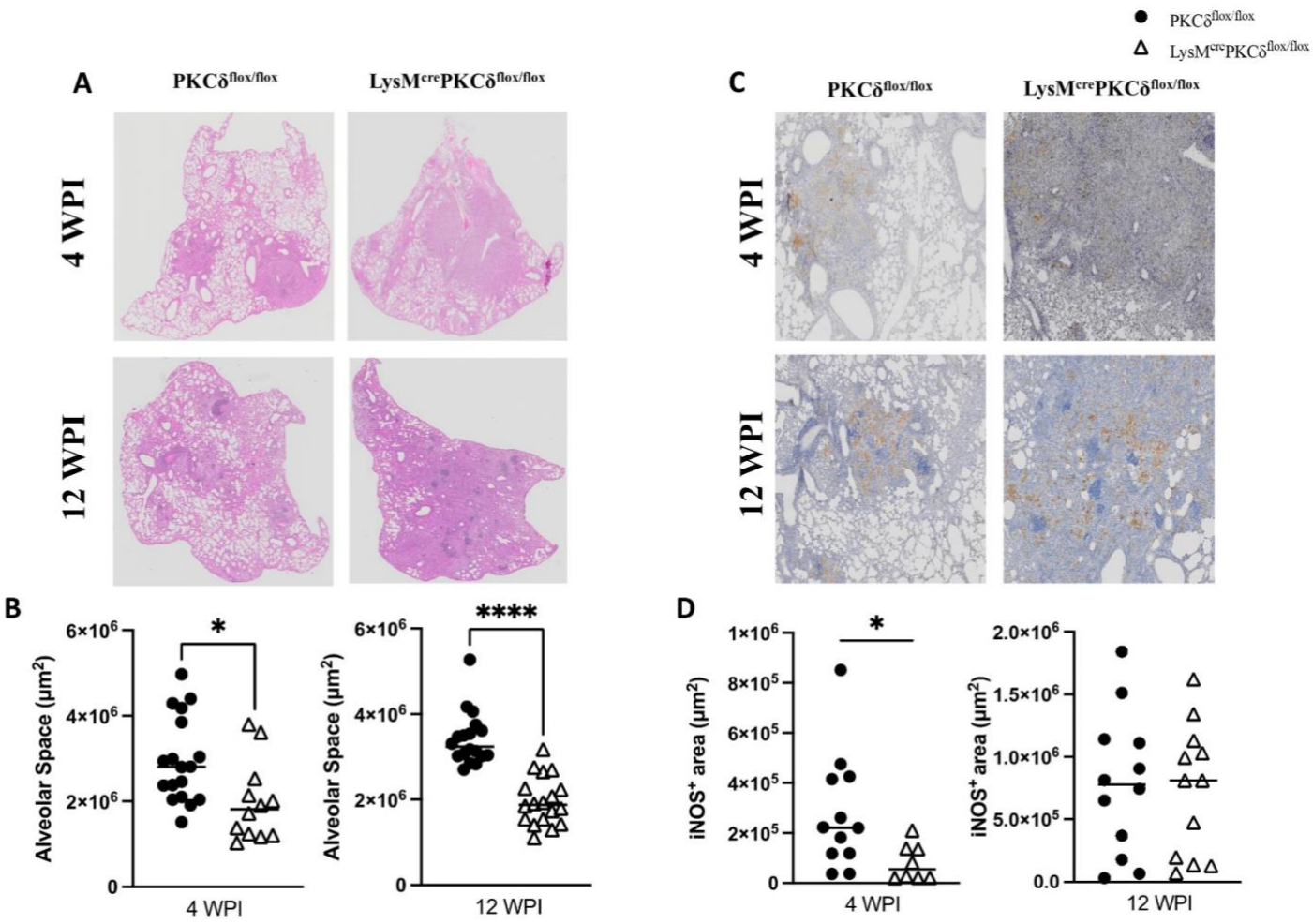

Figure 2. Elevated lung pathology in the male LysM^{cre}PKCδ$^{flox/flox}$ mice at the acute and chronic stage of Mtb infection. Mtb infected lung sections from LysM^{cre}PKCδ$^{flox/flox}$ and PKCδ$^{flox/flox}$ mice were stained for H&E and iNOS histopathology analysis at 4 weeks and 12 weeks. Quantification of [A-B] alveolar space and [C-D] iNOS^{+} area represented with their respective (40X) scanned images. All data shown are representative of two independent experiments. Statistical analyses were performed using an unpaired student t-test. Asterisks are defining significance compared to the control group as: *$p < 0.05$, ****$p < 0.0001$.

3.4.3. Marginal shift towards lung T memory cell-mediated immune response in male LysM^{cre}PKCδ$^{flox/flox}$ mice during acute Mtb infection

In recent advances, how early phases of mycobacterial growth and dissemination impact the generation of the T-cell immune response, is evident in numerous T-cell mediated pathology studies[146]. Although early encounters of the Mtb pathogen by alveolar macrophage (AM) is a naturally occurring host defense mechanism upon Mtb infection, these cells may play a pivotal role in triggering T cell responses[147]. Previously, PKCδ$^{-/-}$ mice showed no variability in conventional T cell recruitment during Mtb infection, but extensive T memory cell responses have not been delineated in the study[88]. These prompted us to explore the consequences of PKCδ deficiency in macrophages on T cell-mediated immune response along with major lymphocyte frequencies during the acute stage of Mtb infection. Flow cytometry analysis revealed no marked increase in the frequencies of lymphocytes with conventional T cells except Natural Killer (NK) cells in LysM^{cre}PKCδ$^{flox/flox}$ mice when compared to PKCδ$^{flox/flox}$ mice (**Figure 3A-B**). Surprisingly, we found that CD4+/CD8+ Effector/Effector memory and short-lived effector cell (SLEC) frequencies were significantly increased in LysM^{cre}PKCδ$^{flox/flox}$ mice (**Figure 3C-E**). In murine TB, not PD-1 but KLRG1 is established as a superior marker for T cell differentiation upon exhaustion[148]. This aberration in T memory and effector subsets was most likely attributed to the exhaustion of CD4+/CD8+ T cells defined by increased PD-1-KLRG1+ frequencies in LysM^{cre}PKCδ$^{flox/flox}$ mice (**Figure 3F-G**). In addition, we showed that PKCδ deficiency in macrophages does not affect any lymphoid population in thoracic lymph nodes in LysM^{cre}PKCδ$^{flox/flox}$ mice at the acute stage of Mtb infection (**Supplementary Figure 2A-D**). Furthermore, neither lungs nor the lymph nodes of female LysM^{cre}PKCδ$^{flox/flox}$ mice showed any discernible changes in the lymphoid populations (**Supplementary Figure 3A-K**). Together, these results indicated that macrophage-specific ablation of PKCδ induces a marginal shift towards lung T memory cell-mediated immune response during acute Mtb infection *in vivo*.

Figure 3.

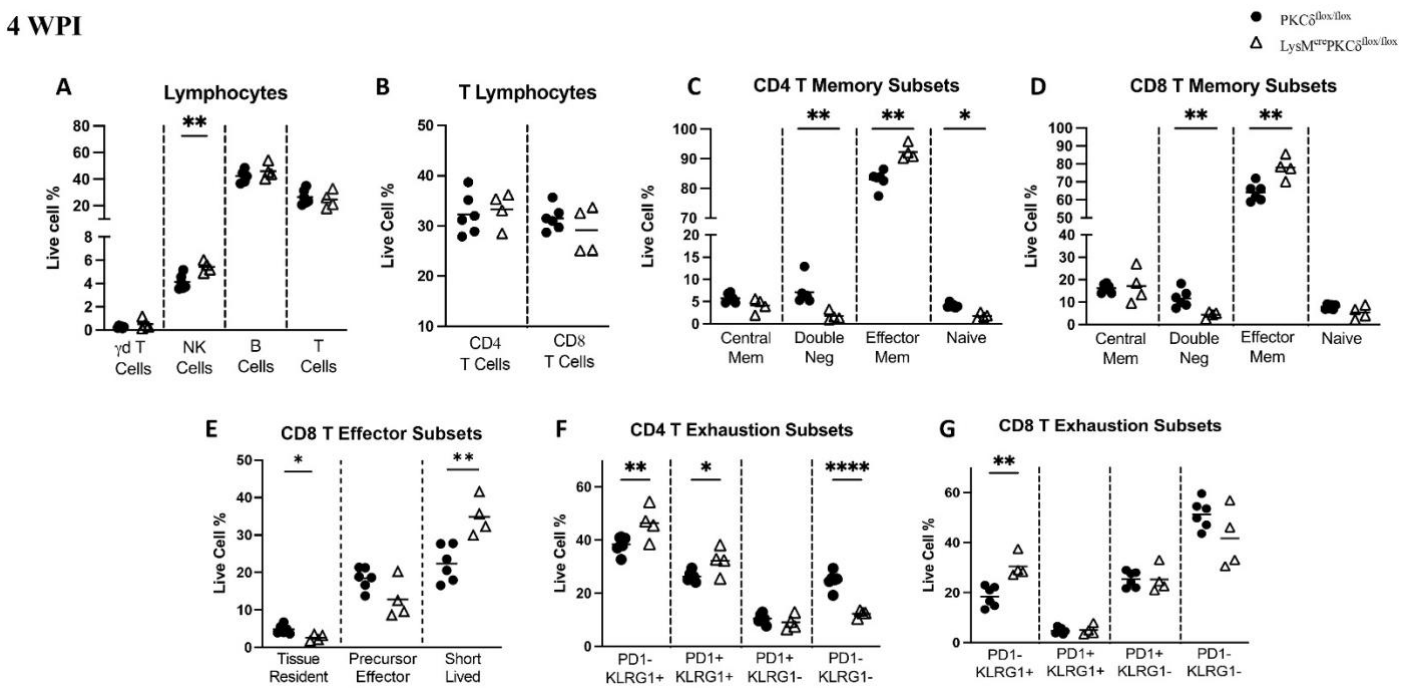

Figure 3. **Marginal shift towards lung T memory cell-mediated immune response in male LysM^{cre}PKCδ$^{flox/flox}$ mice during acute Mtb infection.** Mtb infected lungs were collected, weighed, and processed for single-cell suspension to analyze different immune cell populations using flow cytometric analysis at 4 weeks. [A-G] Lymphoid immune cell populations were detected in LysM^{cre}PKCδ$^{flox/flox}$ and PKCδ$^{flox/flox}$ mice. Surface markers determining different immune cell populations are as following: Lymphoid markers - Gamma delta (γδ) T cells: CD3+gdTCR+; Natural Killer (NK) cells: NK1.1+CD3-; B cells: CD19+CD3-; T cells: CD3+CD19-; CD4 T cells: CD3+CD4+; CD8 T cells: CD3+CD8+; CD4+ Naive: CD3+CD4+CD62L+CD44-; CD4+ Central Memory: CD3+CD4+CD62L+CD44+; CD4+ Effector/Effector Memory: CD3+CD4+CD44+CD62L-; CD4+ Double Negative: CD3+CD4+CD44-CD62L-; CD8+ Naive = CD3+CD8+CD62L+CD44- ; CD8+ Central Memory = CD3+CD8+CD62L+CD44+ ; CD8+ Effector/Effector Memory = CD3+CD8+CD44+ CD62L-; CD8+ Double Negative: CD3+CD4+CD44-CD62L-; CD4+ Exhaustion Memory: CD3+CD4+PD1-KLRG1+; CD8+ Exhaustion Memory: CD3+CD8+PD1-KLRG1+; CD8+ Tissue Resident Memory: CD3+CD8+CD103+CD69+; CD8+ Memory Precursor: CD3+CD8+KLRG1-CD127+; CD8+ Short-lived Effector: CD3+CD8+KLRG1+CD127-. All data shown are representative of two independent experiments. Statistical analyses were performed using an unpaired student t-test. Asterisks are defining significance compared to the control group as: *p < 0.05, **p < 0.01, ***p < 0.001.

3.4.4. Chronic Mtb infection exhibits no effect on lung lymphoid population in male LysM^{cre}PKCδ$^{flox/flox}$ mice

Exponential replication of Mtb ensues in mouse lungs up until the onset of adaptive immunity seizes replication, leading to a chronic infection that is contained however not eradicated[149]. We assessed whether the chronic stage of Mtb infection influenced the lymphoid frequencies in the LysM^{cre}PKCδ$^{flox/flox}$ male mice when compared to PKCδ$^{flox/flox}$ mice. We found no significant differences in the lung lymphoid and conventional T cell frequencies with the sustained burden of Mtb replication at the chronic stage (**Figure 4A-B**). Equalized T memory subsets with unaffected exhaustion were also apparent by flow cytometry analysis of the lung lymphoid population of LysM^{cre}PKCδ$^{flox/flox}$ mice compared to the littermate control (**Figure 4C-G**). Additionally, we showed reduced frequencies of CD4+/CD8+ Effector/Effector memory among the lymphocyte population in the lymph nodes of LysM^{cre}PKCδ$^{flox/flox}$ mice (**Supplementary Figure 4A-D**). Also, no discrepancy in the lymphocyte population was detected in the lungs and lymph nodes of female LysM^{cre}PKCδ$^{flox/flox}$ mice (**Supplementary Figure 5A-K**). Thus, these findings altogether suggest that sustained Mtb burden displays no effect on the lung lymphoid population of LysM^{cre}PKCδ$^{flox/flox}$ mice as compared to PKCδ$^{flox/flox}$ mice.

Figure 4.

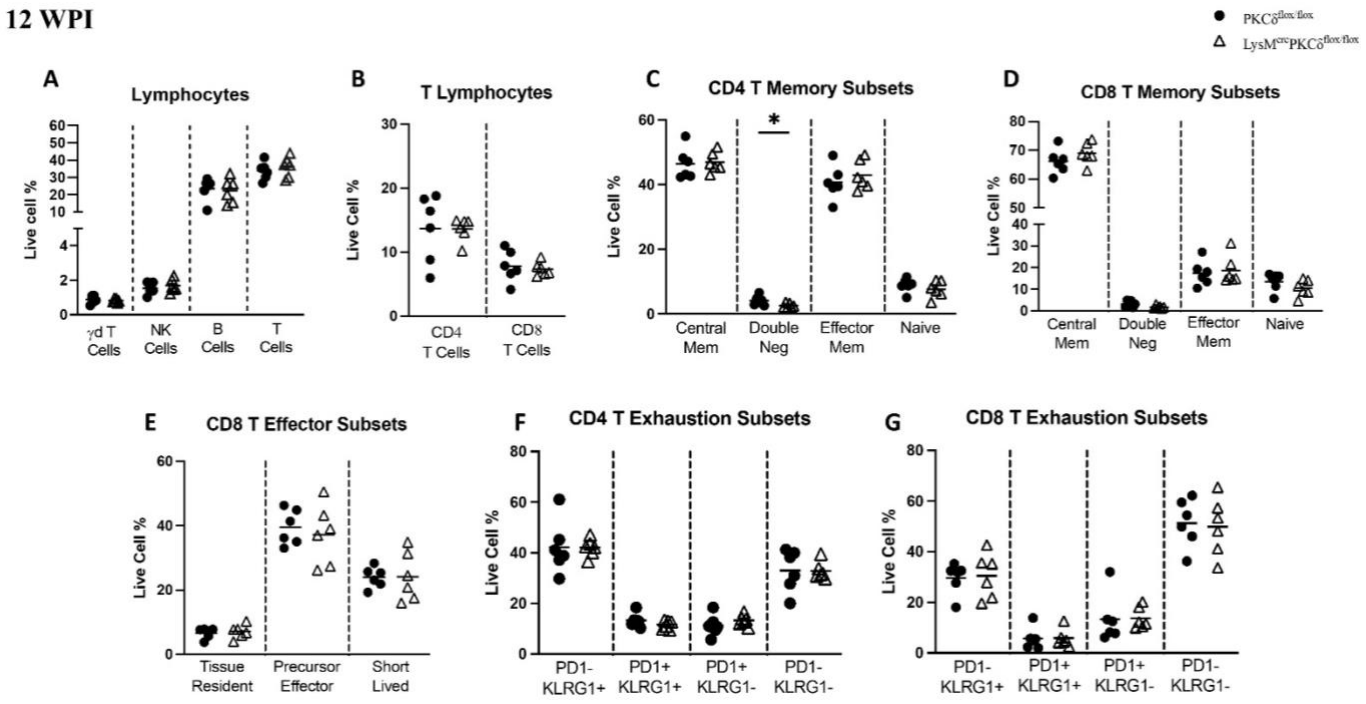

Figure 4. Chronic Mtb infection exhibits no effect on lung lymphoid population in LysM^{cre}PKCδ$^{flox/flox}$ mice. Mtb infected lungs were collected, weighed, and processed for single-cell suspension to analyze different immune cell populations using flow cytometric analysis at 12 weeks. [A-G] Lymphoid immune cell populations were detected in LysM^{cre}PKCδ$^{flox/flox}$ and PKCδ$^{flox/flox}$ mice. Surface markers determining different immune cell populations are as following: Lymphoid markers - Gamma delta (γδ) T cells: CD3+gdTCR+; Natural Killer (NK) cells: NK1.1+CD3-; B cells: CD19+CD3-; T cells: CD3+CD19-; CD4 T cells: CD3+CD4+; CD8 T cells: CD3+CD8+; CD4+ Naive: CD3+CD4+CD62L+CD44-; CD4+ Central Memory: CD3+CD4+CD62L+CD44+; CD4+ Effector/Effector Memory: CD3+CD4+CD44+CD62L-; CD4+ Double Negative: CD3+CD4+CD44-CD62L-; CD8+ Naive = CD3+CD8+CD62L+CD44-; CD8+ Central Memory = CD3+CD8+CD62L+CD44+; CD8+ Effector/Effector Memory = CD3+CD8+CD44+ CD62L-; CD8+ Double Negative: CD3+CD4+CD44-CD62L-; CD4+ Exhaustion Memory: CD3+CD4+PD1-KLRG1+; CD8+ Exhaustion Memory: CD3+CD8+PD1-KLRG1+; CD8+ Tissue Resident Memory: CD3+CD8+CD103+CD69+; CD8+ Memory Precursor: CD3+CD8+KLRG1-CD127+; CD8+ Short-lived Effector: CD3+CD8+KLRG1+CD127-. All data shown are representative of two independent experiments. Statistical analyses were performed using an unpaired student t-test. Asterisks are defining significance compared to the control group as: *$p < 0.05$.

3.4.5. Progressive Mtb burden led to an alteration in myeloid population in the lung of male LysM^{cre}PKCδ$^{flox/flox}$ mice

The complexity of myeloid cell subsets in controlling TB-induced inflammation by their unique immune responses has been tailored either in a protective manner or by providing a favorable environment for pathogen survival[150]. Among major myeloid cells, macrophages harbors Mtb pathogen within TB granuloma, dendritic cells (DC) are responsible for adaptive immunity as the disease continues, and polymorphonuclear neutrophils mount lung damage[150]. Susceptibility of PKCδ$^{-/-}$ mice to Mtb infection showed increased involvement of activated macrophages with reduced alveolar macrophage and DC subsets described by Parihar and colleagues[88]. Based on the mycobacterial burden and increased pulmonary cell recruitment during acute Mtb infection in the LysM^{cre}PKCδ$^{flox/flox}$ mice, we further investigated the cell frequencies of various innate immune responsive myeloid cells in the absence of PKCδ in macrophages. Our findings revealed an increased influx of neutrophil frequencies only in the acute stage of Mtb infection in the LysM^{cre}PKCδ$^{flox/flox}$ mice when compared to PKCδ$^{flox/flox}$ mice (**Figure 5A, D**). This indicates a pro-inflammatory response given the existing evidence of functional versatility and phenotypic heterogeneity of neutrophils with regards to PKCδ inhibition[89]. We did not observe any differences in the frequencies of pulmonary eosinophils, monocytes, and DC subsets in the LysM^{cre}PKCδ$^{flox/flox}$ mice (**Figure 5A-B, D-E**) compared to the littermate control. Also, ontologically distinct macrophage subsets in the absence of PKCδ, surprisingly, revealed a significant reduction in the frequencies of interstitial macrophages (IM), known for pathogen restriction, and intact alveolar macrophages (AM), identified as permissive to the pathogen[151] at the early stages of Mtb infection (**Figure 5C**). This decrease in the IM subset may define the circumstance of early containment of Mtb pathogen and enhanced dissemination at the later stages of infection, with gradual reinforcement of pulmonary IM in the LysM^{cre}PKCδ$^{flox/flox}$ mice (**Figure 5F**). Moreover, the mechanism and functional immunological consequences of lymphatic macrophages during Mtb infection have recently been explored[152]. In our study, myeloid subsets including macrophages in lymph nodes illustrate no significant differences during Mtb infection (**Supplementary Figure 6A-B**). Seemingly, female LysM^{cre}PKCδ$^{flox/flox}$ mice did not show any variations in their myeloid population during the acute and chronic stages of Mtb infection (**Supplementary Figure 7A-B**). Altogether, these results reveal a divergent response by the lung myeloid population, with adversative neutrophils infiltration and reduced IM, conducive to the mycobacterial growth in the male LysM^{cre}PKCδ$^{flox/flox}$ mice.

Figure 5.

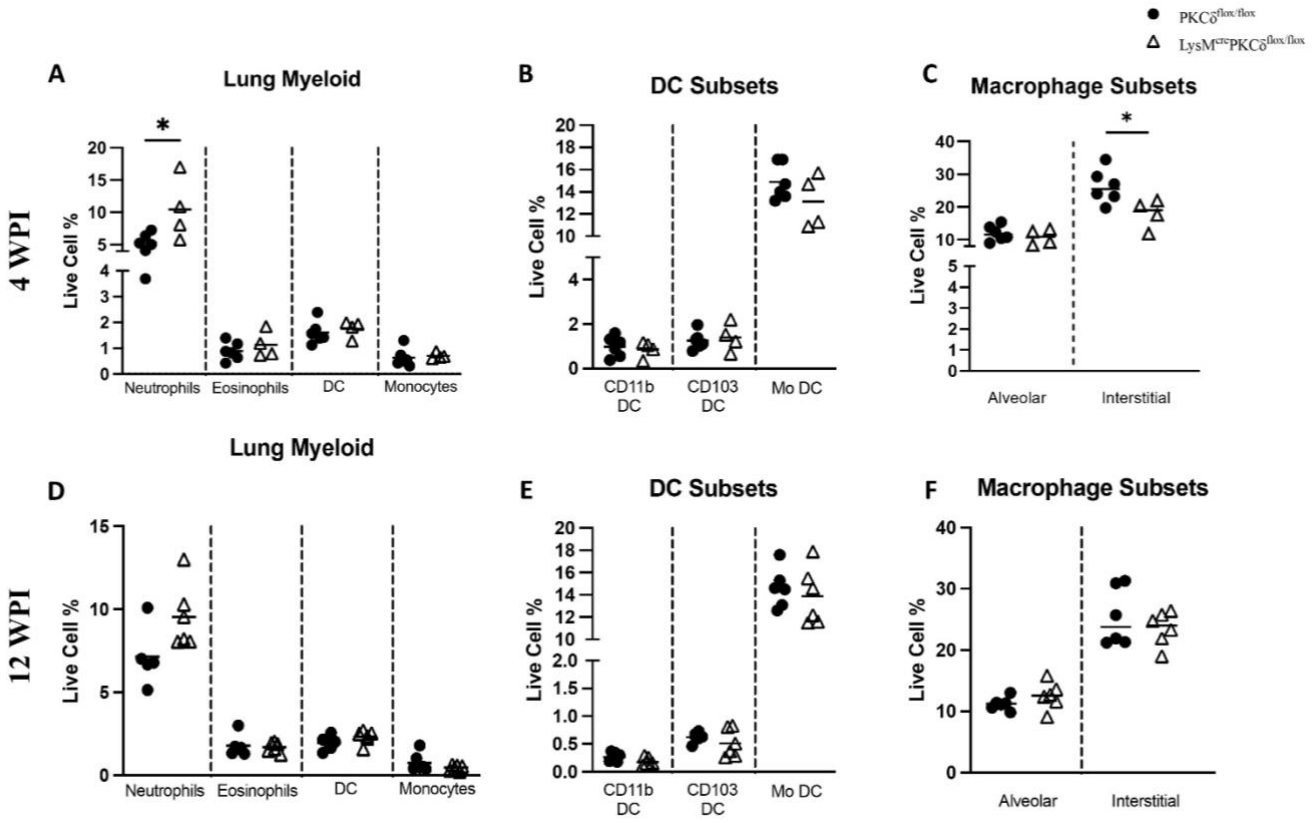

Figure 5. Progressive Mtb burden led to an alteration in myeloid population in the lungs of male LysM^{cre}PKCδ$^{flox/flox}$ mice. Mtb infected lungs were collected, weighed, and processed for single-cell suspension to analyze different immune cell populations using flow cytometric analysis at 4 weeks and 12 weeks. Various myeloid immune cell populations were detected in LysM^{cre}PKCδ$^{flox/flox}$ and PKCδ$^{flox/flox}$ mice at acute[A-C] and chronic[D-F] stages of Mtb infection. Surface markers determining different immune cell populations are as following: Myeloid markers - Neutrophils: Ly6G+CD11b+; Eosinophils: SiglecF+CD11b+CD64-; Dendritic cells (DC): CD11b+CD11c+MHCII+; Monocytes: Ly6G+CD11b+CD64-; Alveolar Macrophages: CD64+MerTK+SiglecF+CD11c+; Interstitial Macrophages: CD64+MerTK+SiglecF+CD11b+CD11c. All data shown are representative of two independent experiments. Statistical analyses were performed using an unpaired student t-test. Asterisks are defining significance compared to the control group as: *$p < 0.05$.

3.4.6. Cytokine profiling of male LysM^{cre}PKCδ$^{flox/flox}$ mice correlates with impeding host defense and favoring mycobacterial growth

Next, we evaluated the cytokine levels in the lung homogenates of LysM^{cre}PKCδ$^{flox/flox}$ mice by conventional ELISA assay at both the acute and chronic stages of Mtb infection. Briefly, acute Mtb infection showed no significant differences in the levels of pro-inflammatory cytokines and chemokines in the lung homogenates of male LysM^{cre}PKCδ$^{flox/flox}$ mice (**Figure 6A-H**). Interestingly, levels of IL-10 and GM-CSF were significantly reduced in LysM^{cre}PKCδ$^{flox/flox}$ mice during acute (**Figure 6B,D**) and chronic (**Figure 6F,H**) stages of Mtb infection. In addition to GM-CSF and IL-10, we also found a reduction in IL-2 production during the chronic stage of Mtb infection (**Figure 6E**). Knowingly, female LysM^{cre}PKCδ$^{flox/flox}$ mice did not display any differences in their lung cytokine and chemokine levels during the acute and chronic stages of Mtb infection (**Supplementary Figure 8A-H**). Previous studies demonstrated the unique functions of GM-CSF, promoting host-defense[153], IL-2, determining the T cell fate in response to Mtb antigens[154], and IL-10, an established potent anti-inflammatory responder[155]. Decreased production of these cytokines by the host in Mtb infection may provide a favorable and proliferative niche for mycobacterial growth, which is evident in our study through an augmented and progressed disease in the absence of PKCδ in macrophages *in vivo*.

Figure 6.

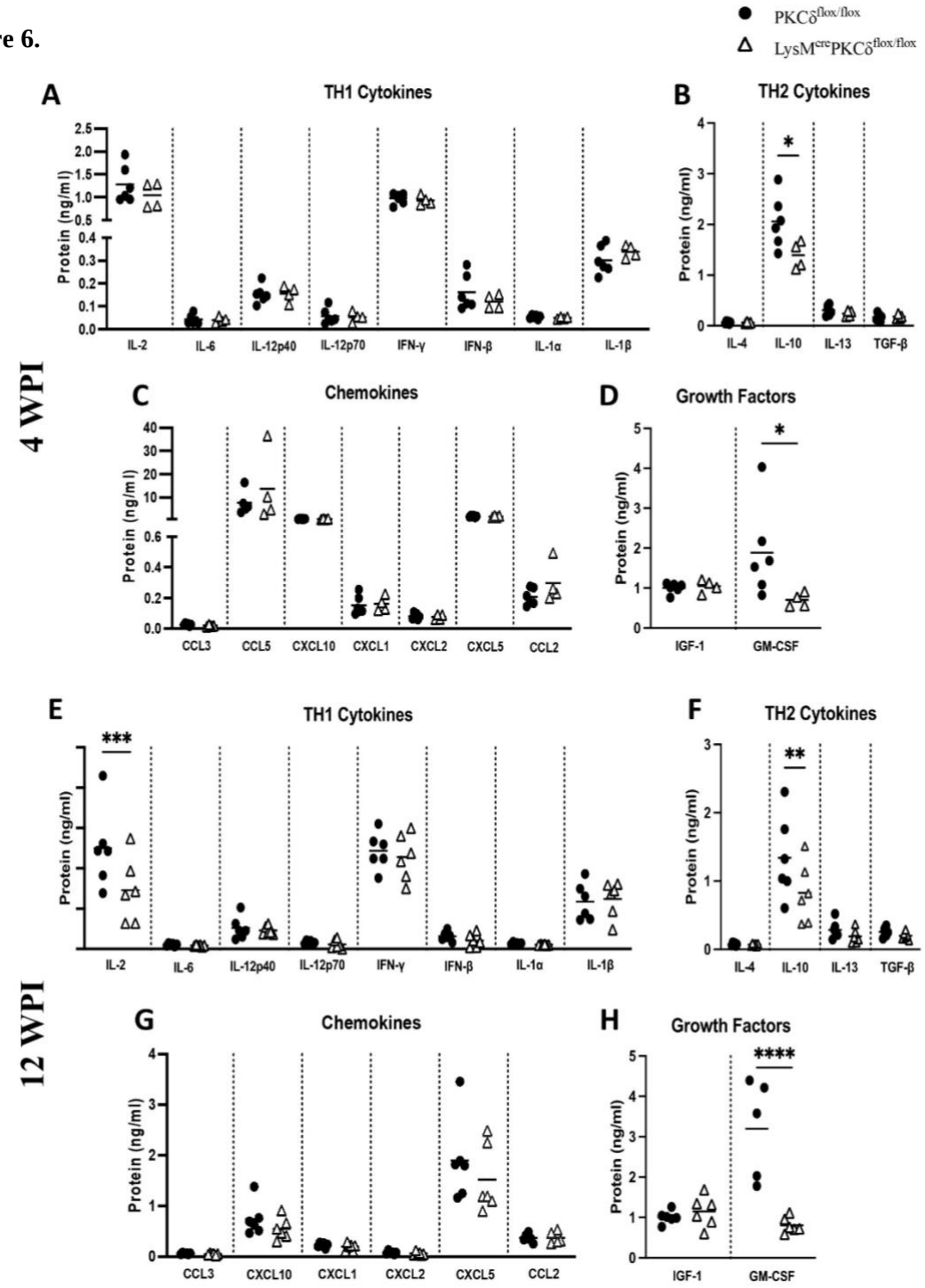

Figure 6. **Cytokine profiling of male LysM^{cre}PKCδ$^{flox/flox}$ mice correlates with impeding host defense and favoring mycobacterial growth.** [A-D] 4 weeks and [E-H] 12 weeks post-infected lung homogenates were collected from both LysM^{cre}PKCδ$^{flox/flox}$ and PKCδ$^{flox/flox}$ mice (n=~6 mice/group) to determine an array of different cytokines TH1: IL-2, IL-6, IL-12p40, IL-12p60, IFN-γ, IFN-β, IL-1α, IL-1β; TH2: IL-4, IL-5, IL-10, IL-13, TGF-β; chemokines (CCL3, CCL5, CXCL10, CXCL1, CXCL2, CXCL5) and growth factors (IGF-1, GM-CSF) levels. All data shown are representative of two independent experiments. Statistical analyses were performed using an unpaired student t-test. Asterisks are defining significance compared to the control group as: **p < 0.01, ***p < 0.001, ****p < 0.0001.

3.5. Discussion

The ability to deal with the threat of tuberculosis to global health is compromised by the lack of our knowledge of key components involved in protective immune response[143], hindering effective vaccine development. Such reliable immune correlates are critical to characterize among numerous immune regulators articulated by the host in response to infection. PKCδ, an inflammation marker with pro-inflammatory signatures during Mtb infection has been established as a key immune regulator by Parihar and colleagues[88]. In order to prevent disease progression from the primary site, it is crucial to control the pathogen at the localized level, which consists of necrotic and cavitary granulomas derived from Mtb infected epithelioid macrophages and a lymphocytic cuff that includes B and T lymphocytes[156]. Previously, myeloid cells like macrophages, myeloid-derived suppressor cells (MDSCs), and neutrophils were found to be heterogeneously distributed throughout the granuloma[156]. The abundance of PKCδ in these inflammatory granuloma regions has been observed earlier in humans[88, 157]. Also, PKCδ is ubiquitously expressed in lymphocytes and myeloid populations, responsible for innate immunity against Mtb pathogen[124, 125]. Though the global deletion of PKCδ in mice demonstrated reduced bacterial killing ability with compromised optimal inflammatory balance[88], the intrinsic myeloid-specific role of PKCδ during *in vivo* Mtb infection has not been delineated yet.

In our study, we have exploited the immunomodulatory functions of macrophage-specific deletion of PKCδ *in vivo* during Mtb infection. Our findings revealed an increased mycobacterial burden with exacerbated lung pathology in the male $LysM^{cre}PKC\delta^{flox/flox}$ mice, indeed confirming a dominant role of macrophage PKCδ in host defense. This also indicates that most likely the macrophages were driving the outcome of TB in germ-line deficiency of PKC-delta[88]. Host defense mechanisms depend on a delicate balance that, if altered, can favor Mtb proliferation, resulting in disease progression, or trigger tissue destruction by initiating an immune response[158]. Evidently, the absence of PKCδ in macrophages induced less production of nitrogen intermediates defined as reduced iNOS histopathology at the early stages of Mtb infection, promoting a pathogen-permissive inflammation detrimental to the host[159]. However, high iNOS production was observed in mice with germline PKCδ deficiency further confirming the erratic iNOS contribution by other immune cells besides macrophages[88].

Chronological events in TB pathogenesis demonstrate a fine link between logarithmical growth of the pathogen and developing Mtb antigen-specific T cell immunity interacting with infected macrophages[142]. It is now well established that CD4+/CD8+ T cells are influential in the control of the Mtb pathogen in both humans and mice[146]. Although, conventional T cell frequencies were not significantly affected by the ablation of PKCδ in macrophages, surprisingly, T cell memory and effector subsets were orchestrated at the early stage of Mtb infection. T cells are required for the control of infection *in vivo*, however, these immune cells cannot eliminate the pathogen or protect from a fatal infection[146]. This may explain the persistence of the pathogen in the presence of robust T memory cell-mediated immune response in the male LysM^{cre}PKCδ$^{flox/flox}$ mice. Importantly, the prolonged challenge with Mtb antigen *in vivo* showed reduced production of IL-2 and reduction in CD8+ T memory cells, promoting impaired antibacterial immunity[142, 146]. Strikingly, we found a significant reduction in the IL-2 levels with restored effector and memory T cell turnover in the male LysM^{cre}PKCδ$^{flox/flox}$ mice similar to the littermate control at the chronic stage of Mtb infection. Certainly, this varied T cell interplay modulating IL-2 levels at various stages of Mtb infection in the absence of PKCδ in macrophages is critical and needs further mechanistic evaluation to confer a concrete link.

Mtb pathogen can also disrupt the innate immunity process by subverting various myeloid cells engaged in the immune response[159, 160]. Recent studies have explained the constitutive negative element – a nutrient-replete niche that supports bacterial growth and tissue damage by neutrophilic inflammation during Mtb infection[161]. Moreover, *NOS2*$^{-/-}$ mice were found to have enhanced neutrophil influx into the lung promoting TB susceptibility[161], which unswervingly supports the significance of compulsive frequencies of neutrophils in the lungs of the male LysM^{cre}PKCδ$^{flox/flox}$ mice producing fewer nitrogen intermediates in response to acute Mtb infection compared to the PKCδ$^{flox/flox}$ mice. Among the major myeloid cells at the site of infection, macrophages play a key role both in disease control as well as progression[151]. Studies have implemented a restrictive nature of interstitial macrophages (IM) exhibiting a distinct metabolic state in contrast to alveolar macrophages[151]. We inferred that increased mycobacterial burden may be directly associated with reduced frequencies of IM in the male LysM^{cre}PKCδ$^{flox/flox}$ mice. Also, mice-derived IM subsets are known to be the foremost producers of IL-10 among macrophage/monocyte lineages[162]. Therefore, reduced IL-10 levels in the lungs of the male LysM^{cre}PKCδ$^{flox/flox}$ mice indeed support this immunophenotypic outcome of depleting

inflammatory macrophages during Mtb infection. Additionally, GM-CSF has also been well-documented in terms of its role in mediating Mtb infection control and inflammation in vivo[163, 164]. Besides, despite no variations in the frequencies of alveolar macrophages, astonishingly, GM-CSF levels were significantly reduced during the disease progression as previous studies demonstrated an unblemished relationship between GM-CSF and alveolar macrophages related bactericidal activity[165]. While GM-CSF can be produced by a variety of host immune cells such as macrophages, conventional/ non-conventional T cells, and alveolar epithelial cells[153], we were limited by the *in vivo* environment to be able to determine the major sources of GM-CSF in the absence of PKCδ in macrophages and whether this reduction is directly linked to alveolar macrophages.

An interesting and unique observation of our study is the apparent sex differences in immunomodulatory functions of macrophage-specific deficiency of PKCδ during Mtb infection. While the male $LysM^{cre}PKC\delta^{flox/flox}$ mice showed both lymphoid and myeloid-centric inflammation with an enriching environment for mycobacterial survival and proliferation, female $LysM^{cre}PKC\delta^{flox/flox}$ mice did not show any differences in the outcome of TB disease. Previous findings by Li and colleagues have demonstrated the male-specific functional role of PKCδ in osteoclasts and significant alteration of differentially expressed genes and signalling dominant in males[126]. As a result, it seems reasonable that the gender difference found in different studies might also occur in other reported experimental disease models. Therefore, it is important to examine phenotypic characteristics in both sexes. Nevertheless, the molecular mechanism underlying macrophage-specific PKCδ deficiency and its gender-biased role needs to be explored further.

In summary, our data provide adequate evidence demonstrating the deletion of PKCδ in macrophages worsened disease outcomes with exaggerated lung pathology. More importantly, we showed that macrophage-specific PKCδ is critical in the pathogenesis of TB with an early lymphocytic immune response and decreased inflammatory macrophages promoting bacterial persistency and dissemination *in vivo*. This work contributes to our understanding of the immunomodulatory functions of macrophage-specific PKCδ deficiency and might aid as a key immune regulator employed by the host myeloid cell to control the exacerbation of Mtb infection *in vivo*.

3.6. Acknowledgements

We are extremely grateful to the UCT Research Animal Facility (RAF) and Mr. Rodney Lucas for providing us the facility to conduct animal research, Ms. Munadia Ansarie for her contribution to animal breeding, genotyping, and maintenance, and Ms. Zarinah Sonday for providing us sterile lab environment. We also express gratitude to the Wellcome Centre for Infectious Diseases Research in Africa (CIDRI-Africa) for supporting this study with WUN CIDRI Ph.D. Scholarship 2019-2022. The study was carried out using the BSL3 platform with core funding from the Wellcome Trust (203135/Z/16/Z).

3.7. Supplementary Figures

Supplementary Figure 1.

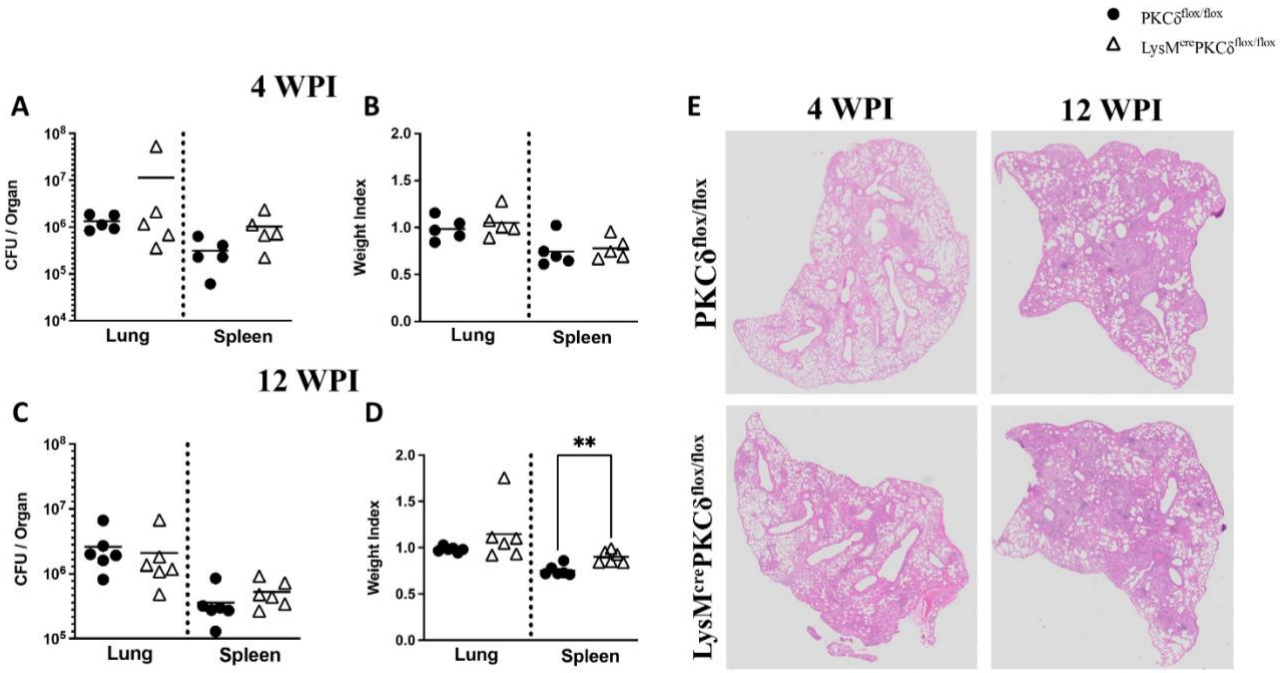

Supplementary Figure 1. Acute and Chronic Mtb infection showed no impact on the mycobacterial burden and lung pathology in the female LysM^{cre}PKCδ$^{flox/flox}$ mice. HN878 Mtb strain was challenged intranasally to female LysM^{cre}PKCδ$^{flox/flox}$ and PKCδ$^{flox/flox}$ mice at 150 CFU/mouse (n=5-6 mice/group). Animals were euthanized to determine lung/spleen CFU burden, and lung/spleen weight index at [A-B] acute stage (4 wpi) and [C-D] chronic stage (12 wpi) of Mtb infection. All data are shown as mean and are representative of two independent experiments (n=6 mice/group). [E] At 4 weeks and 12 weeks post-infected Mtb infected lung sections with their respective (40X) scanned images from female LysM^{cre}PKCδ$^{flox/flox}$ and PKCδ$^{flox/flox}$ mice were stained for H&E. Statistical analyses were performed using an unpaired student t-test. Asterisks are defining significance compared to the control group as: **$p < 0.01$.

Supplementary Figure 2.

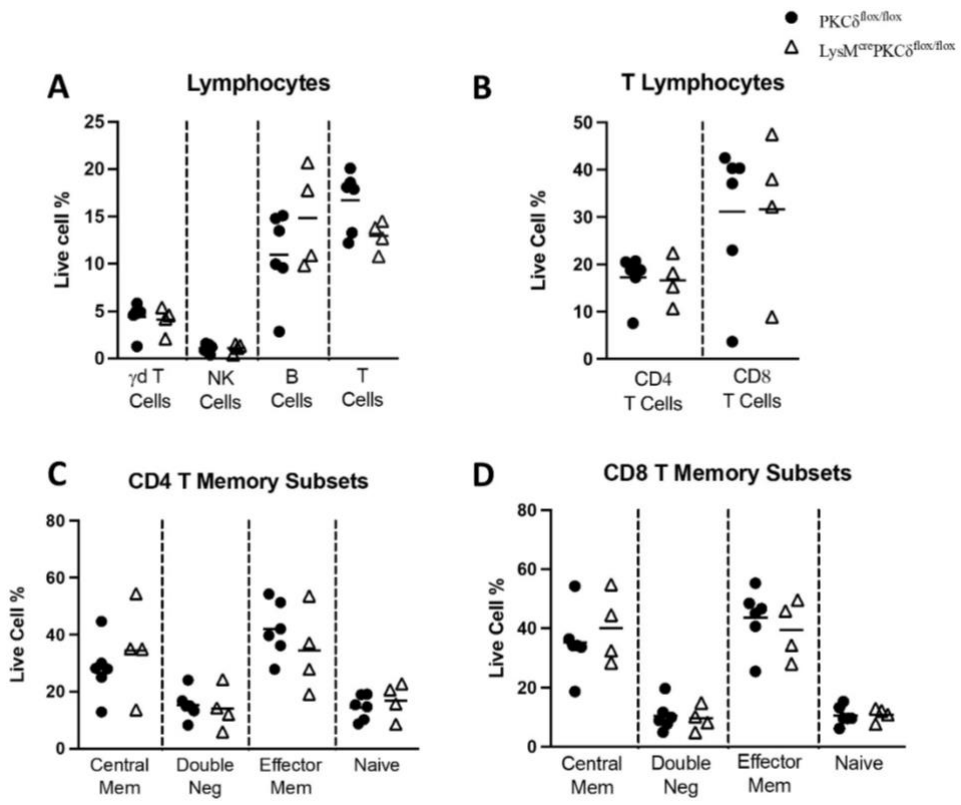

Supplementary Figure 2. Lymphoid cell population of thoracic lymph nodes in male LysM^{cre}PKCδ$^{flox/flox}$ mice during the acute stage of Mtb infection. [A-D] Mtb infected lymph nodes were collected, weighed, and processed for single-cell suspension from both PKCδ$^{flox/flox}$ and LysM^{cre}PKCδ$^{flox/flox}$ male mice at 4 weeks following surface stained and acquired for different immune cell populations using flow cytometric analysis. Surface markers determining different immune cell populations are as following: Lymphoid markers - Gamma delta (γδ) T cells: CD3+gdTCR+; Natural Killer (NK) cells: NK1.1+CD3-; B cells: CD19+CD3-; T cells: CD3+CD19-; CD4 T cells: CD3+CD4+; CD8 T cells: CD3+CD8+; CD4+ Naive: CD3+CD4+CD62L+CD44-; CD4+ Central Memory: CD3+CD4+CD62L+CD44+; CD4+ Effector/Effector Memory: CD3+CD4+CD44+CD62L-; CD4+ Double Negative: CD3+CD4+CD44-CD62L-; CD8+ Naive = CD3+CD8+CD62L+CD44- ; CD8+ Central Memory = CD3+CD8+CD62L+CD44+ ; CD8+ Effector/Effector Memory = CD3+CD8+CD44+ CD62L-; CD8+ Double Negative: CD3+CD4+CD44-CD62L-. All data shown are representative of two independent experiments. Statistical analyses were performed using an unpaired student t-test.

Supplementary Figure 3.

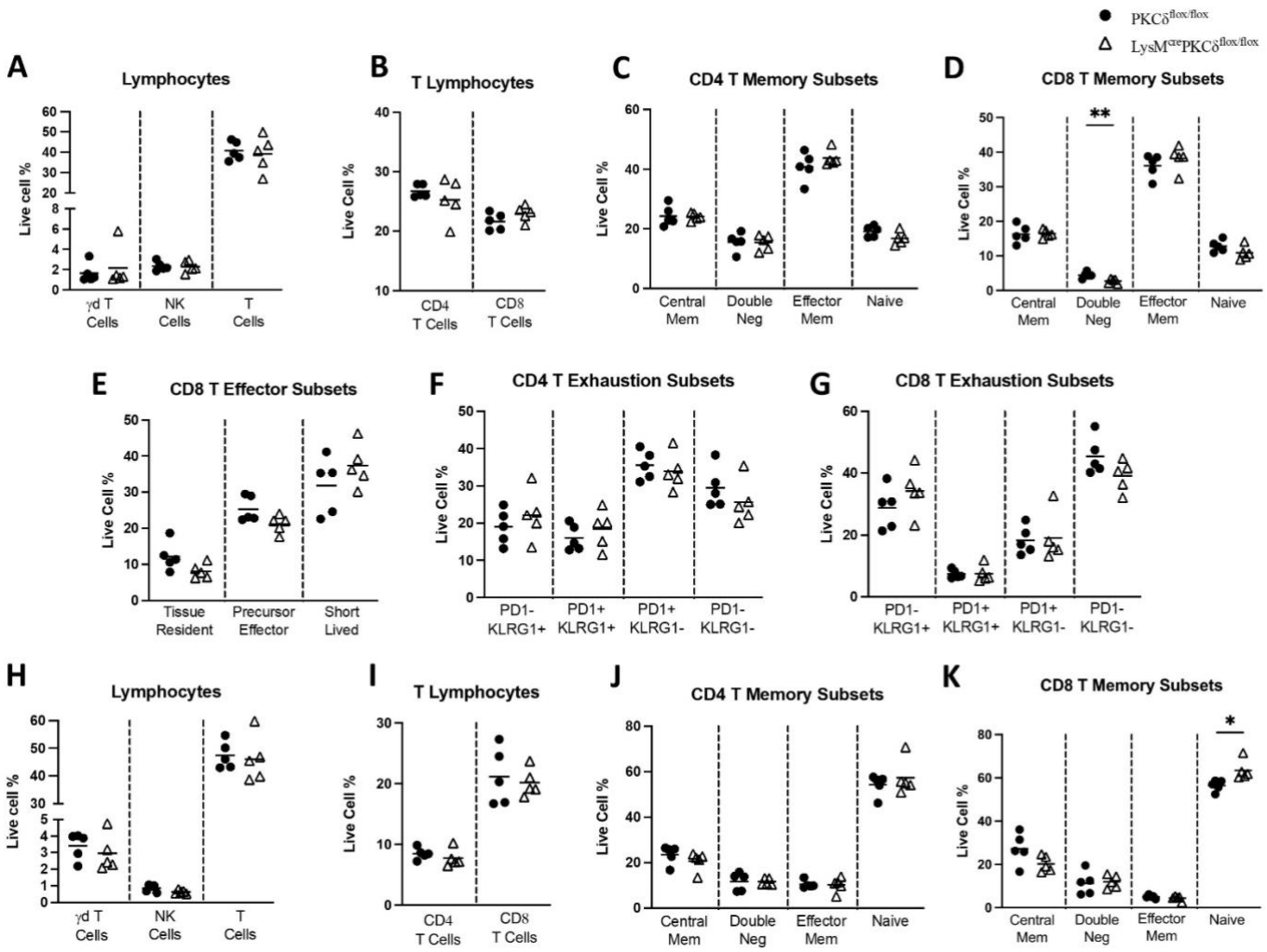

Supplementary Figure 3. Acute Mtb infection showed no impact on female LysM^{cre}PKCδ$^{flox/flox}$ mice. Representative [A-G] lung lymphoid population, [H-K] lymph node lymphoid population at 4 weeks post Mtb infection. Surface markers determining different immune cell populations are as following: lymphoid markers (lung/lymph node) - Gamma delta (γδ) T cells: CD3+gdTCR+; Natural Killer (NK) cells: NK1.1+CD3-; T cells: CD3+CD19-; CD4 T cells: CD3+CD4+; CD8 T cells: CD3+CD8+; CD4+ Naive: CD3+CD4+CD62L+CD44-; CD4+ Central Memory: CD3+CD4+CD62L+CD44+; CD4+ Effector/Effector Memory: CD3+CD4+CD44+CD62L-; CD4+ Double Negative: CD3+CD4+CD44-CD62L-; CD8+ Naive = CD3+CD8+CD62L+CD44- ; CD8+ Central Memory = CD3+CD8+CD62L+CD44+ ; CD8+ Effector/Effector Memory = CD3+CD8+CD44+ CD62L-; CD8+ Double Negative: CD3+CD4+CD44-CD62L-; CD4+ Exhaustion Memory (lung): CD3+CD4+PD1-KLRG1+; CD8+ Exhaustion Memory (lung): CD3+CD8+PD1-KLRG1+; CD8+ Tissue Resident Memory: CD3+CD8+CD103+CD69+; CD8+ Memory Precursor: CD3+CD8+KLRG1-CD127+; CD8+ Short-lived Effector: CD3+CD8+KLRG1+CD127-. All data shown are representative of two independent experiments. Statistical analyses were performed using an unpaired student t-test. Asterisks are defining significance compared to the control group as : *$p < 0.05$, **$p < 0.01$.

Supplementary Figure 4.

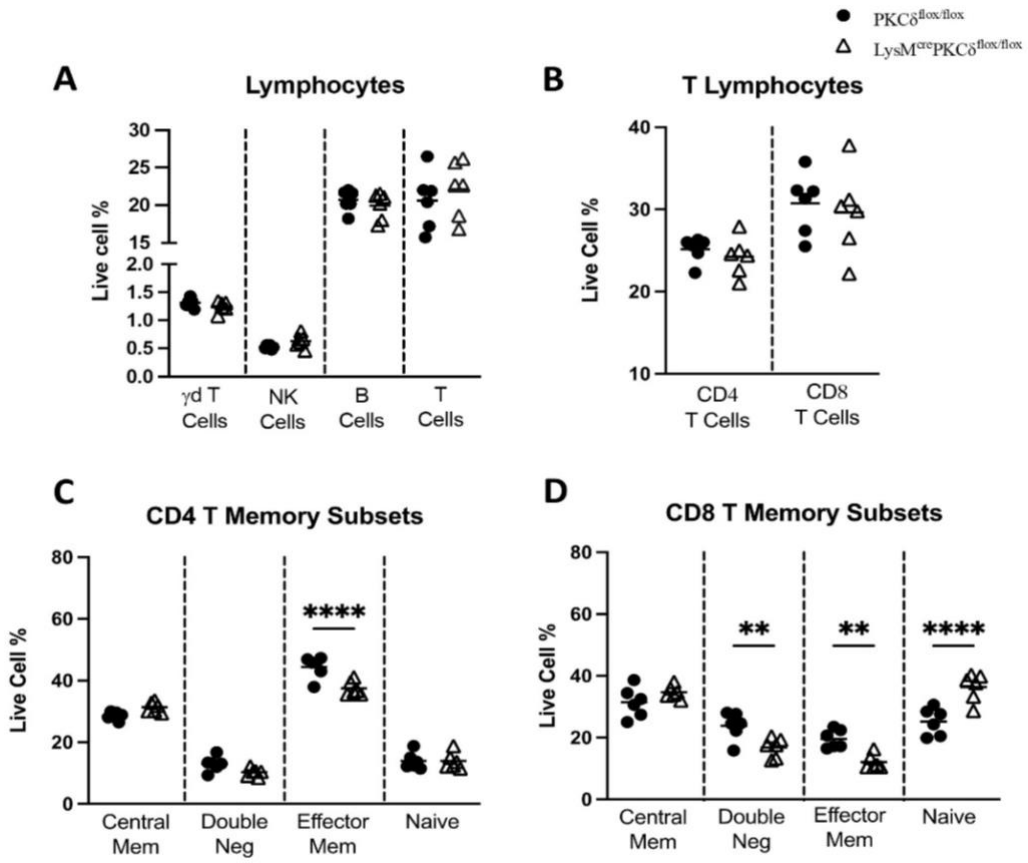

Supplementary Figure 4. Lymphoid cell population of thoracic lymph nodes in male LysM^{cre}PKCδ$^{flox/flox}$ mice during the chronic stage of Mtb infection. [A-D] Mtb infected lymph nodes were collected, weighed, and processed for single-cell suspension from both PKCδ$^{flox/flox}$ and LysM^{cre}PKCδ$^{flox/flox}$ male mice at 12 weeks following surface stained and acquired for different immune cell populations using flow cytometric analysis. Surface markers determining different immune cell populations are as following: Lymphoid markers - Gamma delta (γδ) T cells: CD3+gdTCR+; Natural Killer (NK) cells: NK1.1+CD3-; B cells: CD19+CD3-; T cells: CD3+CD19-; CD4 T cells: CD3+CD4+; CD8 T cells: CD3+CD8+; CD4+ Naive: CD3+CD4+CD62L+CD44-; CD4+ Central Memory: CD3+CD4+CD62L+CD44+; CD4+ Effector/Effector Memory: CD3+CD4+CD44+CD62L-; CD4+ Double Negative: CD3+CD4+CD44-CD62L-; CD8+ Naive = CD3+CD8+CD62L+CD44- ; CD8+ Central Memory = CD3+CD8+CD62L+CD44+ ; CD8+ Effector/Effector Memory = CD3+CD8+CD44+ CD62L-; CD8+ Double Negative: CD3+CD4+CD44-CD62L-. All data shown are representative of two independent experiments. Statistical analyses were performed using an unpaired student t-test. Asterisks are defining significance compared to the control group as : **$p < 0.01$, ****$p < 0.0001$.

Supplementary Figure 5.

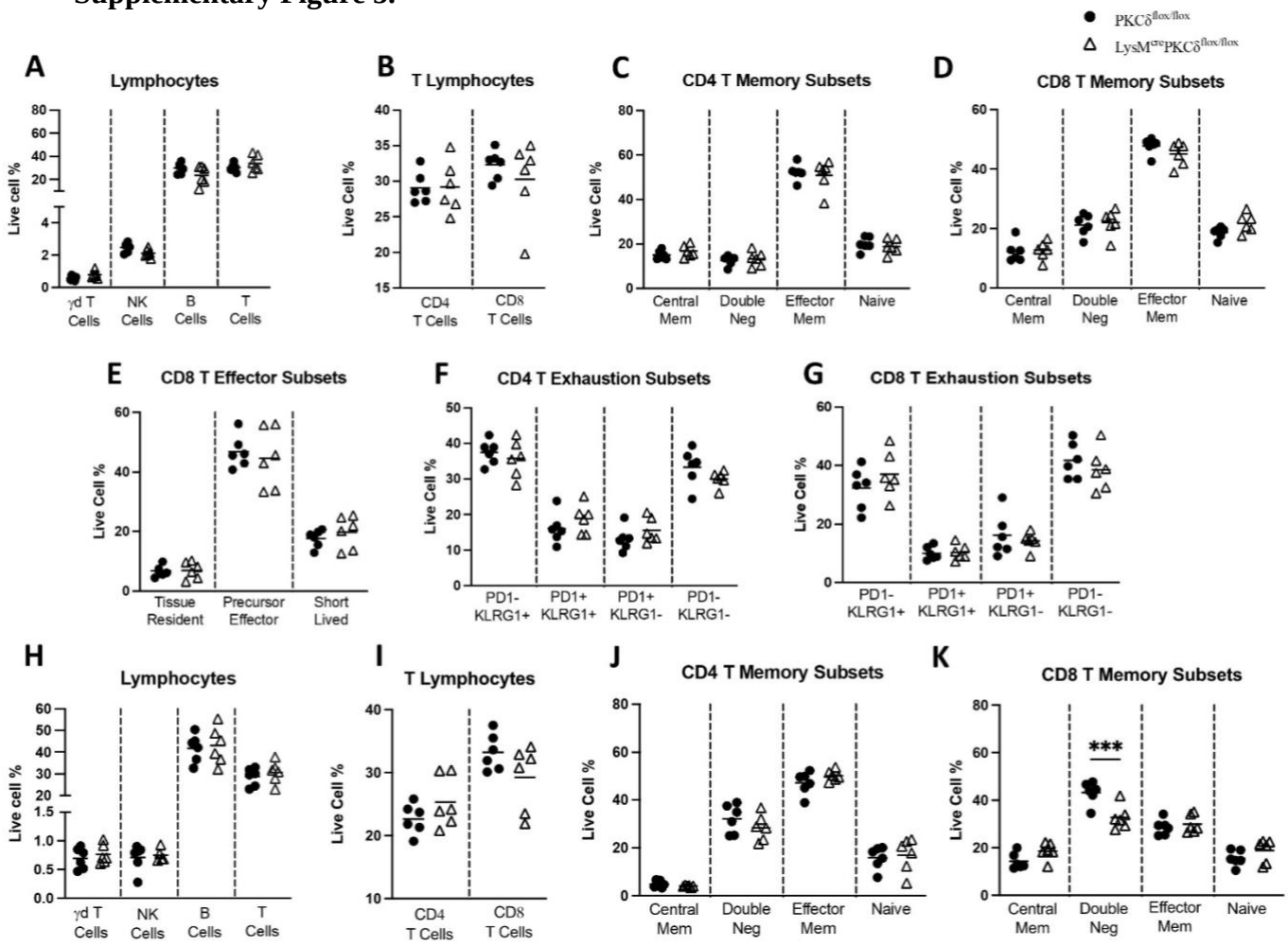

Supplementary Figure 5. Chronic Mtb infection showed no major impact on female LysM^{cre}PKCδ$^{flox/flox}$ mice. Representative [A-G] lung lymphoid population, [H-K] lymph node lymphoid population at 12 weeks post Mtb infection. Surface markers determining different immune cell populations are as following: lymphoid markers (lung/lymph node) - Gamma delta (γδ) T cells: CD3+gdTCR+; Natural Killer (NK) cells: NK1.1+CD3-; B cells: CD19+CD3-; T cells: CD3+CD19-; CD4 T cells: CD3+CD4+; CD8 T cells: CD3+CD8+; CD4+ Naive: CD3+CD4+CD62L+CD44-; CD4+ Central Memory: CD3+CD4+CD62L+CD44+; CD4+ Effector/Effector Memory: CD3+CD4+CD44+CD62L-; CD4+ Double Negative: CD3+CD4+CD44-CD62L-; CD8+ Naive = CD3+CD8+CD62L+CD44- ; CD8+ Central Memory = CD3+CD8+CD62L+CD44+ ; CD8+ Effector/Effector Memory = CD3+CD8+CD44+ CD62L-; CD8+ Double Negative: CD3+CD4+CD44-CD62L-; CD4+ Exhaustion Memory (lung): CD3+CD4+PD1-KLRG1+; CD8+ Exhaustion Memory (lung): CD3+CD8+PD1-KLRG1+; CD8+ Tissue Resident Memory: CD3+CD8+CD103+CD69+; CD8+ Memory Precursor: CD3+CD8+KLRG1-CD127+; CD8+ Short-lived Effector: CD3+CD8+KLRG1+CD127-. All data shown are representative of two independent experiments. Statistical analyses were performed using an unpaired student t-test. Asterisks are defining significance compared to the control group as: ***$p < 0.001$.

Supplementary Figure 6.

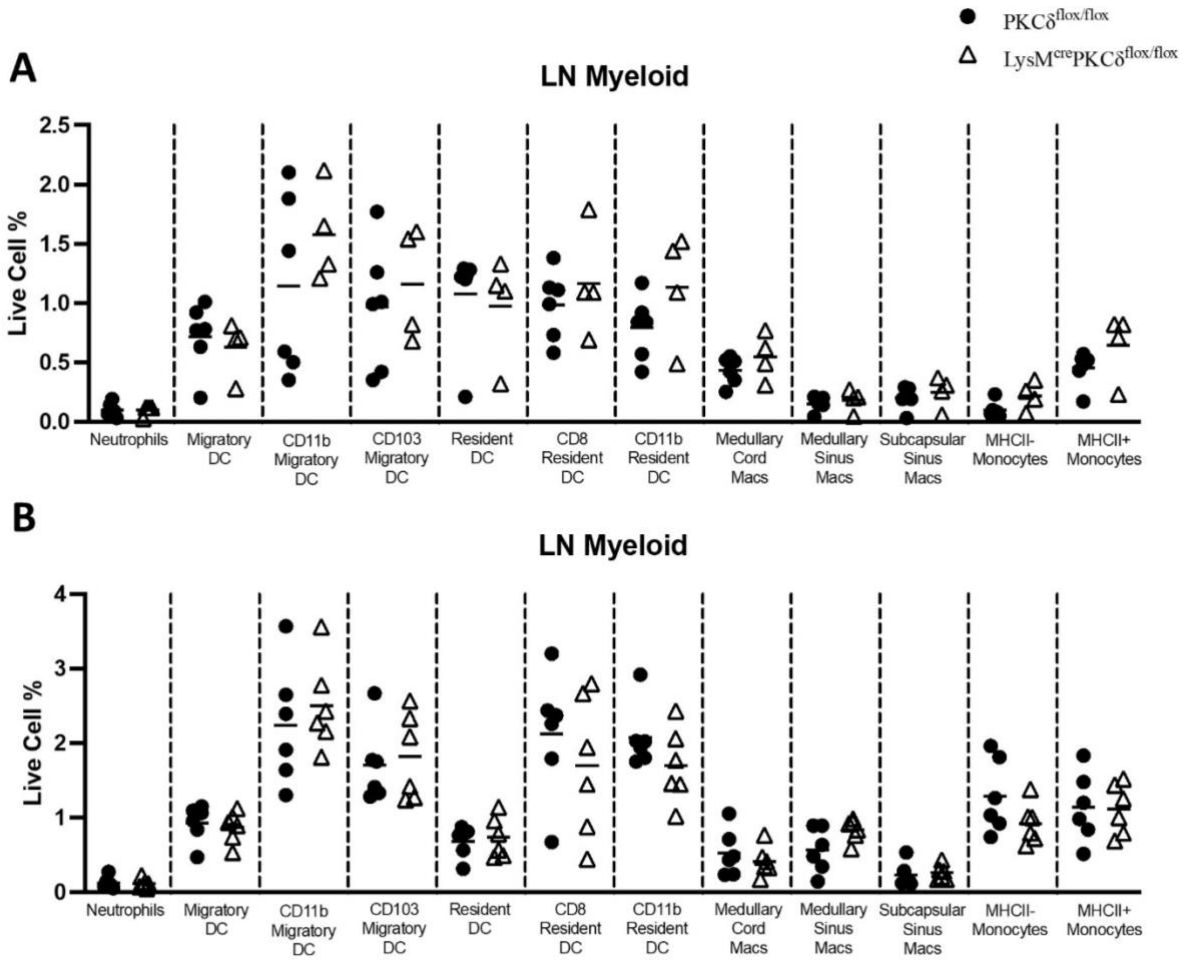

Supplementary Figure 6. Myeloid cell population of thoracic lymph nodes in male LysM^{cre}PKCδ$^{flox/flox}$ mice during the acute and chronic stage of Mtb infection. Representative of various lymph node myeloid cell populations at the [A] acute and [B] chronic stage of Mtb infection. Surface markers determining different immune cell populations are as following: myeloid markers (lymph node): Neutrophils: Ly6G+CD11b+; Migratory DC: CD11c+MHCIIhigh; CD11b+ Migratory DC: CD11c+MHCIIhighCD11b+CD103-; CD103+ Migratory DC: CD11c+MHCIIhighCD103+CD11b-; Resident DC: CD11c+MHCIIlow; CD8+ Resident DC: CD11c+MHCIIlowCD8+CD11b-; CD11b+ Resident DC: CD11c+MHCIIlowCD11b+CD8-; Medullary Cord Macrophages: CD11b+F4/80+CD169-; Medullary Sinus Macrophages: CD11b+F4/80-CD169+; Subcapsular Sinus Macrophages: CD11b+F4/80+CD169+; MHCII- Monocytes: Ly6C+MHCIIlow; MHCII+ Monocytes: Ly6C+MHCIIhigh. All data shown are representative of two independent experiments. Statistical analyses were performed using an unpaired student t-test.

Supplementary Figure 7.

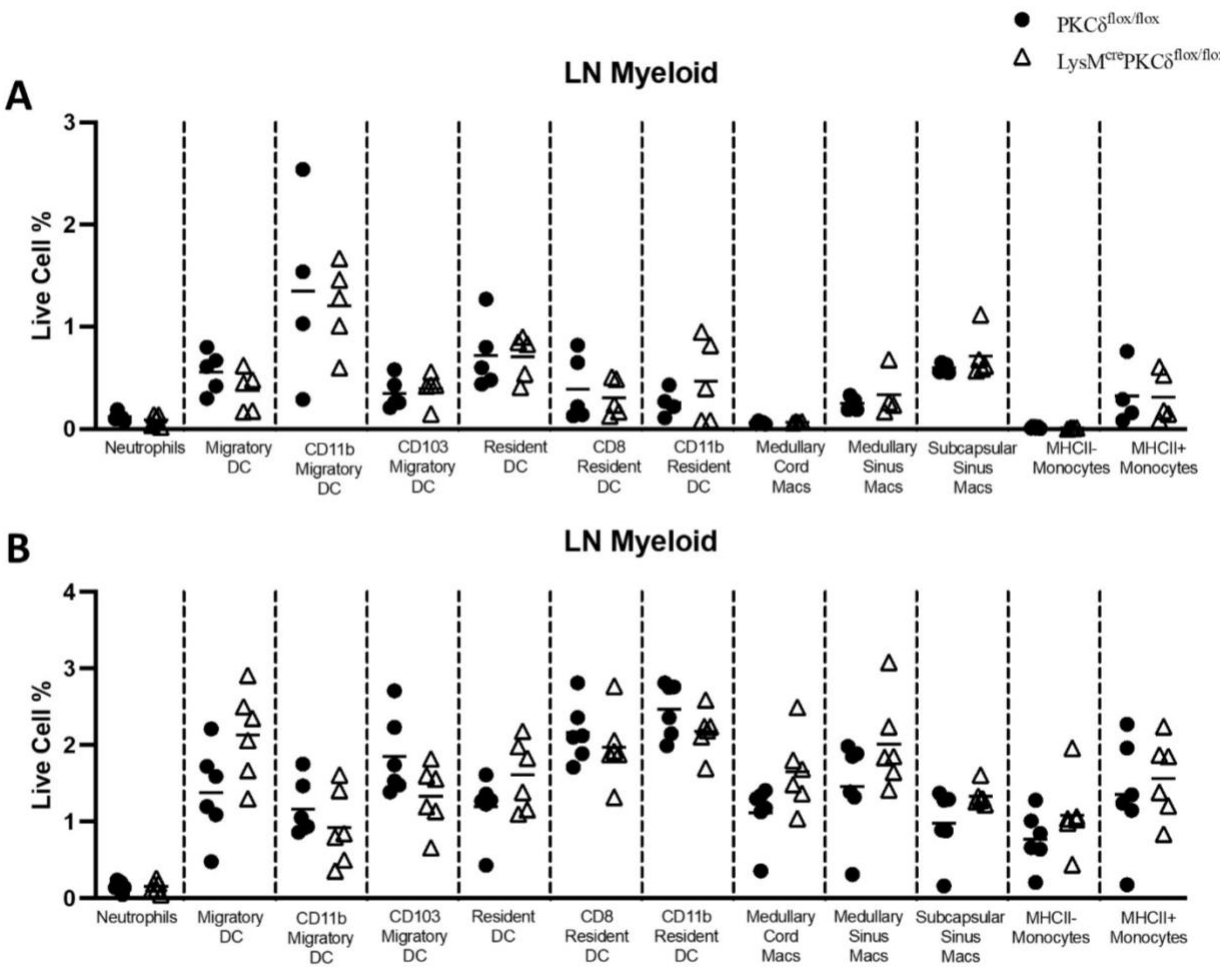

Supplementary Figure 7. Myeloid cell population in thoracic lymph nodes in female LysM^{cre}PKCδ$^{flox/flox}$ mice during the acute and chronic stage of Mtb infection. Representative of various lymph node myeloid cell populations at the [A] acute and [B] chronic stage of Mtb infection. Surface markers determining different immune cell populations are as following: myeloid markers (lymph node): Neutrophils: Ly6G+CD11b+; Migratory DC: CD11c+MHCIIhigh; CD11b+ Migratory DC: CD11c+MHCIIhighCD11b+CD103-; CD103+ Migratory DC: CD11c+MHCIIhighCD103+CD11b-; Resident DC: CD11c+MHCIIlow; CD8+ Resident DC: CD11c+MHCIIlowCD8+CD11b-; CD11b+ Resident DC: CD11c+MHCIIlowCD11b+CD8-; Medullary Cord Macrophages: CD11b+F4/80+CD169-; Medullary Sinus Macrophages: CD11b+F4/80-CD169+; Subcapsular Sinus Macrophages: CD11b+F4/80+CD169+; MHCII- Monocytes: Ly6C+MHCIIlow; MHCII+ Monocytes: Ly6C+MHCIIhigh. All data shown are representative of two independent experiments. Statistical analyses were performed using an unpaired student t-test.

Supplementary Figure 8.

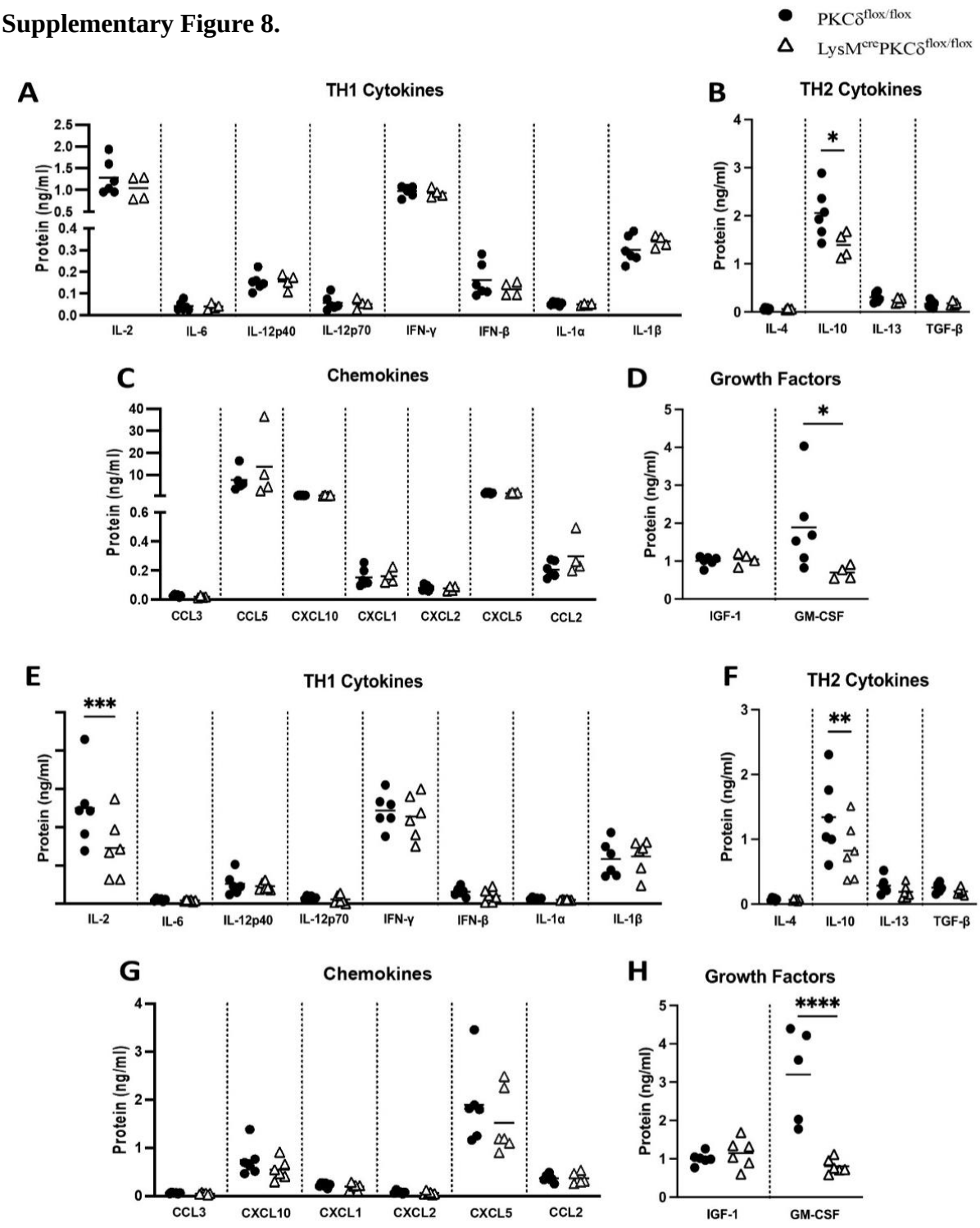

Supplementary Figure 8. Cytokine profiling of female LysM^{cre}PKCδ$^{flox/flox}$ mice exhibits no effects on cytokines, chemokines, and growth factors. [A-D] 4 weeks and [E-H] 12 weeks post-infected lung homogenates were collected from both female PKCδ$^{flox/flox}$ and LysM^{cre}PKCδ$^{flox/flox}$ mice to determine an array of different cytokines TH1: IL-2, IL-6, IL-12p40, IL-12p60, IFN-**γ**, IFN-**β**, IL-1**α**, IL-1**β**; TH2: IL-4, IL-5, IL-10, IL-13, TGF-**β**; chemokines (CCL3, CCL5, CXCL10, CXCL1, CXCL2, CXCL5) and growth factors (IGF-1, GM-CSF) levels. All data shown are representative of two independent experiments. Statistical analyses were performed using an unpaired student t-test.

CHAPTER 4: Manuscript in preparation

Protein Kinase C δ: a critical hub for immunomodulatory functions in macrophages during *Mycobacterium tuberculosis* infection *in vitro*

Rudranil Hazra[1,2], Shelby-Sara Jones[1,3], Mumin Ozturk[3,4], Sibongiseni K.L. Poswayo[3], Robert Rousseau[3], Saiyukthi Naidoo[3], Nashied Peton[5], Anca F. Savulescu[6], Raymond Moseki[1], Frank Brombacher[1,3], Robert J. Wilkinson[1,7], Suraj P. Parihar[1,2,3*]

[1] Wellcome Centre for Infectious Diseases Research in Africa (CIDRI-Africa), Institute of Infectious Diseases and Molecular Medicine (IDM), Faculty of Health Sciences, University of Cape Town, Cape Town 7925, South Africa.

[2] Division of Medical Microbiology, Institute of Infectious Diseases and Molecular Medicine (IDM), Department of Pathology, Faculty of Health Sciences, University of Cape Town, Cape Town 7925, South Africa.

[3] Division of Immunology, South African Medical Research Council (SAMRC) Immunology of Infectious Diseases, and International Centre for Genetic Engineering and Biotechnology (ICGEB), Cape Town Component, Institute of Infectious Diseases and Molecular Medicine (IDM), Department of Pathology, Faculty of Health Sciences, University of Cape Town, Cape Town 7925, South Africa.

[4] Epigenomics & Single Cell Biophysics Group, Department of Cell Biology FNWI, Radboud University, Nijmegen, Netherlands.

[5] Drug Discovery and Development Centre (H3D), University of Cape Town, Cape Town 7925, South Africa.

[6] Division of Chemical, Systems & Synthetic Biology, Institute of Infectious Diseases & Molecular Medicine (IDM), Faculty of Health Sciences, University of Cape Town, Cape Town, South Africa.

[7] Francis Crick Institute and Department of Infectious Diseases, Imperial College London, London, UK.

[*] Correspondence: A/Prof. Suraj P. Parihar, suraj.parihar@uct.ac.za

Keywords: PKCδ, Immunomodulatory functions, *Mycobacterium tuberculosis*

4.1. Abstract

Mycobacterium tuberculosis (Mtb) has acquired the strategy of prolonged survival inside the host by evading its defense mechanisms. As a primary host during initial Mtb infection, macrophages modulate an array of inflammatory functions to provide protection and restrict bacterial dissemination from the primary site. Several macrophage immune determinants are responsible for modulating inflammatory responses during Mtb infection. One such crucial macrophage immune determinant, Protein Kinase C δ (PKCδ), has been previously recognized for its protective role via killing effector functions aiding in bacterial clearance. Increased PKCδ expression has also been shown to be a marker of lung inflammation in active TB patients. In this study, we have comprehensively investigated the role of PKCδ in macrophages during Mtb infection utilizing $LysM^{cre}PKC\delta^{flox/flox}$ derived BMDMs compared to the littermate control ($PKC\delta^{flox/flox}$). Our data show an unblemished phenotype of increased bacterial burden in the absence of PKCδ in macrophages whereas overexpression reversed the phenotype. Mechanistically, the increased bacterial burden is also associated with varying antimicrobial effector functions and elevated proinflammatory cytokine levels in the absence of PKCδ in BMDMs. Further investigation reveals an increased mRNA expression of the non-canonical inflammasome mediators and their dependency on dysregulated cellular metabolic ATP production in PKCδ deficient BMDMs compared to the littermate control. Interestingly, exogenous granulocyte-macrophage colony-stimulating factor (GM-CSF) stimulation of PKCδ deficient BMDMs shows reduced mycobacterial burden with restrictive cellular metabolic dysregulation caused by Mtb infection. Our study also reveals an increased mycobacterial burden in PKCδ silenced human monocyte-derived macrophages (MDMs) with a reduction in the level of pro-inflammatory cytokines. Moreover, we show an increased expression of PKCδ at the site of infection in bronchoalveolar lavage (BAL) samples from active TB patients compared to the household contacts. Also, PKCδ-mediated macrophage biological process enrichment was observed through metaproteome analysis. Altogether, these data suggest that the macrophage-specific PKCδ is crucial and a potential host immune responsive determinant that has a delicate role in protection against Mtb infection.

4.2. Introduction

Mycobacterium tuberculosis (Mtb), the causative agent of Tuberculosis (TB) has evolved with humans since prehistoric times and exists as the oldest global pandemic[166]. Currently, TB stands as the second deadliest death-causing disease worldwide after COVID-19[1]. The devastating consequences of COVID-19 also affected the usual treatment trends of standing TB cases and reduced notifications of newly formed active TB disease in individuals[1]. Prolonged treatment duration, drug-related toxicity, and existing co-morbidities contribute to patients' non-compliance, leading to the development of drug-resistant TB disease and mortality. With an increasing incidence of drug resistance TB cases, current concerns are also inclined toward the inability to distinguish unique host elements fostering susceptibility or resistance to TB disease[166]. To mitigate these dire limitations, research advancements in recent years developed an emerging strategy known as host-directed therapy (HDT) to modulate the host response against Mtb infection to improve diseases outcome[60]. The functional strategy of HDT comprises the identification of unique host determinants and fine-tuning them to modulate various host antimicrobial effector functions to limit inflammation and tissue damage by Mtb infection[60]. Hence, detecting such HDT determinants and understanding their role in TB pathogenesis is a crucial approach, conducive to the eradication of dormant Mtb bacilli with existing anti-TB treatments[60, 66, 139].

The initiation of host immunity to infection advances following the phagocytic uptake of Mtb bacilli by macrophages in the pulmonary microenvironment[74]. Primary Mtb infection-mediated systemic immunity has been extensively studied, revealing macrophage-driven response as a 'central dogma' of protection[167]. Knowingly, macrophages are the frontline immune cells modulating the inflammatory process, maintaining immune homeostasis, and restricting mycobacterial burden and dissemination from the primary site of infection[166]. However, Mtb can thrive within the macrophages and evade all these host immune responses by utilizing them in its favor[168]. Mtb-macrophage interplay embraces various aspects of cellular intrinsic mechanisms such as the production of free-radical intermediates (Reactive oxygen, nitrogen), phagolysosomal fusion, cellular apoptosis, antigen presentation for subsequent adaptive immunity, and cytokine-driven assembly of peripheral immune cells and inflammatory responses[169]. Hence, understanding the macrophage immune evasion mechanisms modulated by Mtb is important to identify novel immune modulators for better control of TB. Previously, one such immune modulator, Protein Kinase C δ (PKCδ), has been recognized as a marker of inflammation in TB disease progression and

a crucial kinase for maintaining macrophage-killing effector functions, leading to the protection against Mtb infection in mice[88]. In this study, the authors exploited the deficiency of PKCδ modulated immune response against Mtb infection in mice[88]. The increased intracellular mycobacterial burden in bone-marrow-derived macrophages (BMDMs) isolated from global PKCδ knockout mice ($PKC\delta^{-/-}$), also displayed reduced production of reactive oxygen species (ROS) and nitric oxide (NO) intermediates. This study also showed that PKCδ-mediated bacterial killing is independent of phagosome maturation and autophagy, which are the key macrophage antimicrobial strategies against Mtb infection[88]. The global knockout ($PKC\delta^{-/-}$) mice model, however, may omit the peripheral PKCδ exhibiting cellular influence on macrophages during Mtb infection *in vivo*, making it unable to examine the macrophage-inclusive role of PKCδ in modifying antimicrobial effector activities. To address this, we have isolated BMDMs from the macrophage-specific PKCδ knockout model ($LysM^{cre}PKC\delta^{flox/flox}$) to exploit the orchestrated immune response in the ablation of PKCδ only in macrophages during Mtb infection. Our results mirrored the increased susceptibility of $LysM^{cre}PKC\delta^{flox/flox}$ mice to Mtb infection (Chapter 3) in isolated BMDMs compared to the littermate BMDMs. Interestingly, overexpression of PKCδ in a murine macrophage cell line, on the other hand, reduces the mycobacterial load. We further investigated, how Mtb survival was carried out by PKCδ-deficient macrophage influenced different antimicrobial effectors functions. Elevated proinflammatory cytokine-mediated localized inflammasome response was also detected in PKCδ deficient BMDMs during Mtb infection. Exceptionally, we have identified cellular metabolic ATP dysregulation in the absence of PKCδ in BMDMs during Mtb infection, which was restricted by exogenous granulocyte-macrophage colony-stimulating factor (GM-CSF) stimulation, leading to reduced bacterial replication. Our results show similar findings of increased bacterial replication in human monocyte-derived macrophages (MDMs) with a reduction in the major pro-inflammatory cytokine levels. Additionally, proteomic analysis revealed that PKCδ mediated dysregulation of regulatory proteins during Mtb infection contributes to various macrophage biological processes. Overall, the inflammatory responses elicited by PKCδ demonstrated that this novel kinase is a crucial hub for immunoregulatory functions in macrophages during Mtb infection.

4.3. Methods

4.3.1. Generation of bone-marrow-derived macrophages

As previously described, bone-marrow-derived macrophages (BMDMs) were generated from 8-12 weeks old $PKC\delta^{flox/flox}$ and $LysM^{cre}PKC\delta^{flox/flox}$ mice [132]. Briefly, bone marrow cells were flushed out from femurs and cultured for 10 days at 37°C under 5% CO_2 in sterile tissue culture grade Petri dishes (140mm x 20mm Petri dish, Nunc, Denmark) consisting of PLUTZNIK media (DMEM containing 30% L929 cell-conditioned medium, 10% fetal calf serum, 5% horse serum, 1 mM sodium pyruvate, 2 mM L-glutamine, 0.1 mM β-mercaptoethanol, 100 U/ml penicillin G, and 100 µg/ml streptomycin. BMDMs were harvested and plated in desired culture plates in complete media (DMEM with 10% fetal calf serum) to proceed with the downstream experimental procedure.

4.3.2. Lentiviral overexpression

RAW264.7 murine macrophage cell line was obtained from ATCC, cultured, passaged, and seeded at $0.5x10^5$ cells in a tissue culture grade 24-well plate for following lentivirus-packaged ORF clone of PKCδ (MR225184L4V, Origene) transduction according to the manufacturer's protocol. Briefly, frozen lentivirus particles were thawed and added to the cells with a fresh culture medium (DMEM with 10% fetal calf serum) of 500µl at a multiplicity of infection (MOI) 5 with 8 µg/ml of Polybrene (Sigma). Cells were incubated with the lentivirus-contained medium for 18-20 hours at 37°C and replaced with a fresh medium, followed by the stable cell selection with 2.5 µg/ml Puromycin (ThermoFisher) for 10-14 days. PKCδ overexpressed cells were detected using a ZOE fluorescence microscope (BioRad) for GFP expression, followed by the collection of RNA and protein for overexpression confirmation by qRT-PCR and western blot, respectively, and downstream Mtb infection (MOI 1) experiment.

4.3.3. Mtb infection and determination of mycobacterial burden

A virulent strain of Mtb (HN878) was grown in complete 7H9 media to log phase and glycerol stocks were made for *in-vitro* infection of the BMDMs and MDMs as previously described[77]. Stock solutions of Mtb were thawed and washed once with 1X phosphate-buffered saline (PBS) to get rid of glycerol before infection. Seeded BMDMs and MDMs were

infected with a multiplicity of infection (MOI) 1 and 5, respectively. At indicated time points, cells were washed with 1X phosphate-buffered saline (PBS), lysed with 0.1% Triton X-100, followed by 10- and 100- fold dilution, and plated on Middlebrook 7H10 (BD Biosciences) agar plates supplemented with 10% OADC and 0.5% glycerol. Agar plates were incubated for 14-21 days at 37°C before colonies were counted. RNA and protein were collected at indicated time points from Mtb infected cells for downstream process. A similar procedure was followed for the enumeration of mycobacterial load in PKCδ overexpressed and control RAW264.7 murine macrophage cells.

4.3.4. Western blot analysis

As previously described, sodium dodecyl sulfate-polyacrylamide gel electrophoresis (SDS-PAGE) and Western Blot analysis were performed [67]. Briefly, PKCδ overexpressed and control RAW264.7 murine macrophage cells (3×10^6) were seeded in a 6-well tissue culture graded plate containing complete media (DMEM containing 10% fetal calf serum) overnight at 37°C under a 5% CO_2 incubator. Cells were washed and lysed with ice-cold RIPA buffer containing protease and phosphatase inhibitors for 30 min at 4°C. BCA Protein Assay Kit (Thermofisher Scientific Pierce™, cat# 23225) was used to determine the total protein concentration. An equal amount (20 µg) of protein were boiled at 100°C for 5 min with 1X loading dye (2% SDS, 5% 2-mercaptoethanol, 10% glycerol, 0.002% bromophenol blue, 0.62 M Tris-HCl, pH 6.8). Samples were then electrophoresed on 12% SDS-PAGE gel (Mini-PROTEAN® system, Bio-Rad) and transferred to nitrocellulose membrane (Sigma) using the Mini Trans-Blot® Cell system (Bio-Rad). The membrane blocking was done for 2 hours on a shaker at room temperature with 5% w/v BSA, 1X TBS (20 mM Tris with 150 mM NaCl), and 0.1% Tween20 (blocking buffer). Next, the membrane was probed with recombinant anti-PKC delta antibody (Abcam; ab182126) or GAPDH [Santa Cruz Biotechnology; (sc47724)] primary antibodies (in 5% BSA blocking buffer; 1:1000 dilution) according to the manufacturer's protocol at 4°C overnight and goat anti-rabbit IgG H&L (Abcam; ab97040) secondary antibody (in 5% BSA blocking buffer; 1:10000 dilution) at room temperature for one hour. Immunoblots were developed using the KPL LumiGLO® Reserve Chemiluminescent Substrate Kit (SeraCare Life Sciences; cat# 5430-0042(54-61-02)) on the iBright FL1000 Imaging System (Thermofisher Scientific).

4.3.5. Quantitative real-time polymerase chain reaction (qRT-PCR)

RNA was extracted using the RNeasy Mini Kit (Qiagen, cat# 74106) from stored RNA samples in 350 µl of RLT lysis buffer with 3.5 µl β-mercaptoethanol. 400ng normalized RNA was reverse transcribed using a High-Capacity cDNA Reverse Transcription Kit (Applied Biosystems, cat# 4368814) with random primers to yield first-strand cDNA following the manufacturer's protocol. Desired gene expressions were amplified using Fast SYBR™ Green Master Mix (Applied Biosystems, cat# 4385612) and analyzed using Quantstudio 7 (Applied Biosystems, USA). The qRT-PCR conditions were as follows: Stage 1 (x1 cycle): Pre-incubation 95°C for 10 min; Stage 2 (x45 cycle): Denaturation 95°C for 15 sec, Annealing 60°C for 10 sec, Extension 72°C for 15 sec, Final acquisition 80°C for 1 sec. Desired gene expressions were normalized using an endogenous housekeeping control Hprt. Primer sequences are listed in *Appendix B* with their respective gene accession number.

4.3.6. Enzyme-Linked Immunosorbent Assay (ELISA) and Griess assay

BMDMs were seeded in a 96-well cell culture plate and infected with Mtb (MOI 1) at indicated time points, followed by the procurement of cell-free supernatant analyzed using a standard sandwich ELISA assay. Coating, standard, and detection antibodies were obtained from BD Biosciences, Biolegend, and R&D Scientific. The assay was performed to detect proinflammatory cytokines: IL-6, IL-1**α**, and IL-1**β** according to the manufacturer's dilutions and protocol. TMB microwell peroxidase substrate (KPL International) for streptavidin-HRP conjugates or 1 mg/ml p-nitrophenyl phosphate disodium salt hexahydrate (Sigma, cat# N2765) for streptavidin-AP conjugates. Nitrite levels in Mtb infected cell-free supernatants were measured using the Griess reagent assay. Briefly, cell supernatants were incubated with 1% sulfanilamide in 2.5% phosphoric acid for 10 minutes at room temperature in the dark, followed by 0.1% naphthyl-ethylene-diamine in 2.5% phosphoric acid for another 10 minutes. VersaMax™ microplate spectrophotometer (Molecular Devices, Sunnyvale, California) was used to measure optical densities.

4.3.7. Cellular and mitochondrial Reactive Oxygen Species (ROS) assay

BMDMs were seeded in a 96-well cell culture plate and infected with Mtb (MOI 1) at indicated time points, followed by incubation with either 5 µM CellROX Green Reagent

(ThermoFisher) or 100 nM MitoTracker Red CM-H2XRos (ThermoFisher) for 30 minutes at 37°C. Cells were then washed with 1X phosphate buffer saline (PBS) three times. Wells with only media were used as blank. Fluorescence was measured on Spectramax iD3 multi-mode reader (Molecular Devices) with the excitation of 485 nm and emission of 525 nm for CellROX and excitation of 579 nm and emission of 599 nm for MitoTracker intensity.

4.3.8. pHrodo labeling of Mtb and detection of phagosome maturation

Mtb stocks were thawed and labeled with 100 nM pHrodo iFL Green STP ester, amine-reactive dye (TheroFisher) in 100 mM sodium bicarbonate buffer (pH 8.5) at room temperature for 30 minutes. Labeled Mtb the washed with 1X phosphate buffer saline (PBS) three times before infection of BMDMs. Phagolysosomal pH-mediated fluorescence was recorded at indicated time points with excitation of 500 nm and emission of 540 nm on Spectramax iD3 multi-mode reader (Molecular Devices).

4.3.9. Flow cytometry

Mtb infected BMDMs were washed once with 1X phosphate buffer saline (PBS) and stained with dead cell marker (575V Viability Dye, BD Biosciences) for 15 min at room temperature. After that cells were washed with FACS buffer (0.5% BSA, 0.5% Sodium azide (NaN3), 1x PBS) and surface stained for the following surface markers: CD11b – PerCPCy5.5 (Clone M1/70), F4/80 – PeCy7 (Clone BM8), CD86 – AF700 (GL-1), MHCII – APC (Clone M5/114.15.2). Surface-stained cells were permeabilized and blocked (Permeabilization buffer + 2% IRS + 1% 2.4G2 FcgRII/III blocker) at 4°C for 10 minutes, followed by the staining for intracellular marker: active Caspase-3 – PE (Clone 51-68655X) at 4°C for 30 minutes. Intracellularly stained cells were resuspended in FACS buffer and acquired using BD LSR Fortessa (BD Biosciences Immunohistochemistry Systems) and data was analyzed by FlowJo v10.6.1 software (TreeStar, US). All stained cells positive for specific markers are calculated as a percentage of live cells.

4.3.10. Seahorse XF real-time ATP rate assay

BMDMs (5 x 10^4) were seeded in Seahorse XFp cell culture mini plates before Mtb infection. Cell culture medium was removed, washed with pre-warmed Seahorse assay media (10 mL of Seahorse XF DMEM Medium, pH 7.4 with 10 mM of XF glucose, 1 mM of XF pyruvate, 2 mM of XF glutamine), and replaced with Mtb (MOI 1) containing assay media to the total volume of 50 µl per well. Seahorse XF real-time ATP rate assay sensor cartridge and utility plate were subjected to overnight hydration and a 1-hour calibration period in the Seahorse XF HS Mini analyzer before the assay run. Oligomycin (1.5 µM and Rotenone (0.5 µM) were loaded to the injection ports of the Seahorse XF real-time ATP rate assay sensor cartridge and replaced the utility plate with Mtb infected Seahorse XFp cell culture mini plate to start the assay. Wells with only assay media were used as blank. Total 3 assay cycles were performed to record basal and mitochondrial inhibitors (Oligomycin and Rotenone) mediated oxygen consumption rate (OCR) and extra-cellular acidification rate (ECAR), which allows the calculation of total ATP production rate and pathway-specific dependency of cellular energy production. Assay-related algorithms can be more profound in the manufacturer's user guide (Kit 103591-100).

4.3.11. Generation of human-monocyte-derived macrophages

Peripheral blood mononuclear cells (PBMCs) were obtained from healthy donor buffy coats and were isolated using Lymphoprep (Alere Technologies) density gradient method. CD14 monocytes were isolated from PBMCs through CD14+ magnetic bead separation kit (MACS Miltenyi) following the manufacturer's protocol and differentiated at 1x10^6 cells/ml in a 60 mm cell culture dish (Nunc, Denmark) for 7 days at 37°C in RPMI media (Sigma) supplemented with 1 mM Sodium Pyruvate (Sigma), 2 mM L-Glutamine (Sigma), 10% human AB Serum (hAB) (Sigma), and 50ng/ml recombinant human M-CSF (Biolegend). Following the 7-day differentiation, macrophages were then harvested by incubation with Accutase (Sigma) at 37°C for 20 minutes to gently detach the cells followed by centrifugation at 300 x g for 10 minutes. Cell pellets were resuspended in fresh prewarmed RPMI media (Sigma) supplemented with 1 mM Sodium Pyruvate (Sigma), 2 mM L-Glutamine (Sigma), 5 % hAB (Sigma), counted, and seeded in desired tissue culture grade plates for further downstream experimental procedures.

4.3.12. siRNA transfection

Human MDMs were seeded at 80% confluency in a cell culture grade 96-well plate overnight at 37°C in a 5% CO_2 incubator. TransIT-X2 transfection reagent (Mirusbio) and serum-free medium (Gibco) were prewarmed to room temperature. Next, Silencer-select siRNA (ThermoFisher) specific for PKC isoforms was added to the prewarmed serum-free medium followed by the addition of TransIT-X2 transfection reagent to allow the formation of the complex for 30 minutes at room temperature. The complex was then added dropwise to the seeded MDMs at a final concentration of 25 nM per well and incubated for 24-72 hours before continuing with Mtb infection. Similarly, BMDMs were transfected with 10 nM Silencer-select siRNA (ThermoFisher) specific for novel PKC isoforms with both TransIT-X2 transfection reagent (Mirusbio) and Lipofectamine RNAiMAX Reagent (ThermoFisher) according to manufacturer's protocol. Knockdown efficiency was determined by qRT-PCR.

4.3.13. Luminex assay

Human MDMs were seeded in a 96-well cell culture plate and infected with Mtb (MOI 5) at indicated time points, followed by the procurement of cell-free supernatant analyzed using Human Magnetic Luminex Screening assay kit (R&D Biosystems). A panel of 10 analytes was measured according to the manufacturer's protocol. The analyte panel is as follows: IL-6, IL-1α, IL-1β, IL12p40, IL-10, IFN-β, TNF-α, IL-18, CCL2, and RANTES. Data acquisition was done on Bioplex 2.0 Workstation (Biorad).

4.3.14. Liquid chromatography with tandem mass spectrometry (LC-MS/MS)

Proteomic analysis was conducted using the Dionex Ultimate 3500 RSLC Nano System (Thermo Fisher) coupled to a Q Exactive mass spectrometer (ThermoFisher) as described previously[170]. Briefly, collected protein (200 μg) from uninfected and Mtb infected BMDMs were digested overnight with trypsin at the ratio of 1:100 at 30°C. Digested peptides were prepared for MS analysis by desalting in reverse phase C18 chromatography (Millipore). 50 μg proteome peptides in 4 μl were used in the injection port of the LC-MS/MS system and ran at a flow rate of 400 nl/min at 40°C. MS1 and MS2 spectra were acquired at a resolution of 75000 within 250 ms and 175000 within 80 ms, respectively. Raw files were processed and

analyzed using Perseus v1.6.5.0 (Maxquant) and MS/MS spectra were searched against the *Mus musculus* proteome database (http://www.uniprot.org/proteomes/UP000000589). Protein annotation (GO terms) and functional pathway enrichment were conducted using stringApp and the KEGG database.

4.3.15. Statistical analysis

All data were represented as mean values and analyzed using GraphPad Prism v9.0. Statistical analyses were performed using an unpaired student t-test. Asterisks are defining significance compared to the control group as: *p < 0.05, **p < 0.01, ***p < 0.001, ****p < 0.0001.

4.4. Results

4.4.1. Ablation and overexpression of PKCδ in macrophages led to distinct mycobacterial burden outcomes *in vitro*

Based on the pivotal role of macrophage-specific PKCδ mediated immune modulation in mice during Mtb infection (Chapter 3), we analyzed whether these macrophages from LysM^{cre}PKCδ$^{flox/flox}$ mice could exert similar effects within an *in vitro* setting. First, we isolated bone-marrow-derived macrophages (BMDMs) from both LysM^{cre}PKCδ$^{flox/flox}$ and PKCδ$^{flox/flox}$ mice and infected them with Mtb at a multiplicity of infection (MOI) 1. As expectedly, we found a significant increase in the mycobacterial burden at 48 hour-post infections (hpi) in LysM^{cre}PKCδ$^{flox/flox}$ BMDMs compared to PKCδ$^{flox/flox}$ (**Figure 1A**). To further extend our insights into the tenacity of macrophage-specific PKCδ during Mtb infection, we overexpressed PKCδ in RAW264.7 murine macrophage cell line to assess whether it could rescue the effects of PKCδ deficiency (**Figure 1B-D**). Remarkably, we found a significant decrease in the mycobacterial burden in PKCδ overexpressed cells compared to the control cells at 72 and 144 hpi (**Figure 1E**). These results show that PKCδ is a fine regulator of the protective functions in macrophages during Mtb infection.

Figure 1.

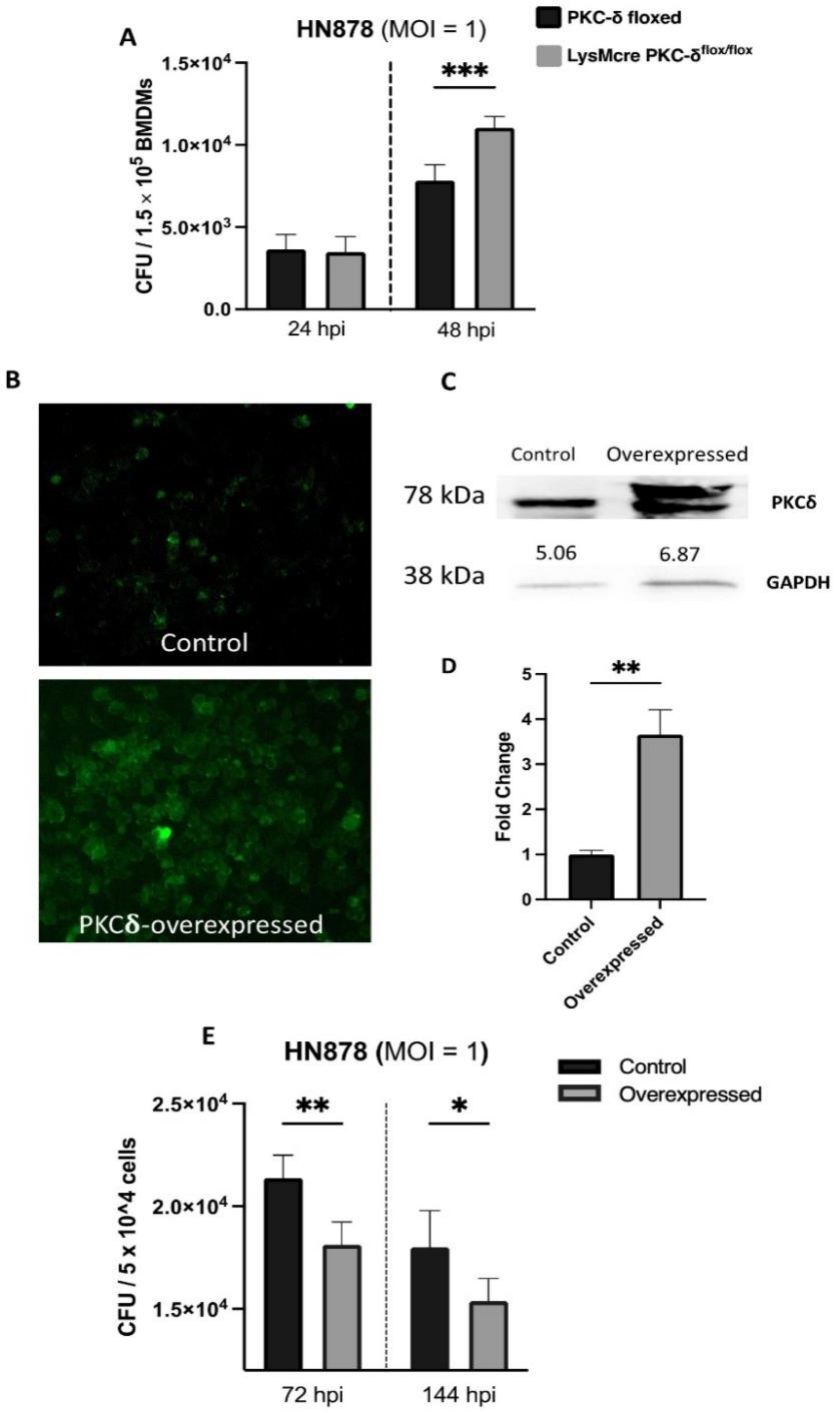

Figure 1. PKCδ in macrophages led to distinct mycobacterial burden outcomes *in vitro*. [A] Determination of mycobacterial burden in bone-marrow-derived macrophages from LysM^{cre}PKCδ$^{flox/flox}$ and PKCδ$^{flox/flox}$ mice at indicated time points. [B] Lentivirus-mediated overexpression of PKCδ in RAW264.7 murine macrophage cell line confirmed by ZOE fluorescence imaging, [C] western blot, and [D] qRT-PCR. [E] Determination of mycobacterial burden in PKCδ-overexpressed RAW264.7 murine macrophage cells at indicated time points compared to control cells. All data shown are representative of two independent experiments. Statistical analyses were performed using an unpaired student t-test. Asterisks are defining significance compared to the control group as: *$p < 0.05$, **$p < 0.01$, ***$p < 0.001$.

4.4.2. Varying antimicrobial effector functions in PKCδ deficient bone-marrow-derived macrophages during Mtb infection

The profound pathogenic capability of the bacterium can be attributed to its ability to produce an abundance of bacterial effectors that circumvent the host's immune system. Mtb can favorably affect various host antimicrobial effector activities displayed by macrophages[171]. However, the significance of PKCδ in the antimicrobial capabilities of macrophages has not yet been clearly defined, which prompted us to further investigate various antimicrobial effector functions in PKCδ deficient BMDMs during Mtb infection. To reduce Mtb survival, macrophages use reactive oxygen species (ROS) to restrict the growth of cytosolic bacteria which are escaped from the phagolysosomal compartment, as a primary component of their antibacterial defense[172, 173]. Surprisingly, we found elevated levels of cellular ROS production at 24 and 48 hpi in LysM^{cre}PKCδ$^{flox/flox}$ compared to PKCδ$^{flox/flox}$ BMDMs (**Figure 2A**). Knowingly, invading bacterial-influenced production of mitochondrial ROS can directly encounter the bacteria within the phagosomal compartment in macrophages[173]. A similar increase was observed in the mitochondrial ROS levels at 24 and 48 hpi in LysM^{cre}PKCδ$^{flox/flox}$ compared to PKCδ$^{flox/flox}$ BMDMs (**Figure 2B**). Also, previous research has shown the consecutive fusion of Mtb trapped phagosome with lysozyme is required to acquire microbicidal activity, which leads to bacterial destruction inside macrophages[168]. We determined that phagosome maturation is reduced at early 4 hpi in LysM^{cre}PKCδ$^{flox/flox}$ compared to PKCδ$^{flox/flox}$ BMDMs however no major effect overall (**Figure 2C**). During Mtb infection, it has been demonstrated that Mtb restricts the translocation of inducible nitric oxide synthase (iNOS), a major nitric oxide (NO) producing enzyme, to phagosomes[174]. qRT-PCR results revealed that iNOS expression in LysM^{cre}PKCδ$^{flox/flox}$ was reduced at 24 and 48 hpi with subsequently reduced levels of NO production at 48 hpi compared to PKCδ$^{flox/flox}$ BMDMs (**Figure 2D-E**). Moreover, Mtb bacilli and their antigens can also be packaged in apoptotic bodies through the apoptotic process, eliminating the niche for the growth of Mtb infection[175]. Previously, it has been shown that siRNA inhibition of PKCδ in vascular smooth muscle cells (SMCs) restricts both initiation and execution of caspase-3-mediated apoptosis[176]. Similar results of reduction in the caspase-3 activity were noticed in LysM^{cre}PKCδ$^{flox/flox}$ at 24 hpi compared to PKCδ$^{flox/flox}$ BMDMs (**Figure 2F**). In addition, we found that bacterial augmentation was associated with decreased macrophage activation via reduced surface expression of major histocompatibility complex II (MHCII) in LysM^{cre}PKCδ$^{flox/flox}$ compared to PKCδ$^{flox/flox}$ BMDMs (**Figure 2G-H**). Collectively, these

findings imply that the absence of PKCδ in macrophages orchestrates a variety of antimicrobial effector activities that favor Mtb development despite high cellular ROS levels.

Figure 2.

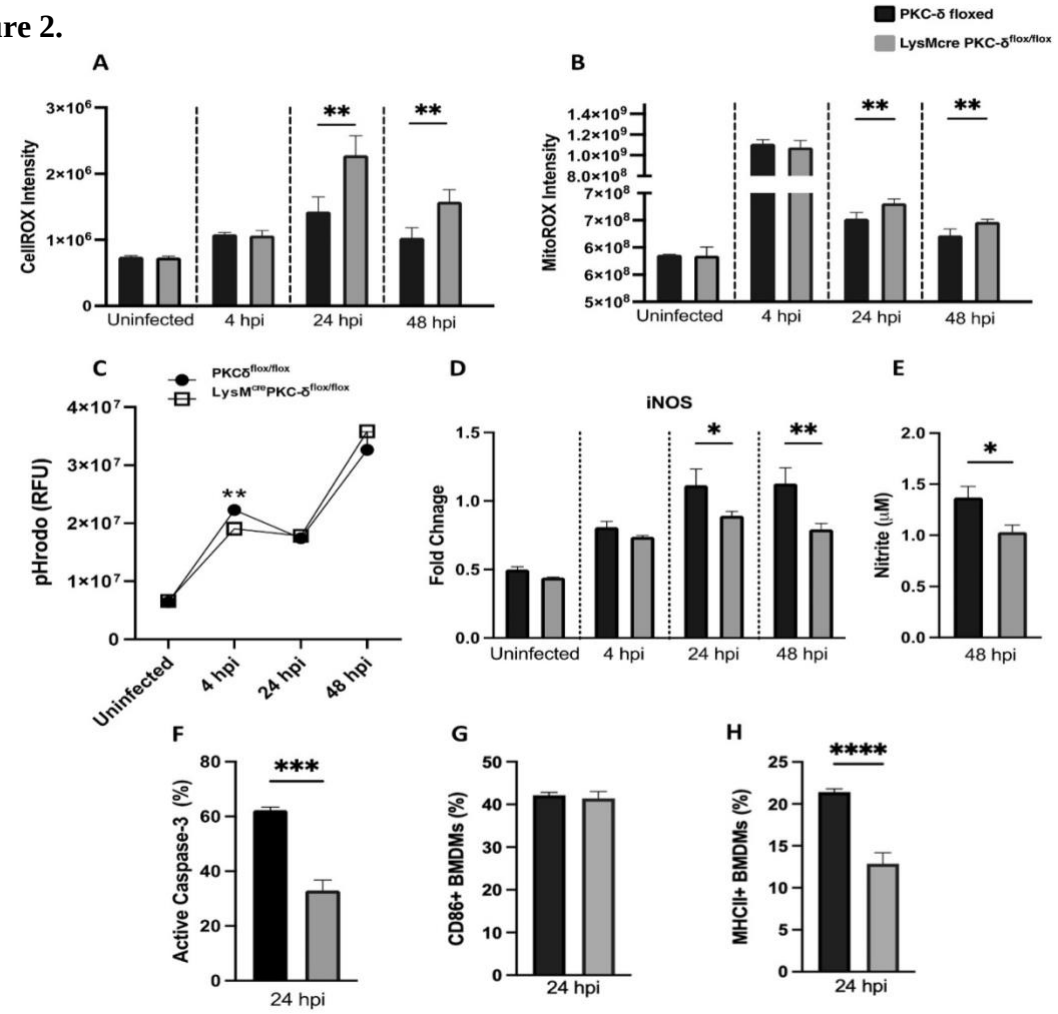

Figure 2. Varying antimicrobial effector functions in PKCδ deficient bone-marrow-derived macrophages during Mtb infection. [A-B] Accumulation of cellular and mitochondrial ROS were determined at indicated time points in bone-marrow-derived macrophages from LysM^{cre}PKCδ$^{flox/flox}$ and PKCδ$^{flox/flox}$ mice during Mtb infection. [C] Determination of phagosome maturation (Relative fluorescence unit) based on pH change in the phagolysosomal compartment in bone-marrow-derived macrophages from LysM^{cre}PKCδ$^{flox/flox}$ and PKCδ$^{flox/flox}$ mice. [D] iNOS expression and subsequent [E] nitrite levels in bone-marrow-derived macrophages from LysM^{cre}PKCδ$^{flox/flox}$ and PKCδ$^{flox/flox}$ mice at indicated Mtb infected time points. [F] Determination of Caspase-3 activity by flow cytometry in bone-marrow-derived macrophages from LysM^{cre}PKCδ$^{flox/flox}$ and PKCδ$^{flox/flox}$ mice during Mtb infection. [G-H] Detection of macrophage activation markers (CD86 and MHCII) by flow cytometry in bone-marrow-derived macrophages from LysM^{cre}PKCδ$^{flox/flox}$ and PKCδ$^{flox/flox}$ mice at 24 hours post Mtb infection. All data shown are representative of two independent experiments. Statistical analyses were performed using an unpaired student t-test. Asterisks are defining significance compared to the control group as: *$p < 0.05$, **$p < 0.01$, ***$p < 0.001$, ****$p < 0.0001$.

4.4.3. Elevated proinflammatory cytokines level in PKCδ deficient bone-marrow-derived macrophages during Mtb infection

The crucial significance of cytokines in controlling Mtb infection resides in the requirement for cell-to-cell interaction for effective migration as well as for explicit instructions during the expression of immunity[177]. A protective function for interleukin-6 (IL-6) in the generation of early protective responses through IFN-γ is supported by *in vivo* studies[178, 179]. Also, following Mtb exposure, mice lacking either interleukin-1α (IL-1α) or interleukin-1β (IL-1β) or both are vulnerable to acute and chronic infection, respectively[177]. Although, it is unclear whether the continuous release of these cytokines is deleterious or propitious to the host. Unlike in the *in-vivo* model (Chapter 3), we found a significant increase in IL-6, IL-1α, and IL-1β production in LysM^{cre}PKCδ$^{flox/flox}$ compared to PKCδ$^{flox/flox}$ BMDMs at indicated time points during Mtb infection (**Figure 3A-C**). As a result, an enhanced mycobacterial load in PKCδ deficient macrophages may benefit from heightened levels of proinflammatory cytokines production during Mtb infection.

Figure 3.

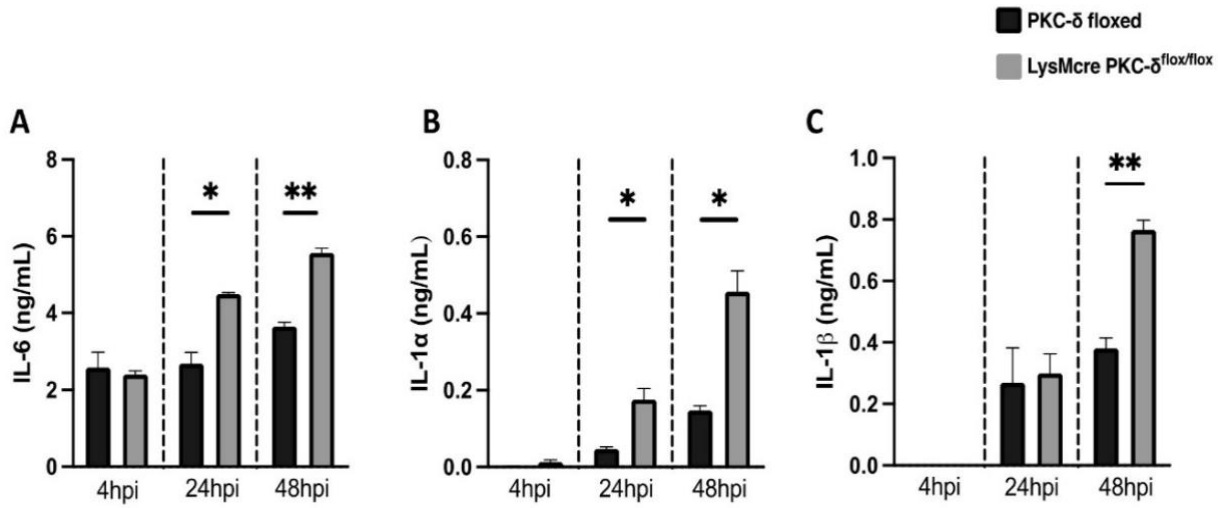

Figure 3. Elevated proinflammatory cytokines level in PKCδ deficient bone-marrow-derived macrophages during Mtb infection. [A-C] Determination of pro-inflammatory cytokine (IL-6, IL-1α, IL-1β) levels in bone-marrow-derived macrophages from LysM^{cre}PKCδ$^{flox/flox}$ and PKCδ$^{flox/flox}$ mice during Mtb infection. All data shown are representative of two independent experiments. Statistical analyses were performed using an unpaired student t-test. Asterisks are defining significance compared to the control group as: *$p < 0.05$, **$p < 0.01$.

4.4.4. PKCδ deficiency triggers inflammasome mediators and exhibits a distinct metabolic state in bone-marrow-derived macrophages during Mtb infection

The high pro-inflammatory cytokines IL-1β and IL-18 are activated by either canonical or non-canonical inflammasomes, which are important signaling platforms that detect pathogenic bacteria[177, 180]. We thus assessed the inflammasome components in the absence of PKCδ in BMDMs from LysM^{cre}PKCδ$^{flox/flox}$ mice because of the higher amounts of IL-1β production. Previously, studies discovered that pyroptosis, a caspase-1-dependent programmed cell death, can aid in the activation of an inflammatory response by releasing IL-1β and IL-18[181]. We found no significant differences in the mRNA expression of caspase-1 between LysM^{cre}PKCδ$^{flox/flox}$ and PKCδ$^{flox/flox}$ BMDMs (**Figure 4A**). Interestingly, a non-canonical inflammasome mediator upstream of NLRP3 assembly, caspase-11, has been shown to produce adequate amounts of IL-1β and IL-18 in an inflammatory environment[182, 183]. Surprisingly, we found significantly higher mRNA expression of caspase-11 in LysM^{cre}PKCδ$^{flox/flox}$ compared to PKCδ$^{flox/flox}$ BMDMs (**Figure 4B**), indicating PKCδ deficiency in macrophages predisposes them to non-canonical inflammasome-driven pyroptosis during Mtb infection. Furthermore, macrophages lacking NLRP3 do not promote the production of IL-1β and IL-18[182]. BMDMs from LysM^{cre}PKCδ$^{flox/flox}$ mice showed higher mRNA expression of NLRP3 than PKCδ$^{flox/flox}$ macrophages during Mtb infection (**Figure. 4C**). Furthermore, Saiga and colleagues revealed that AIM2$^{-/-}$ mice are more vulnerable to Mtb infection, implying that AIM2-mediated inflammasome activation plays a role during Mtb infection[184]. We found significantly higher levels of AIM2 expression in LysM^{cre}PKCδ$^{flox/flox}$ compared to PKCδ$^{flox/flox}$ macrophages at 48hpi (**Figure 4D**), suggesting that PKCδ-mediated pyroptosis in macrophages appears to be primarily dependent on the caspase-11-NLRP3, with a minor skewing of AIM2-mediated inflammasome activation at later time point. As expected, we also found higher expression of IL-1β but not IL-18 in LysM^{cre}PKCδ$^{flox/flox}$ compared to PKCδ$^{flox/flox}$ BMDMs during Mtb infection (**Figure 4E-F**) which indicates a minor role of IL-18 in inflammasome-mediated host defense as previously proven by other investigations[182]. To assess the energy metabolism, we measured the adenosine triphosphate (ATP) synthesis rate by LysM^{cre}PKCδ$^{flox/flox}$ BMDMs since studies have shown that ATP is necessary for P2X purinergic receptor 7 (P2X7) mediated activation of the inflammasome and subsequent generation of IL-1β[185-187]. Utilizing Seahorse Bioanalyzer, we found that the total ATP production rate was unchanged in macrophages at the naive state but drastically increased in LysM^{cre}PKCδ$^{flox/flox}$ BMDMs during Mtb infection (**Figure 4G-H**). The pathogenic success of

Mtb is inextricably connected to its capacity to rebalance metabolic processes in infected macrophages[188]. Additionally, we found that the enhanced ATP production in LysM^{cre}PKCδ$^{flox/flox}$ BMDMs during Mtb infection induced a relative increase in glycolysis than oxidative phosphorylation (OXPHOS)/ mitochondrial origin of cellular energy metabolism (**Figure 4H**). These findings collectively shed light on an aspect of PKCδ mediated inflammasome activation and associated cellular metabolic regulation in macrophages during Mtb infection that has not previously been known.

Figure 4.

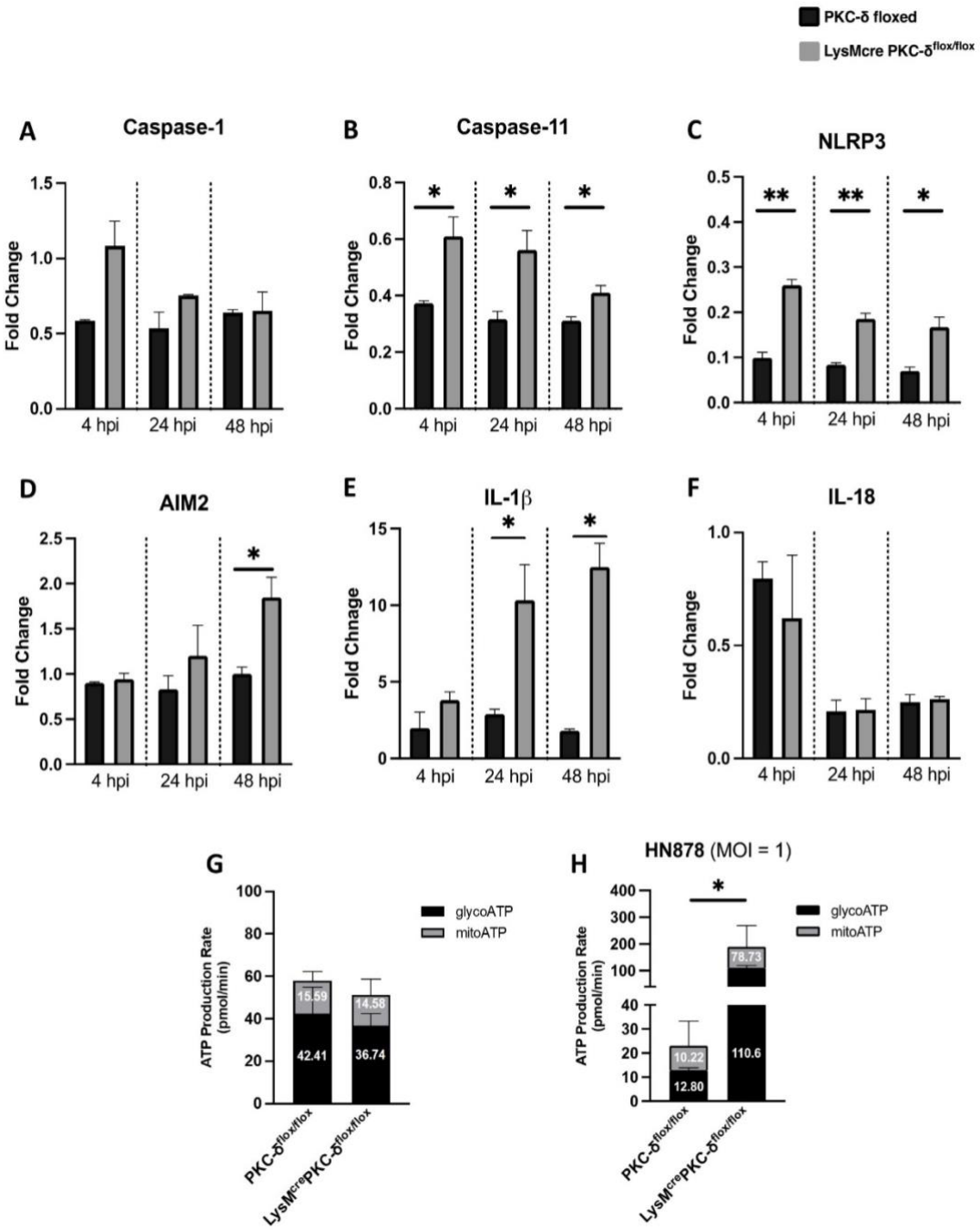

Figure 4. PKCδ deficiency triggers inflammasome mediators and exhibits a distinct metabolic state in bone-marrow-derived macrophages during Mtb infection. [A-D] mRNA expression of inflammasome pathway mediators (Caspase-1, Caspase-11, NLRP3, and AIM2) in bone-marrow-derived macrophages from LysM^{cre}PKCδ$^{flox/flox}$ and PKCδ$^{flox/flox}$ mice during Mtb infection. [E-F] Inflammasome elicited cytokines (IL-1β and IL-18) mRNA expression in bone-marrow-derived macrophages from LysM^{cre}PKCδ$^{flox/flox}$ and PKCδ$^{flox/flox}$ mice during Mtb infection. [G-H] Total ATP production rate and metabolic dependence of bone-marrow-derived macrophages from LysM^{cre}PKCδ$^{flox/flox}$ and PKCδ$^{flox/flox}$ mice at the naive state and during Mtb infection. All data shown are representative of two independent experiments. Statistical analyses were performed using an unpaired student t-test. Asterisks are defining significance compared to the control group as: *$p < 0.05$, **$p < 0.01$.

4.4.5. Exogenous GM-CSF reduces the mycobacterial burden and restricts dysregulation of metabolic state in PKCδ deficient bone-marrow-derived macrophages during Mtb infection

Growing investigations support the conception that granulocyte-macrophage colony-stimulating factor (GM-CSF) may play an important role in immunity against Mtb infection[189]. Our *in vivo* study (Chapter 3) revealed a significant reduction in the levels of GM-CSF production in LysM^{cre}PKCδ$^{flox/flox}$ compared to PKCδ$^{flox/flox}$ mice with increased susceptibility to acute and chronic Mtb infection. To reciprocate this phenotype, we investigated the expression of GM-CSF in Mtb infected BMDMs from both LysM^{cre}PKCδ$^{flox/flox}$ and PKCδ$^{flox/flox}$ mice *in vitro*. As anticipated, LysM^{cre}PKCδ$^{flox/flox}$ had much lower GM-CSF mRNA expression than PKCδ$^{flox/flox}$ BMDMs during Mtb infection (**Figure 5A**). As colony-stimulating factor 2 receptor subunit alpha (CSF2RA), the receptor for GM-CSF, confers specificity to GM-CSF signaling[153], we also found a similar reduction in the expression of CSF2RA at 48 hpi in LysM^{cre}PKCδ$^{flox/flox}$ compared to PKCδ$^{flox/flox}$ BMDMs (**Figure 5B**). According to earlier research, GM-CSF in macrophage signaling is linked to the suppression of Mtb infection[80]. Henceforth, in LysM^{cre}PKCδ$^{flox/flox}$ BMDMs, we further investigated the effects of exogenous GM-CSF to assess if it might counteract the negative effects of elevated bacterial load and alters the cellular metabolic dysregulation. Surprisingly, GM-CSF stimulated LysM^{cre}PKCδ$^{flox/flox}$ showed reduced mycobacterial burden compared to PKCδ$^{flox/flox}$ BMDMs during Mtb infection (**Figure 5C**). Furthermore, GM-CSF stimulated LysM^{cre}PKCδ$^{flox/flox}$ BMDMs also limited modest dysregulation of the cellular metabolic state of glycolysis and complete restriction of oxidative phosphorylation (OXPHOS)/ mitochondrial origin of ATP synthesis compared to PKCδ$^{flox/flox}$ BMDMs, despite total ATP production being

higher in LysM^{cre}PKCδ$^{flox/flox}$ BMDMs (**Figure 5D**). These results, in fact, demonstrate a strong connection between GM-CSF signaling and the protective function of PKCδ in macrophages during Mtb infection.

Figure 5.

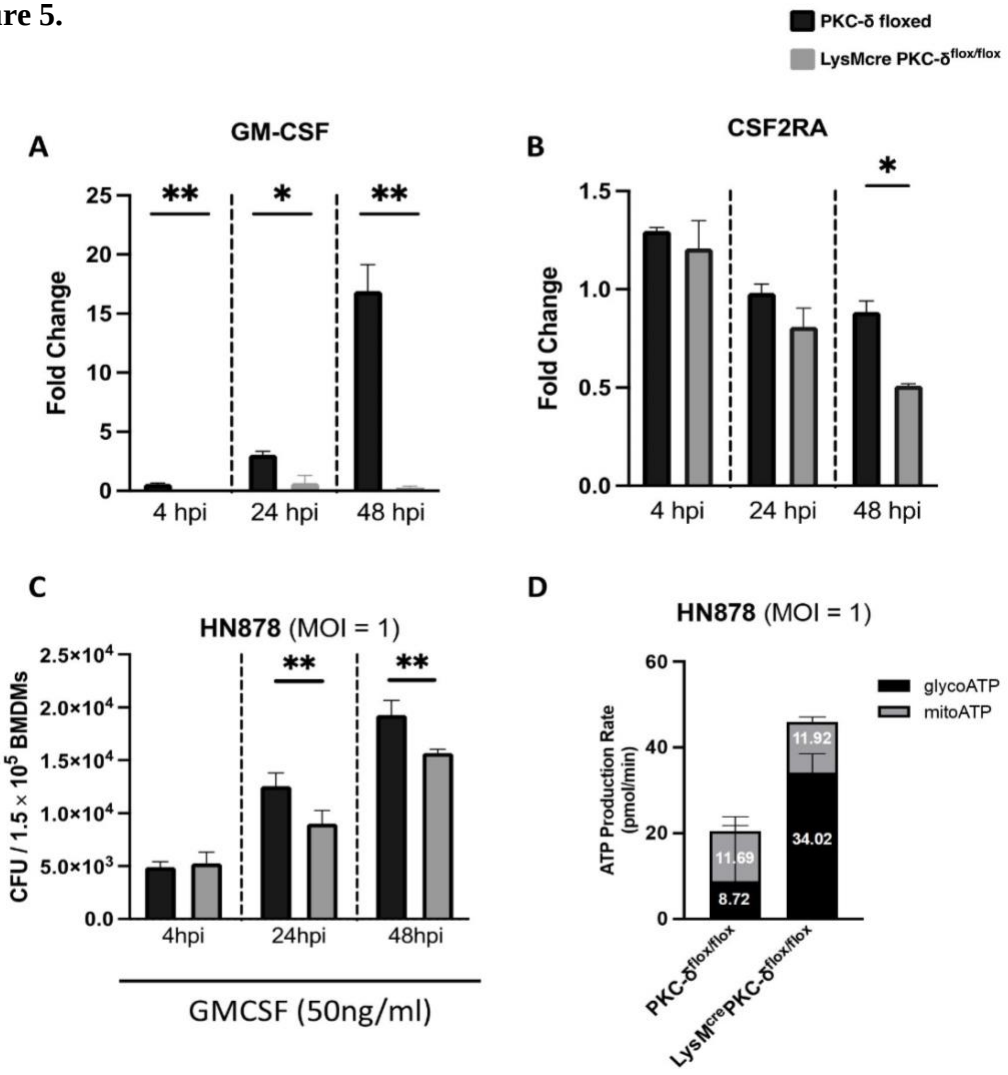

Figure 5. Exogenous GM-CSF reduces the mycobacterial burden and restricts dysregulation of metabolic state in PKCδ deficient bone-marrow-derived macrophages during Mtb infection. [A-B] mRNA expression of GM-CSF and CSF2RA in bone-marrow-derived macrophages from LysM^{cre}PKCδ$^{flox/flox}$ and PKCδ$^{flox/flox}$ mice during Mtb infection at indicated time points. [C] Determination of mycobacterial burden in GM-CSF stimulated (50 ng/ml) bone-marrow-derived macrophages from LysM^{cre}PKCδ$^{flox/flox}$ and PKCδ$^{flox/flox}$ mice at indicated time points. [D] Total ATP production rate and metabolic dependence of GM-CSF stimulated bone-marrow-derived macrophages from LysM^{cre}PKCδ$^{flox/flox}$ and PKCδ$^{flox/flox}$ mice during Mtb infection. All data shown are representative of two independent experiments. Statistical analyses were performed using an unpaired student t-test. Asterisks are defining significance compared to the control group as: *$p < 0.05$, **$p < 0.01$.

4.4.6. siRNA-mediated knockdown of PRKCD increases mycobacterial burden in human monocyte-derived macrophages

The perception of differences between rodent and human macrophages is a controversial aspect of macrophage biology[190]. To further assess the relevance of our findings in human macrophages, first, we assessed the expression kinetics of human PRKCD in isolated monocyte-derived macrophages (MDMs) during Mtb infection. We found that the mRNA expression of PRKCD increased significantly from 4 hpi to 24 hpi and then remained stable as the infection progressed (**Figure 6A**). Of interest, we also silenced PRKCD in human monocyte-derived macrophages by conventional siRNA-mediated knockdown and achieved a progressive drop in expression, as shown by knockdown efficiency of ~90% and above (**Figure 6B**). We then infected these PRKCD-silenced MDMs and discovered a similar rise in mycobacterial burden at 48 and 72 hpi in comparison to MDMs that had received negative control (NC)/ scramble siRNA treatment (**Figure 6C**). Moreover, the visual representation of this phenotype is further confirmed using imaging where we detected a profound increase in the bacterial burden at 72 hpi, which correlates to the increased mean-fluorescence intensity (MFI) of Mtb bacilli in PRKCD-silenced MDMs compared to the negative control (NC)/ scramble siRNA-treated MDMs (**Figure 6D-E**). These findings show that PRKCD in human MDMs exhibits the similar phenotypic feature of increased mycobacterial load as in murine BMDMs following Mtb infection.

Figure 6.

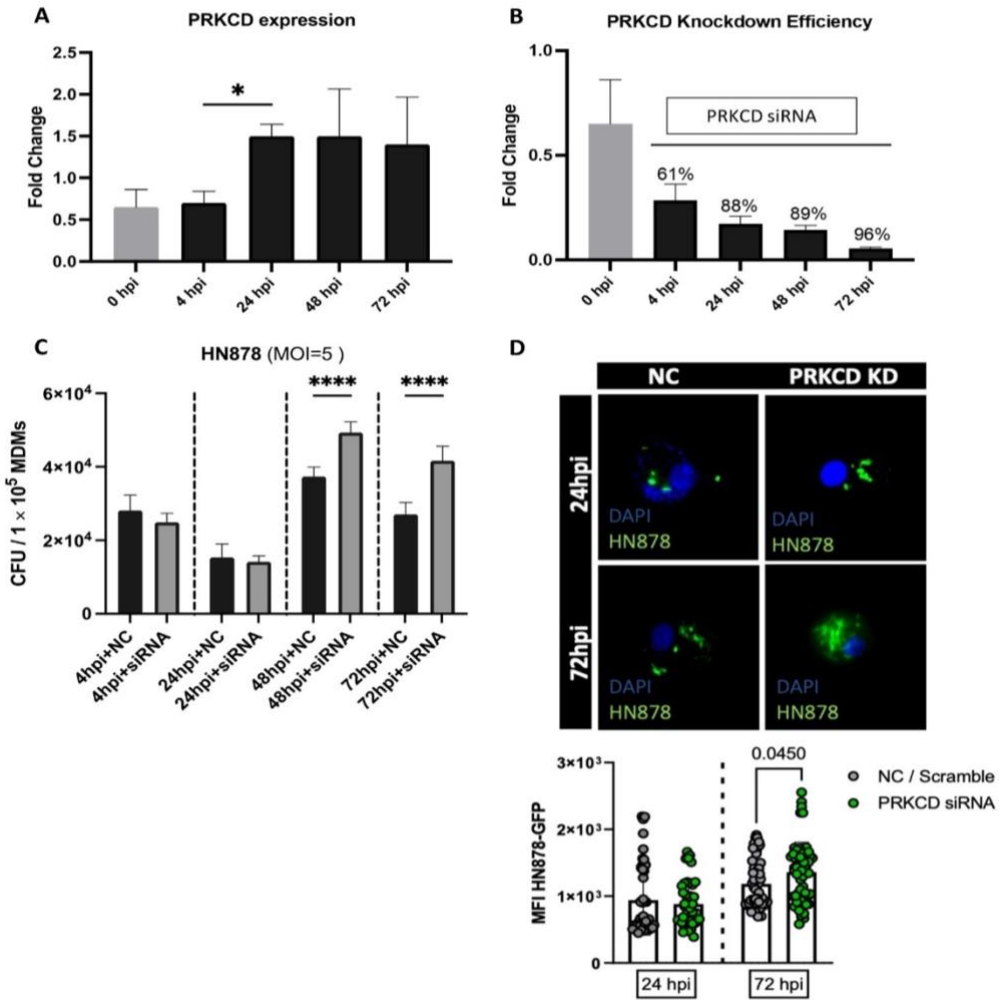

Figure 6. siRNA-mediated knockdown of PRKCD increases mycobacterial burden in human monocyte-derived macrophages. [A] mRNA expression of PRKCD in human monocyte-derived macrophages at indicated time points during Mtb infection. [B] siRNA mediated knockdown efficiency of PRKCD in human monocyte-derived macrophages during Mtb infection. [C] Determination of mycobacterial burden in the negative control (NC)/ scramble siRNA treated and PRKCD deficient human monocyte-derived macrophages at indicated time points. [D] Visual representation of elevated HN878-GFP burden in PRKCD depleted human primary monocyte-derived macrophages. Images show staining for DAPI (Blue, Nuclear stain) and GFP- tagged HN878 Mtb strain (Green) at 24 hpi and 72 hpi in the negative control (NC)/ scramble siRNA treated and PRKCD siRNA-treated human primary monocyte-derived macrophages using StellarVision microscope by synthetic aperture optics technology. [E] Comparison between the mean fluorescence intensity (MFI) of HN878-GFP at 24 hpi and 72 hpi using Fiji (Image processing module). All data shown are representative of two independent experiments. Statistical analyses were performed using an unpaired student t-test. Asterisks are defining significance compared to the control group as: *$p < 0.05$, **$p < 0.01$.

4.4.7. Knockdown of PRKCD in human monocyte-derived macrophages results in a reduction of pro-inflammatory cytokines during Mtb infection

The global transcriptional landscape revealed that immunological diseases and infections frequently result in dysregulated cytokine expression that appears to differ between species[191]. To find out the rationale behind this finding in our experimental model, we have measured an array of cytokines and chemokines in PRKCD-silenced MDMs in comparison to macrophages that received negative control (NC)/ scramble siRNA treatment during Mtb infection. This demonstrated a significant reduction in the major proinflammatory cytokines (IL-6, IL-1α, IL-1β, IL-12p40, and IFN-γ) in PRKCD-silenced MDMs compared to the negative control (NC)/ scramble siRNA-treated macrophages (**Figure 7A-E**), suggesting that human PRKCD in MDMs utilizes a distinct modality of cytokine-mediated signaling that differs from the phenotype observed in murine BMDMs following Mtb infection. In addition, we did not find any significant difference in the levels of macrophage-specific anti-inflammatory cytokines and chemokines between PRKCD-silenced MDMs and negative control (NC)/ scramble siRNA-treated macrophages (**Supplementary Figure 1A-F**).

Figure 7.

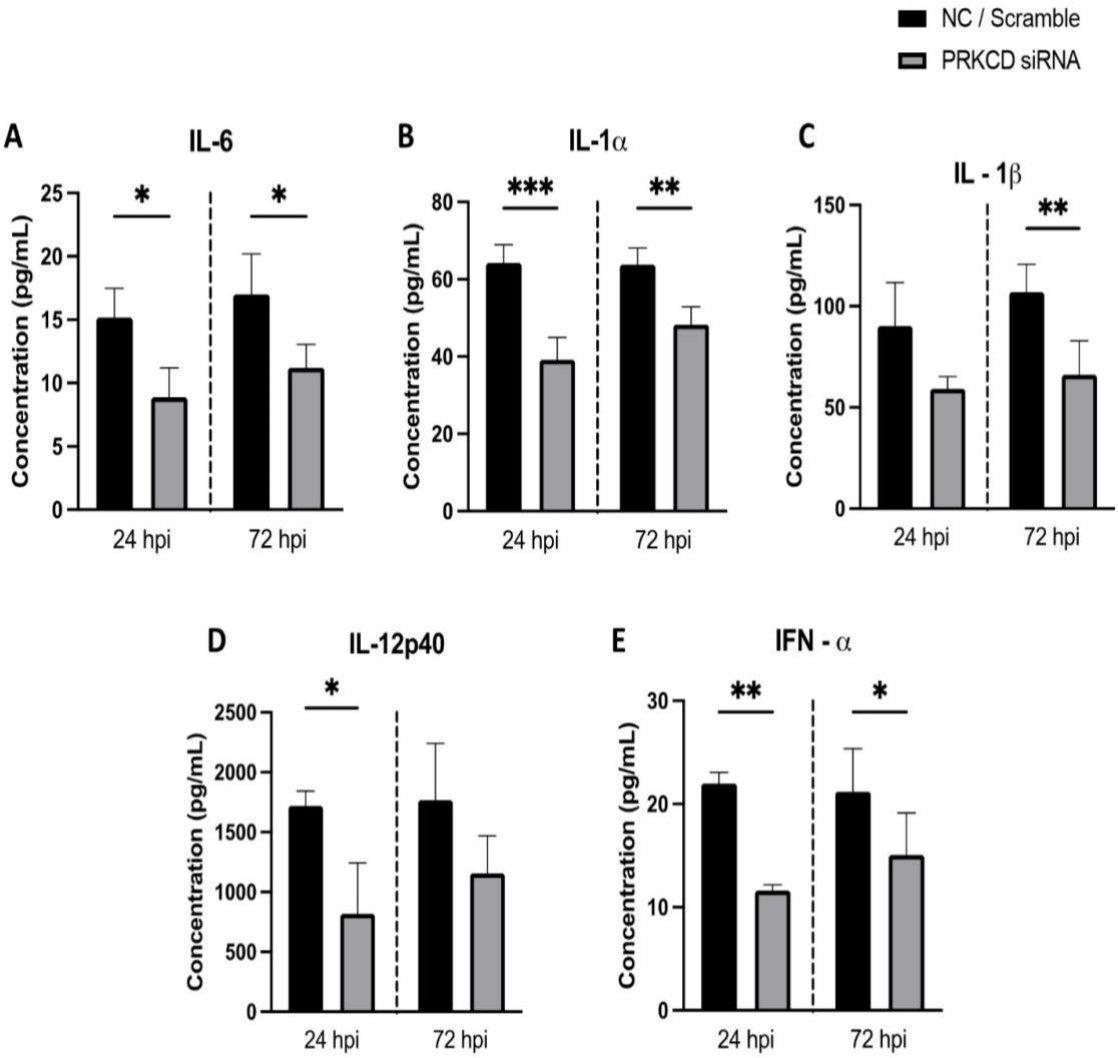

Figure 7. Knockdown of PKCδ in human monocyte-derived macrophages results in a reduction of pro-inflammatory cytokines during Mtb infection. [A-E] Customized human magnetic multiplex immunobead Luminex assay kit (R&D Biosystems) containing antibodies against IL-6, IL-1α, IL-1β, IL-12p40, IFN-γ was used to measure cytokines level in negative control/ scramble and siRNA-treated HN878 (MOI=5) infected human primary monocyte-derived macrophages. The assay was carried out based on manufacturer protocol and the data acquisition was done on Bioplex 2.0 Workstation (Biorad). Standards and unknown concentrations were determined using a logistic regression mode. All data shown are representative of two independent experiments. Statistical analyses were performed using an unpaired student t-test. Asterisks are defining significance compared to the control group as: *$p < 0.05$, **$p < 0.01$, ***$p < 0.001$.

4.4.8. PKCδ as a pervasive kinase among novel PKC family

As Mtb infection induces robust immunological responses in the absence of PKCδ in macrophages, we explored whether its expression changes during the transition from infection to active TB disease. We analyzed gene expression in bronchoalveolar lavage (BAL) samples from the site of infection i.e. lungs obtained from active TB patients, as it exhibits the most favorable clinical manifestation of TB disease[192]. Expectedly, PKCδ mRNA expression was significantly higher in the active TB group compared to the household contact group (**Figure 8A**). By assessing South Africa (SA) cohort data from Dawany and colleagues' study[193], we also found that in concurrence with HIV disease, PKCδ mRNA expression increased in active TB patients compared to only HIV-positive participants (**Figure 8B**). Recently, we have also curated the phosphorylation profile of PKCδ from a global proteome signature done by Vanderboom and colleagues[194], which revealed a significant reduction in the serine-664 (S664) phosphorylation of PKCδ in the COVID-19 positive patients compared to COVID-19 negative individuals (**Figure 8C**). Hence, PKCδ presents a constraint to be employed as a prognostic marker due to the non-specificity to TB and high expression overlap between different diseases. Remarkably, the increased mRNA expression of PKCδ was also profound in the RNA-seq data from the lung tissue of outbred mice and macaques that progressed to TB disease among other novel PKC isoforms (**Figure 8D-G**). Altogether, PKCδ stands out as a pervasive kinase during TB disease progression among other novel PKC isoforms. We further knocked down other novel PKC isoforms (theta; q, eta; h, epsilon; e) in murine BMDMs, which led to a similar increase in mycobacterial burden (**Supplementary Figure 2A-F**), providing a solid foundation for further research.

Figure 8.

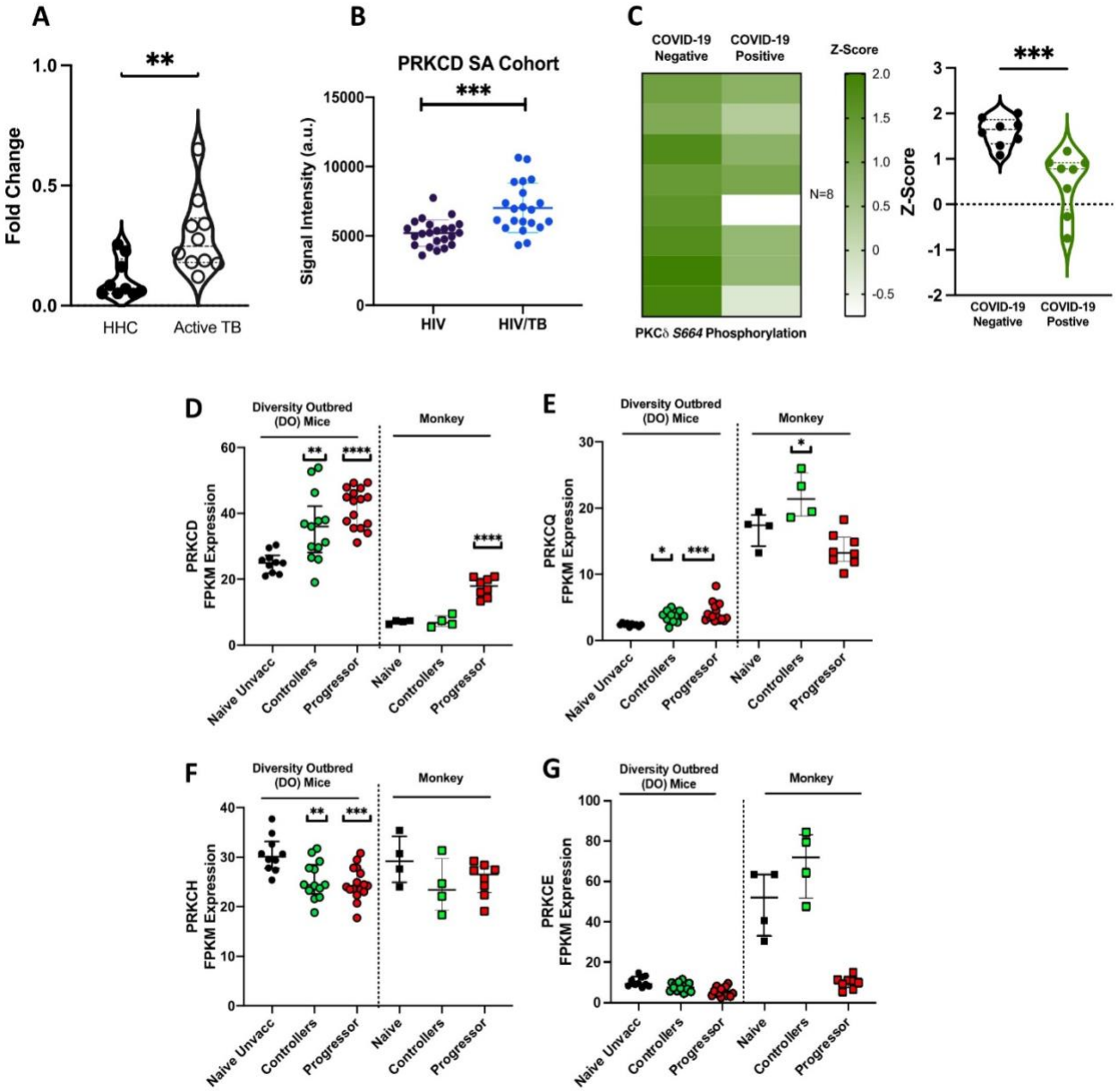

Figure 8. PKCδ as a pervasive kinase among novel PKC family. [A] mRNA expression of PRKCD in bronchoalveolar lavage (BAL) samples acquired from active TB patients and household contacts (HHC) (N=10). [B] Expression profile (mRNA signal intensity in arbitrary units) of PKCδ in HIV and HIV/TB co-infected patients in South Africa (N=23). Data was manually extrapolated and plotted from a publicly available dataset (PMID: 24587128). [C] Heat map (Z-score) of PKCδ phosphorylation at *S664* site in COVID-19 negative and COVID-19 positive patients. Data was manually extrapolated, re-analyzed, and plotted from a publicly available dataset (PMID: 34400346). [D-G] RNA-seq data for novel protein kinase C isoforms in Mtb infected lung tissues of diversity outbred mice and macaques either controlled or progressed to TB disease compared to the naive unvaccinated group. Data were extracted and re-analyzed (PMID: 31996462). Statistical analyses were performed using an unpaired student t-test. Asterisks are defining significance compared to the control group as: *p < 0.05, **p < 0.01, ***p < 0.001, ****p < 0.0001.

4.4.9. Metaproteome analysis of PKCδ-deficient bone marrow-derived macrophages revealed dysregulated protein clusters contributing to cellular functional enrichment during Mtb infection

To investigate the cellular pathways influenced and likely interacting with PKCδ in macrophages, we have quantified a metaproteome cluster from both $PKC\delta^{flox/flox}$ (NFF) and $LysM^{cre}PKC\delta^{flox/flox}$ (TFF) BMDMs at naive state (Uninf_#) and Mtb infected (Inf_#) state using Liquid Chromatography-Tandem Mass-Spectrometry (LC-MS/MS). Combined heat map cluster analysis shows no significant differences in the protein clusters in the uninfected state, rendering a distributed classification tree of NFF and TFF samples on the horizontal unit of the heatmap (**Figure 9A**). This strongly supports our characterization study showing $LysM^{cre}PKC\delta^{flox/flox}$ mice model is indistinguishable in comparison to $PKC\delta^{flox/flox}$ mice (Chapter 2). In addition, a total of 1658 proteins were quantified in the Mtb infected cluster, among which 829 proteins were considered on their reproducibility between the replicates, fold-change, and p-value (**Figure 9A**). Volcano plot through a stringent magnitude and significance revealed the top 10-most upregulated and downregulated proteins in the absence of PKCδ in BMDMs during Mtb infection (**Figure 9B, Supplementary Figure 3A**). Previously, Wang et al. showed a significant dysregulation in the Toll-like receptor signaling and antigen presentation induced by *Mycobacterium marinum* in a murine macrophage cell line (RAW264.7) through quantitative proteomics and concurrent biological functional enrichment analysis[195]. Similarly, our Gene Ontology (GO) enrichment analysis showed a significant amelioration in several biological process among which Toll-like receptor signaling, antigen processing and presentation, lipoprotein catabolic process, and negative regulation of protein dephosphorylation were noticeable with an enrichment score of above 10 (**Figure 9C**). These processes agree with macrophage mechanisms that we report here. Overall, these results showed a wide spectrum of PKCδ involvement in macrophage biological functions during Mtb infection at the proteome level.

Figure 9.

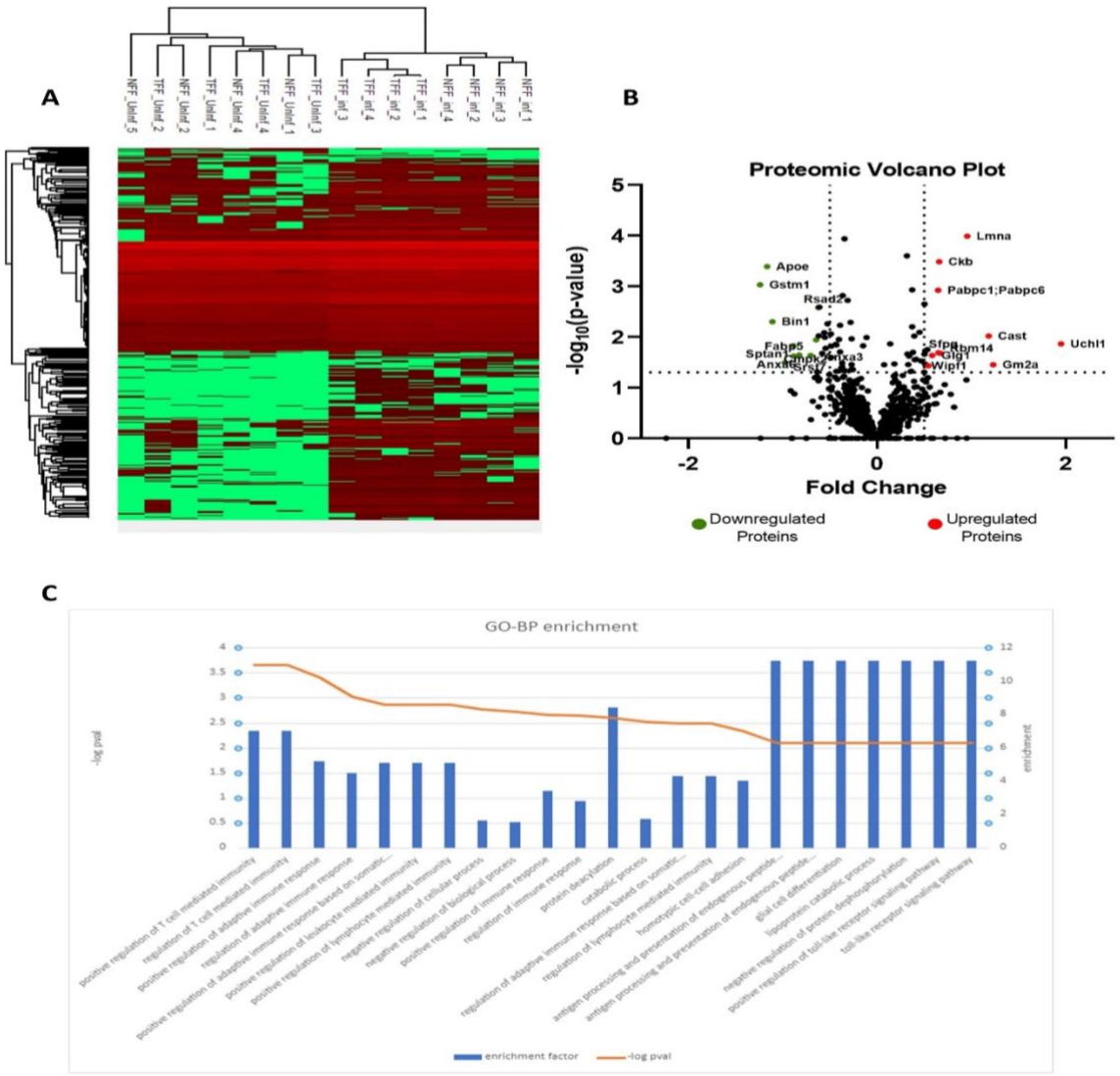

Figure 9. Metaproteome analysis of PKCδ-deficient bone marrow-derived macrophages revealed dysregulated protein clusters contributing to cellular functional enrichment during Mtb infection. [A] Heat-map analysis of metaproteome of bone marrow-derived macrophages from PKCδ$^{flox/flox}$ (NFF) and LysM^{cre}PKCδ$^{flox/flox}$ (TFF) mice at naive (Uninfected) and 30 minutes (MOI 1) post Mtb Infected (Infected) state. Protein clusters are arranged according to the similarity between their constituents. Horizontal and vertical clustering trees are depicting sample legends and differentially expressed proteins, respectively. (N=4) [B] Volcano plots for Mtb infected protein cluster (Total 829 proteins) with top 10-most upregulated (red) and downregulated (green) proteins. Dotted lines are denoting threshold (Fold change ≥ 0.5; p-value ≥ 0.05(i.e. -log$_{10}^{p\text{-value}}$ ≥ 1.3)) on X- and Y-axis, respectively. [C] QuickGO-BP (Biological Process) enrichment analysis of Mtb infected bone marrow-derived macrophages from PKCδ$^{flox/flox}$ (NFF) and LysM^{cre}PKCδ$^{flox/flox}$ (TFF) mice. Selected 74 proteins were annotated using the QuickGO annotation search following categorizing for different biological pathways using the KEGG database. Statistical analyses were performed using an unpaired student t-test using Perseus v1.6.5.0 (Maxquant).

4.5. Discussion

The capacity of Mtb to colonize, endure, and reproduce within macrophages is a defining feature of the disease pathophysiology[196]. Understanding the ways in which Mtb interacts with macrophages holds the promise of revealing physiological processes that are essential to bacterial virulence and host immunity. Our research centered on how the Mtb pathogen circumvented the immune system where only macrophages lacked the protective kinase PKCδ. To achieve this, we have previously established a macrophage-specific-knockout model ($LysM^{cre}PKC\delta^{flox/flox}$) (Chapter 2) and outlined the role of PKCδ during *in vivo* Mtb infection (Chapter 3). This provided us with the additional impetus to research macrophage-inclusive immunomodulation in the ablation of PKCδ during Mtb infection in an *in vitro* environment. In this study, we began by mirroring a similar approach to determine the mycobacterial load in PKCδ-deficient BMDMs isolated from $LysM^{cre}PKC\delta^{flox/flox}$ mice, which showed a similar increase in the burden compared to $PKC\delta^{flox/flox}$ mice. The overexpression of PKCδ altered this phenotype in a murine macrophage cell line, indicating the plasticity of this kinase and moderately corroborating our prior hypothesis that macrophage-specific PKCδ governs the fate of Mtb infection among other host immune cells.

The phagocytic absorption of Mtb bacilli by macrophages in the pulmonary milieu initiates host protection from infection and integrates various cellular intrinsic mechanisms[74, 169]. We observed the switching of various cell death modalities in the absence of PKCδ in macrophages during Mtb infection. Traditionally, cellular ROS during bacterial infection has been described as a bactericidal effector function during pathogen engulfment by macrophages[197]. Surprisingly, we found a significant increase in the cellular ROS levels in the $LysM^{cre}PKC\delta^{flox/flox}$ BMDMs compared to $PKC\delta^{flox/flox}$, which is counterintuitive and raises an existing question of whether ROS has a direct antimicrobial effect against infection or only operates as signaling molecules in favor for Mtb survival? which is still unknown. Mice lacking NOX2, a prominent ROS-generating transmembrane protein, have been demonstrated to be less susceptible to Mtb infection[198]. Also, studies demonstrated that excessive or incorrectly localized ROS can be detrimental, leading to damage to the host[197]. To further examine, we discovered that $LysM^{cre}PKC\delta^{flox/flox}$ BMDMs had higher mitochondrial ROS levels than $PKC\delta^{flox/flox}$, indicating that PKCδ is a nexus for restricting excessive ROS-mediated inflammation in macrophages following Mtb infection. The production of ROS and nitrogen intermediates by macrophages increases the bacterial killing potential within phagosomes, whereas Mtb can modify phagosome activity, which gives it the chance to alter the host's

overall behavior in ways that will favor its survival[199]. Mechanistically, PKCδ$^{-/-}$ mice showed an immune regulation independent of phagosome maturation during Mtb infection, as described by Parihar and colleagues previously[88]. Our results showed a moderate reduction in the early phagosome maturation in LysM^{cre}PKCδ$^{flox/flox}$ BMDMs compared to PKCδ$^{flox/flox}$ which was abolished at later infection time points, implying a minor involvement of PKCδ in phagosome maturation. In line with our previous finding in LysM^{cre}PKCδ$^{flox/flox}$ mice (Chapter 3), we also detected less expression of iNOS and NO levels, strongly suggesting that PKCδ is essential for NO-mediated control of enhanced bacterial burden in macrophages. We also probed additional antimicrobial effector mechanisms in which PKCδ emerged as a key player in the caspase-3-mediated apoptosis that drives infected macrophage killing as well as the MHCII-mediated antigen presentation during Mtb infection *in vitro*. These notable antimicrobial function orchestrations by PKCδ offer sufficient evidence for it to be acknowledged as a crucial hub for immunomodulation during Mtb infection in murine macrophages.

Furthermore, research suggests a link between elevated mitochondrial ROS and enhanced IL-1β production via activation of the NLRP3 inflammasome[199]. A subsequent study contradicted this finding, revealing a critical function for cytosolic ROS in the activation of the NLRP3 inflammasome via xanthine oxidase (XO) during Mtb infection[187]. The role of IL-1β during Mtb infection is complicated, with some studies suggesting a role in host protection and other studies showing an influence on host vulnerability[200]. Numerous research examining genetic variability in the human IL-1β gene and clinical outcomes provide some of the best evidence for a correlation between elevated IL-1β and the severity of TB disease in individuals[201, 202]. Additionally, a recent study hypothesized that pharmacological and genetic suppression of NLRP3 inflammasome would decrease bacterial viability in macrophages for Mtb strains that produce a strong IL-1β response[203]. Based on our observations of ROS elevation, we have found an increase in IL-1β secretion in LysM^{cre}PKCδ$^{flox/flox}$ BMDMs compared to PKCδ$^{flox/flox}$, which in turn were associated with the activation of NLRP3 and AIM2 inflammasome signaling. Our investigation also revealed an unknown immune response dependency towards caspase-11 mediated non-canonical inflammasome activation in PKCδ deficient BMDMs during Mtb infection. Although the precise mechanism is unclear, the detrimental role of excessive production of IL-1β might be favorable for augmented bacterial growth and persistency in the context of PKCδ deficiency in macrophages during Mtb infection, which needs further investigation. The process through

which biochemicals are utilized to produce energy in the form of ATP is known as cellular energy metabolism[204]. Numerous investigations have demonstrated that NLRP3-mediated increased IL-1β production during inflammation is ATP-dependent[205, 206]. This observation was apparent in our results with increased ATP production in LysM^{cre}PKCδ$^{flox/flox}$ BMDMs compared to PKCδ$^{flox/flox}$, rendering a functional implication for bacterial persistence through metabolic reprogramming in the absence of PKCδ in murine macrophages during Mtb infection. The metabolic study further showed enhanced ATP generation in the absence of PKCδ was redundant towards OXPHOS and biased toward glycolytic metabolism in murine macrophages during Mtb infection. Recently, Mills and colleagues have described a crucial role in this rise in glycolytic activity, with ATP from the glycolytic pathway needed to power ATP synthase (Complex V), which in turn enhances mitochondrial membrane potential and allows Complex I to produce pro-inflammatory mitochondrial ROS[207]. Another study done by Mishra and colleagues showed that macrophages derived from active TB patients exhibit lower levels of GM-CSF[189], which indeed supports our results in the context of PKCδ deficiency in murine macrophages during Mtb infection *in vitro*. Remarkably, exogenous GM-CSF supplementation in LysM^{cre}PKCδ$^{flox/flox}$ BMDMs reduced mycobacterial burden with a subsequent restriction of uncontrolled metabolic reprogramming seen in Mtb infection, pointing to a critical role played by GM-CSF in the immunological regulation caused by PKCδ deficiency that promotes Mtb development.

Previously, the whole blood profile showed a significant increase in the mRNA expression of PKCδ in active TB patients compared to healthy and LTBI individuals[88]. When we employed human MDMs during Mtb infection, the experimental results showed that this signature was similar. Furthermore, conventional knockdown of PKCδ in MDMs showed a similar rise in the mycobacterial burden, indicating PKCδ is also optimal for macrophage restriction of Mtb infection in humans. Although the fact that PKCδ silenced MDMs secreted less major pro-inflammatory cytokines than murine BMDMs, suggests a distinct cellular intrinsic mode switching in humans. The response of Mtb infection to intracellular settings varies substantially depending on the macrophage cell type used, whether primary or immortalized, human or murine; consequently, caution should be exercised when interpreting findings from a single cell type[208]. Despite its limitations as a predictive marker for TB disease, our thorough analysis demonstrated a substantial clinical manifestation of higher mRNA expression of PKCδ in BAL samples from active TB patients compared to household contacts, presenting a prospective target for future therapeutic intervention. Also, our

proteomic analysis revealed dysregulation in several regulatory proteins upstream of PKCδ enriching Toll-like receptor (TLR) mediated signaling during Mtb infection, supporting the previous findings of involvement of PKCδ in TLR signaling[109]. Another study by Li et al. previously described that macrophage-specific deletion of PKCδ in ApoE$^{-/-}$ mice showed enhanced atherosclerosis with increased macrophage numbers and amplified expression of inflammatory cytokines. We found that ApoE was significantly downregulated in our metaproteome analysis during Mtb infection, indicating a synergistic role of ApoE and PKCδ in macrophages. Enticingly, Rsad2 was also downregulated, which has been shown to be differentially expressed in vascular smooth muscle cells (VSMCs) during inflammatory diseases induced by PKCδ. An intracellular lipid-binding protein, Fabp5, known to be a positive regulator of PKC activation via ROS modulation, was significantly downregulated in the absence of PKCδ in macrophages observed by proteomic analysis. Although, proteomic data rendered a temperate degree of observation of the cellular biological process regulated by PKCδ in macrophages during Mtb infection, but the major and critical functional role of kinases can only be divulged by investigating its broad phosphorylation targets. This suggests a warrant for future phosphoproteome study in the context of PKCδ in macrophages during Mtb infection. Besides, another drawback of our work was that we investigated the significance of PKCδ in macrophages as a niche while excluding polarized M1 and M2 subtypes, which might be of interest in future research.

Collectively, our findings reveal a hitherto undiscovered involvement of PKCδ in primary macrophages during Mtb infection. This systemic analysis provided a crucial role of PKCδ in immune and proteome modulation during Mtb infection with perturbed antimicrobial functions and dysregulated cellular metabolic profile conducive to the augmented bacterial growth *in vitro*. Clinical presentation of increased PKCδ expression was also attributed to the expression of PKCδ in MDMs, once inhibited, a similar increase in Mtb burden was observed, suggesting that PKCδ is a key hub for immunoregulatory function in macrophages during Mtb infection.

4.6. Acknowledgements

We are extremely grateful to the UCT Research Animal Facility (RAF) and Mr. Rodney Lucas for providing us the facility to conduct animal research, Ms. Munadia Ansarie for her contribution to animal breeding, genotyping, and maintenance, and Ms. Zarinah Sonday, Ms.

Fatima Abrahams for providing us sterile lab environment. We also express gratitude to the Wellcome Centre for Infectious Diseases Research in Africa (CIDRI-Africa) for supporting this study with WUN CIDRI Ph.D. Scholarship 2019-2022. The study was carried out using the BSL3 platform with core funding from the Wellcome Trust (203135/Z/16/Z).

4.7. Supplementary Figures

Supplementary Figure 1.

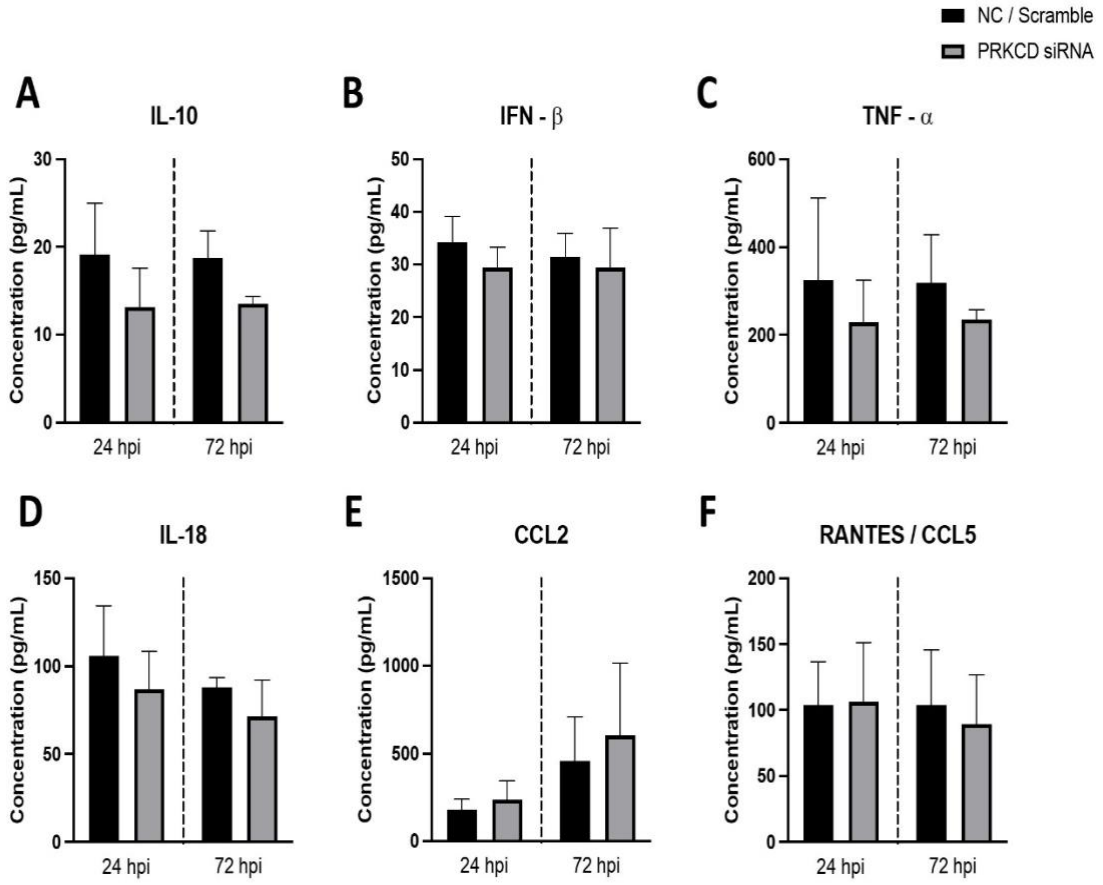

Supplementary Figure 1. Inflammatory cytokines and chemokines level in PKCδ deficient human monocyte-derived macrophages during Mtb infection. [A-F] Customized human magnetic multiplex immunobead Luminex assay kit (R&D Biosystems) containing antibodies against IL-10, IFN-β, TNF-α, IL-18, CCL2, and RANTES was used to measure cytokines levels in negative control/ scramble and siRNA-treated HN878 (MOI=5) infected human primary monocyte-derived macrophages. The assay was carried out based on manufacturer protocol and the data acquisition was done on Bioplex 2.0 Workstation (Biorad). Standards and unknown concentrations were determined using a logistic regression mode. All data shown are representative of two independent experiments. Statistical analyses were performed using an unpaired student t-test.

Supplementary Figure 2.

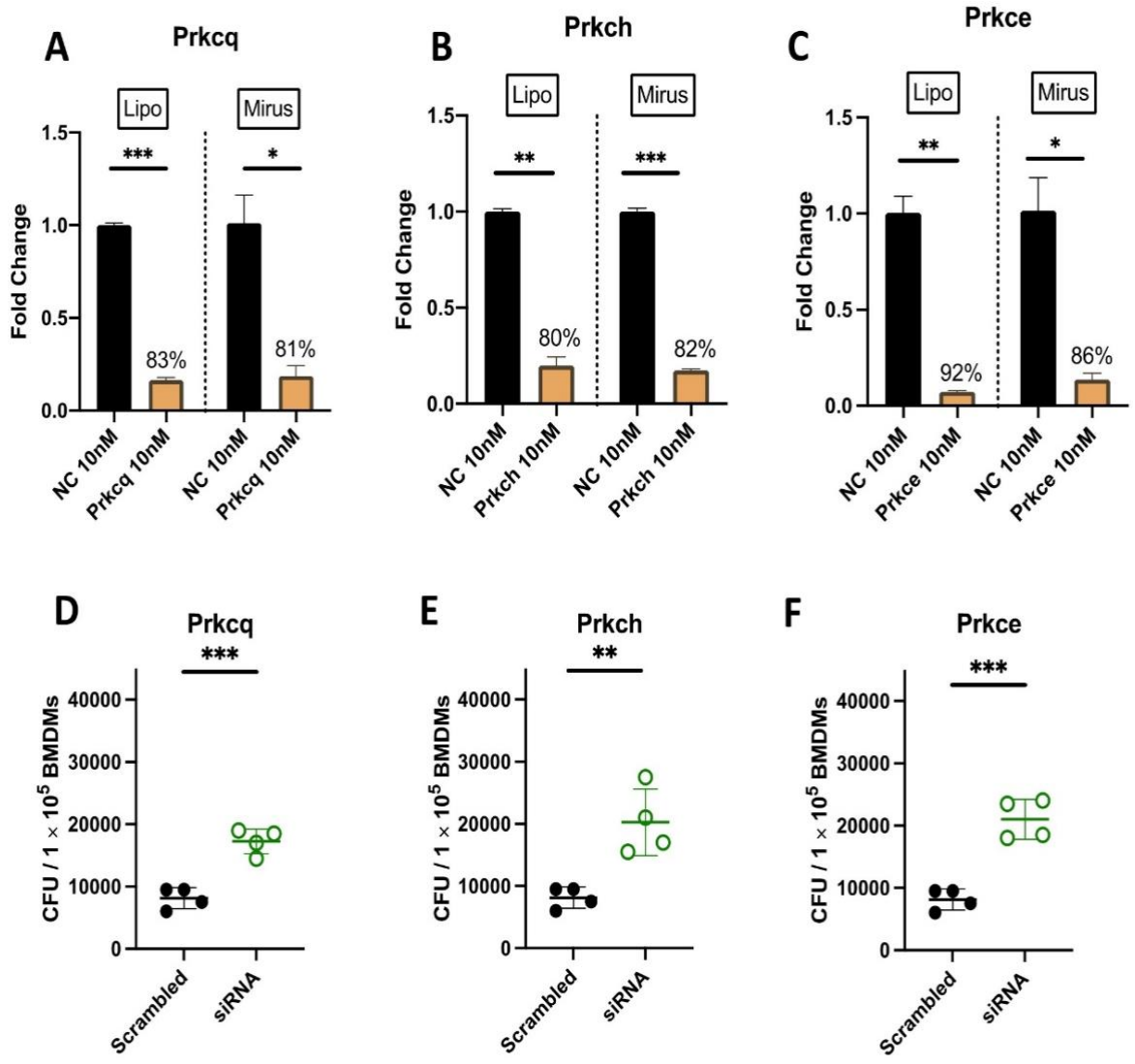

Supplementary Figure 2. Knockdown of novel PKC isoforms increases mycobacterial burden in bone-marrow-derived macrophages. [A-C] Knockdown efficiency of novel PKC isoforms in bone-marrow derived macrophages using different transfection reagents (Lipofectamine or Mirus). [D-F] Determination of mycobacterial burden in novel PKC isoforms deficient bone-marrow-derived macrophages (theta: Prkcq/ eta: Prkch/ epsilon: Prkce) compared to scramble (control). All data shown are representative of two independent experiments. Statistical analyses were performed using an unpaired student t-test. Asterisks are defining significance compared to the control group as: *$p < 0.05$, **$p < 0.01$, ***$p < 0.001$.

Supplementary Figure 3.

A

Protein Name	Protein Description	Fold change	-$\log_{10}$ p-value
Top 10-most Downregulated Protein			
Gstm1	Glutathione S-transferase Mu 1	-1,2387533	3,03238719
Apoe	Apolipoprotein E	-1,1637034	3,38824815
Bin1	Myc box-dependent-interacting protein 1	-1,1071997	2,30052734
Anxa6	Annexin;Annexin A6	-0,9723945	1,49279553
Fabp5	Fatty acid-binding protein, epidermal	-0,8854117	1,82558967
Cmpk2	UMP-CMP kinase 2, mitochondrial	-0,8809991	1,62213979
Sptan1	Spectrin alpha chain, non-erythrocytic 1	-0,824914	1,64196972
Srsf7	Serine/arginine-rich splicing factor 7	-0,7024798	1,63481444
Anxa3	Annexin A3;Annexin	-0,6425776	1,94516946
Rsad2	Radical S-adenosyl methionine domain-containing protein 2	-0,6203532	2,58047445
Top 10-most Upregulated Protein			
Uchl1	Ubiquitin carboxyl-terminal hydrolase isozyme L1	1,95247364	1,86407295
Gm2a	Ganglioside GM2 activator	1,23173809	1,45100401
Cast	Calpastatin	1,184913	2,02050774
Lmna	Prelamin-A/C;Lamin-A/C	0,95626163	3,99068022
Rbm14	RNA-binding protein 14	0,67405256	1,67745186
Ckb	Creatine kinase B-type	0,65995264	3,48522998
Sfpq	Splicing factor, proline- and glutamine-rich	0,65253162	1,69101528
Pabpc1;Pabpc6	Polyadenylate-binding protein 1;Polyadenylate-binding protein	0,64907169	2,92166277
Glg1	Golgi apparatus protein 1	0,58370638	1,63379933
Wipf1	WAS/WASL-interacting protein family member 1	0,54458904	1,42943453

Supplementary Figure 3. List of top 10-most upregulated and downregulated proteins in the absence of PKCδ in bone-marrow-derived macrophages. [A] Table shows the top 10-most upregulated and downregulated protein list identified by proteomic analysis using a stringent cutoff of fold-change ≥ 0.5; p-value ≥ 0.05(i.e. $-\log_{10}{}^{\text{p-value}} \geq 1.3$)) among 829 proteins. Protein name and descriptions were determined by Gene Ontology (GO) term and Kyoto encyclopedia of genes and genomes (KEGG) pathway enrichment.

Appendix B: Primer pairs for qRT-PCR

Gene	Accession number	Forward Primer (5'-3')	Reverse Primer (5'-3')
Mouse PKCδ	M69042	CTGGGTAACTTAACAAGACC	CTGCTAAATAACATGTTCGGTCC
Mouse PKCε	M18331	CATCGATCTCTCGGGATCATCG	CGGTTGTCAAATGACAAGGCC
Mouse PKCη	M62980	AGCTAGCCGTCTTCCACGAGACGC	GGACGACGCAGGTGCACACTTGG
Mouse PKCθ	D11061	AGCTAGCCGTCTTCCACGAGACGC	GGACGACGCAGGTGCACACTTGG
Mouse caspase 1	NM_009807	ACAAGGCACGGGACCTATG	TCCCAGTCAGTCCTGGAAATG
Mouse caspase 11	NM_009807	AGAGGGCATGGAGTCAGAGA	GCCATGAGACATTAGCACCA
Mouse NLRP3	NM_145827	ATTACCCGCCCGAGAAAGG	TCGCAGCAAAGATCCACACAG
Mouse AIM2	NM_001013779	GTCACCAGTTCCTCAGTTGTG	CACCTCCATTGTCCCTGTTTTAT
Mouse IL-1β	NM_008361	GCTTCAGGCAGGCAGTATC	AGGATGGGCTCTTCTTCAAAG
Mouse IL-18	NM_008360	ACTTTGGCCGACTTCACTGT	GGGTTCACTGGCACTTTGAT
Mouse GM-CSF	XM_006532127	ACCACCTATGCGGATTTCAT	TCATTACGCAGGCACAAAAC
Mouse CSF2RA	NM_009970	ACGTGGCGCGATGCAT	ACTTGTCACTGCTGGGGAGTG
Mouse iNOS	NM_011198	AGCCCTCACCTACTTCCTG	CAATCTCTGCCTATCCGTCTC
Mouse HPRT	NM_013556	GTTGGATATGCCCTTGAC	AGGACTAGAACACCTGCT
Human PRKCD	L07860	CACCATCTTCCAGAAAGAACG	CTTGCCATAGGTCCCGTTGTTG
Human RPL13A	NM_001270491	GAAAAAGCGGATGGTGGTTC	CCGGTAGTGGATCTTGGCT

CONCLUSION AND FUTURE STUDIES

The primary aim of this thesis was to establish a macrophage-specific PKCδ knockout mice model ($LysM^{cre}PKC\delta^{flox/flox}$) and investigate the extensive role of this novel kinase in immune modulation during Mtb infection. To achieve this, we have characterized the $LysM^{cre}PKC\delta^{flox/flox}$ mice model, which showed an indistinguishable characteristic of lung and spleen physiology with no observations in immune cell dysregulation and concurrent irregularities in cytokines or chemokine levels when compared to the littermate control mice ($PKC\delta^{flox/flox}$) at naive state. Besides, reduced B cell turnover in our cell-specific characterization study opposed the previous observation of B cell hyperproliferation in PKCδ global knockout mice ($PKC\delta^{-/-}$). Despite having no effect on the study, this might be an interesting artifact that requires further investigation. In the context of acute and chronic Mtb infection, $LysM^{cre}PKC\delta^{flox/flox}$ mice showed an increased susceptibility with augmented mycobacterial growth associated with exacerbated lung pathology in a gender-biased manner. This suggests a broad role for macrophage-specific PKCδ as protection, which is probably what causes the deleterious outcome of TB in $PKC\delta^{-/-}$ mice. Moreover, time-course Mtb infection also revealed a subtle skewing of memory T cell-mediated immunity, reduced interstitial macrophage (IM) subset, and reduced inflammatory cytokines and growth factors conducive to the mycobacterial containment and persistence in the pulmonary microenvironment of the $LysM^{cre}PKC\delta^{flox/flox}$ mice model compared to the $PKC\delta^{flox/flox}$ mice. The requirement of PKCδ in macrophage-killing effector function was further exposed with our systemic *in vitro* investigation. We showed that the absence of PKCδ in bone-marrow-derived macrophages presented a similar increase in mycobacterial burden, whereas overexpression reduces the Mtb growth. With erratic macrophage antimicrobial effector functions, metabolic, and proteomic dysregulation during Mtb infection, PKCδ indeed stands as a key immunomodulatory hub in macrophages. Due to the broad role of this kinase in immune modulation, we also argue that the phosphoproteome analysis in the setting of PKCδ deficiency in macrophages during Mtb infection will reveal major phosphorylation targets of this kinase, which will further provide an immaculate macrophage signaling atlas mediated by PKCδ during Mtb infection. Additionally, the clinical presentation with increased expression in active TB individuals and similar characteristics of increased bacterial burden in the ablation of PKCδ in human monocyte-derived macrophages (MDMs), provides a future perspective for the investigation of the role of PKCδ in immune modulation in humans and as a therapeutic target against TB disease.

REFERENCES

1. World Health, O., *Global tuberculosis report 2021*. 2021, Geneva: World Health Organization.
2. World Health, O., *The end TB strategy*. 2015, World Health Organization: Geneva.
3. Barberis, I., et al., *The history of tuberculosis: from the first historical records to the isolation of Koch's bacillus.* J Prev Med Hyg, 2017. **58**(1): p. E9-E12.
4. Daniel, T.M., J.H. Bates, and K.A. Downes, *History of tuberculosis.* Tuberculosis: pathogenesis, protection, and control, 1994: p. 13-24.
5. Gutierrez, M.C., et al., *Ancient origin and gene mosaicism of the progenitor of Mycobacterium tuberculosis.* PLoS Pathog, 2005. **1**(1): p. e5.
6. Daniel, T.M., *Pioneers of medicine and their impact on tuberculosis*. 2000: University Rochester Press.
7. Frith, J., *History of tuberculosis. Part 1-phthisis, consumption and the white plague.* Journal of Military and Veterans Health, 2014. **22**(2): p. 29-35.
8. Klebs, E., *Über Wirkung des Koch'schen Mittels auf Tuberkulose der Thiere, nebst Vorschlage eines unschaldlichen Tuberkulins.* Wiener med. Wochenschr, 1891: p. 15.
9. Bartolozzi, G., *Vaccini e vaccinazioni, 2002*. Masson.
10. INTERNATIONAL MEDICAL CONGRESS. 10TH, B., *Verhandlungen des X. Internationalen medicinischen congresses: Berlin, 4.-9. august 1890*. 1891: A. Hirschwald.
11. Luca, S. and T. Mihaescu, *History of BCG Vaccine.* Maedica (Bucur), 2013. **8**(1): p. 53-8.
12. Schatz, A., E. Bugie, and S.A. Waksman, *Streptomycin, a substance exhibiting antibiotic activity against gram-positive and gram-negative bacteria. 1944.* Clin Orthop Relat Res, 2005(437): p. 3-6.
13. Lehmann, J., *The treatment of tuberculosis in Sweden with para-aminosalicylic acid; a review.* Dis Chest, 1949. **16**(6): p. 684-703, illust.
14. Crofton, J., *Chemotherapy of pulmonary tuberculosis.* Br Med J, 1959. **1**(5138): p. 1610-4.
15. Margalith, P. and G. Beretta, *Rifomycin. XI. taxonomic study on streptomyces mediterranei nov. sp.* Mycopathologia et mycologia applicata, 1960. **13**(4): p. 321-330.
16. Thomas, J.P., et al., *A new synthetic compound with antituberculous activity in mice: ethambutol (dextro-2,2'-(ethylenediimino)-di-l-butanol).* Am Rev Respir Dis, 1961. **83**: p. 891-3.
17. Calmette, A., *L' Infection Bacillaire Et la Tuberculose: Chez L'Homme Et Chez Les Animaux; Processus D'Infection Et de Defense, Etude Biologique Et Experimentale*. 2013: BiblioLife.
18. *Short-course chemotherapy in pulmonary tuberculosis. A controlled trial by the British Thoracic and Tuberculosis Association.* Lancet, 1976. **2**(7995): p. 1102-4.
19. Tait, D.R., et al., *Final Analysis of a Trial of M72/AS01E Vaccine to Prevent Tuberculosis.* N Engl J Med, 2019. **381**(25): p. 2429-2439.
20. Sulis, G., et al., *Tuberculosis: epidemiology and control.* Mediterr J Hematol Infect Dis, 2014. **6**(1): p. e2014070.
21. Seung, K.J., S. Keshavjee, and M.L. Rich, *Multidrug-Resistant Tuberculosis and Extensively Drug-Resistant Tuberculosis.* Cold Spring Harb Perspect Med, 2015. **5**(9): p. a017863.
22. Kanabalan, R.D., et al., *Human tuberculosis and Mycobacterium tuberculosis complex: A review on genetic diversity, pathogenesis and omics approaches in host biomarkers discovery.* Microbiol Res, 2021. **246**: p. 126674.
23. Kaufmann, S.H., *How can immunology contribute to the control of tuberculosis?* Nat Rev Immunol, 2001. **1**(1): p. 20-30.
24. Welin, A. *Survival strategies of Mycobacterium tuberculosis inside the human macrophage*. 2011.
25. Awuh, J.A. and T.H. Flo, *Molecular basis of mycobacterial survival in macrophages.* Cell Mol Life Sci, 2017. **74**(9): p. 1625-1648.

26. Orme, I.M., R.T. Robinson, and A.M. Cooper, *The balance between protective and pathogenic immune responses in the TB-infected lung.* Nat Immunol, 2015. **16**(1): p. 57-63.
27. Pai, M., et al., *Tuberculosis.* Nat Rev Dis Primers, 2016. **2**: p. 16076.
28. Chiner-Oms, A., et al., *Genome-wide mutational biases fuel transcriptional diversity in the Mycobacterium tuberculosis complex.* Nat Commun, 2019. **10**(1): p. 3994.
29. van der Wel, N., et al., *M. tuberculosis and M. leprae translocate from the phagolysosome to the cytosol in myeloid cells.* Cell, 2007. **129**(7): p. 1287-98.
30. Simeone, R., et al., *Perspectives on mycobacterial vacuole-to-cytosol translocation: the importance of cytosolic access.* Cell Microbiol, 2016. **18**(8): p. 1070-7.
31. Stanley, S.A., et al., *The Type I IFN response to infection with Mycobacterium tuberculosis requires ESX-1-mediated secretion and contributes to pathogenesis.* J Immunol, 2007. **178**(5): p. 3143-52.
32. Mayer-Barber, K.D., et al., *Host-directed therapy of tuberculosis based on interleukin-1 and type I interferon crosstalk.* Nature, 2014. **511**(7507): p. 99-103.
33. Manca, C., et al., *Virulence of a Mycobacterium tuberculosis clinical isolate in mice is determined by failure to induce Th1 type immunity and is associated with induction of IFN-alpha /beta.* Proc Natl Acad Sci U S A, 2001. **98**(10): p. 5752-7.
34. Wolf, A.J., et al., *Initiation of the adaptive immune response to Mycobacterium tuberculosis depends on antigen production in the local lymph node, not the lungs.* J Exp Med, 2008. **205**(1): p. 105-15.
35. Samstein, M., et al., *Essential yet limited role for CCR2(+) inflammatory monocytes during Mycobacterium tuberculosis-specific T cell priming.* Elife, 2013. **2**: p. e01086.
36. Chackerian, A.A., et al., *Dissemination of Mycobacterium tuberculosis is influenced by host factors and precedes the initiation of T-cell immunity.* Infect Immun, 2002. **70**(8): p. 4501-9.
37. Cooper, A.M., et al., *Disseminated tuberculosis in interferon gamma gene-disrupted mice.* J Exp Med, 1993. **178**(6): p. 2243-7.
38. Casanova, J.L. and L. Abel, *The human model: a genetic dissection of immunity to infection in natural conditions.* Nat Rev Immunol, 2004. **4**(1): p. 55-66.
39. Palucci, I. and G. Delogu, *Host Directed Therapies for Tuberculosis: Futures Strategies for an Ancient Disease.* Chemotherapy, 2018. **63**(3): p. 172-180.
40. Barry, C.E., 3rd, et al., *The spectrum of latent tuberculosis: rethinking the biology and intervention strategies.* Nat Rev Microbiol, 2009. **7**(12): p. 845-55.
41. Srivastava, S., J.D. Ernst, and L. Desvignes, *Beyond macrophages: the diversity of mononuclear cells in tuberculosis.* Immunol Rev, 2014. **262**(1): p. 179-92.
42. Stamm, C.E., A.C. Collins, and M.U. Shiloh, *Sensing of Mycobacterium tuberculosis and consequences to both host and bacillus.* Immunol Rev, 2015. **264**(1): p. 204-19.
43. Gordon, S., *Phagocytosis: An Immunobiologic Process.* Immunity, 2016. **44**(3): p. 463-475.
44. Pugin, J., et al., *CD14 is a pattern recognition receptor.* Immunity, 1994. **1**(6): p. 509-16.
45. Lewthwaite, J.C., et al., *Mycobacterium tuberculosis chaperonin 60.1 is a more potent cytokine stimulator than chaperonin 60.2 (Hsp 65) and contains a CD14-binding domain.* Infect Immun, 2001. **69**(12): p. 7349-55.
46. Velasco-Velazquez, M.A., et al., *Macrophage--Mycobacterium tuberculosis interactions: role of complement receptor 3.* Microb Pathog, 2003. **35**(3): p. 125-31.
47. Basu, J., D.M. Shin, and E.K. Jo, *Mycobacterial signaling through toll-like receptors.* Front Cell Infect Microbiol, 2012. **2**: p. 145.
48. Takeuchi, O. and S. Akira, *Pattern recognition receptors and inflammation.* Cell, 2010. **140**(6): p. 805-20.
49. Liu, C.H., H. Liu, and B. Ge, *Innate immunity in tuberculosis: host defense vs pathogen evasion.* Cell Mol Immunol, 2017. **14**(12): p. 963-975.
50. Bogdan, C., M. Rollinghoff, and A. Diefenbach, *Reactive oxygen and reactive nitrogen intermediates in innate and specific immunity.* Curr Opin Immunol, 2000. **12**(1): p. 64-76.

51. Shin, D.M., et al., *Mycobacterium tuberculosis eis regulates autophagy, inflammation, and cell death through redox-dependent signaling.* PLoS Pathog, 2010. **6**(12): p. e1001230.
52. Jamaati, H., et al., *Nitric Oxide in the Pathogenesis and Treatment of Tuberculosis.* Front Microbiol, 2017. **8**: p. 2008.
53. Miller, J.L., et al., *The type I NADH dehydrogenase of Mycobacterium tuberculosis counters phagosomal NOX2 activity to inhibit TNF-alpha-mediated host cell apoptosis.* PLoS Pathog, 2010. **6**(4): p. e1000864.
54. Russell, D.G., *Mycobacterium tuberculosis and the intimate discourse of a chronic infection.* Immunol Rev, 2011. **240**(1): p. 252-68.
55. Ehrt, S., K. Rhee, and D. Schnappinger, *Mycobacterial genes essential for the pathogen's survival in the host.* Immunol Rev, 2015. **264**(1): p. 319-26.
56. Korb, V.C., A.A. Chuturgoon, and D. Moodley, *Mycobacterium tuberculosis: Manipulator of Protective Immunity.* Int J Mol Sci, 2016. **17**(3): p. 131.
57. Kimmey, J.M., et al., *Unique role for ATG5 in neutrophil-mediated immunopathology during M. tuberculosis infection.* Nature, 2015. **528**(7583): p. 565-9.
58. Behar, S.M. and E.H. Baehrecke, *Tuberculosis: Autophagy is not the answer.* Nature, 2015. **528**(7583): p. 482-3.
59. Upadhyay, S., E. Mittal, and J.A. Philips, *Tuberculosis and the art of macrophage manipulation.* Pathog Dis, 2018. **76**(4).
60. Guler, R. and F. Brombacher, *Host-directed drug therapy for tuberculosis.* Nat Chem Biol, 2015. **11**(10): p. 748-51.
61. Piton, J., C.S. Foo, and S.T. Cole, *Structural studies of Mycobacterium tuberculosis DprE1 interacting with its inhibitors.* Drug Discov Today, 2017. **22**(3): p. 526-533.
62. Gygli, S.M., et al., *Antimicrobial resistance in Mycobacterium tuberculosis: mechanistic and evolutionary perspectives.* FEMS Microbiol Rev, 2017. **41**(3): p. 354-373.
63. Andersen, P. and T.M. Doherty, *The success and failure of BCG - implications for a novel tuberculosis vaccine.* Nat Rev Microbiol, 2005. **3**(8): p. 656-62.
64. Kamala, T., et al., *Immune response & modulation of immune response induced in the guinea-pigs by Mycobacterium avium complex (MAC) & M. fortuitum complex isolates from different sources in the south Indian BCG trial area.* Indian J Med Res, 1996. **103**: p. 201-11.
65. Palmer, C.E. and M.W. Long, *Effects of infection with atypical mycobacteria on BCG vaccination and tuberculosis.* Am Rev Respir Dis, 1966. **94**(4): p. 553-68.
66. Guler, R., et al., *Targeting Molecular Inflammatory Pathways in Granuloma as Host-Directed Therapies for Tuberculosis.* Front Immunol, 2021. **12**: p. 733853.
67. Parihar, S.P., et al., *Statin therapy reduces the mycobacterium tuberculosis burden in human macrophages and in mice by enhancing autophagy and phagosome maturation.* J Infect Dis, 2014. **209**(5): p. 754-63.
68. Dutta, N.K., et al., *Statin adjunctive therapy shortens the duration of TB treatment in mice.* J Antimicrob Chemother, 2016. **71**(6): p. 1570-7.
69. Su, V.Y., et al., *Statin Use Is Associated With a Lower Risk of TB.* Chest, 2017. **152**(3): p. 598-606.
70. Cholesterol Treatment Trialists, C., et al., *The effects of lowering LDL cholesterol with statin therapy in people at low risk of vascular disease: meta-analysis of individual data from 27 randomised trials.* Lancet, 2012. **380**(9841): p. 581-90.
71. Ma, S. and C.C. Ma, *Recent development in pleiotropic effects of statins on cardiovascular disease through regulation of transforming growth factor-beta superfamily.* Cytokine Growth Factor Rev, 2011. **22**(3): p. 167-75.
72. Stanley, S.A., et al., *Identification of host-targeted small molecules that restrict intracellular Mycobacterium tuberculosis growth.* PLoS Pathog, 2014. **10**(2): p. e1003946.

73. Vilaplana, C., et al., *Ibuprofen therapy resulted in significantly decreased tissue bacillary loads and increased survival in a new murine experimental model of active tuberculosis.* J Infect Dis, 2013. **208**(2): p. 199-202.
74. Kolloli, A. and S. Subbian, *Host-Directed Therapeutic Strategies for Tuberculosis.* Front Med (Lausanne), 2017. **4**: p. 171.
75. Singhal, A., et al., *Metformin as adjunct antituberculosis therapy.* Sci Transl Med, 2014. **6**(263): p. 263ra159.
76. de Valliere, S., et al., *Enhancement of innate and cell-mediated immunity by antimycobacterial antibodies.* Infect Immun, 2005. **73**(10): p. 6711-20.
77. Ozturk, M., et al., *Evaluation of Berberine as an Adjunct to TB Treatment.* Front Immunol, 2021. **12**: p. 656419.
78. Ehrt, S., et al., *Reprogramming of the macrophage transcriptome in response to interferon-gamma and Mycobacterium tuberculosis: signaling roles of nitric oxide synthase-2 and phagocyte oxidase.* J Exp Med, 2001. **194**(8): p. 1123-40.
79. Saliba, A.E., C.S. S, and J. Vogel, *New RNA-seq approaches for the study of bacterial pathogens.* Curr Opin Microbiol, 2017. **35**: p. 78-87.
80. Bryson, B.D., et al., *Heterogeneous GM-CSF signaling in macrophages is associated with control of Mycobacterium tuberculosis.* Nat Commun, 2019. **10**(1): p. 2329.
81. Pisu, D., et al., *Dual RNA-Seq of Mtb-Infected Macrophages In Vivo Reveals Ontologically Distinct Host-Pathogen Interactions.* Cell Rep, 2020. **30**(2): p. 335-350 e4.
82. Consortium, E.P., *An integrated encyclopedia of DNA elements in the human genome.* Nature, 2012. **489**(7414): p. 57-74.
83. Consortium, F., et al., *A promoter-level mammalian expression atlas.* Nature, 2014. **507**(7493): p. 462-70.
84. Roy, S., et al., *Transcriptional landscape of Mycobacterium tuberculosis infection in macrophages.* Sci Rep, 2018. **8**(1): p. 6758.
85. Bain, C.C. and A.S. MacDonald, *The impact of the lung environment on macrophage development, activation and function: diversity in the face of adversity.* Mucosal Immunol, 2022. **15**(2): p. 223-234.
86. Schwegmann, A., et al., *Protein kinase C delta is essential for optimal macrophage-mediated phagosomal containment of Listeria monocytogenes.* Proc Natl Acad Sci U S A, 2007. **104**(41): p. 16251-6.
87. Guler, R., et al., *PKCdelta regulates IL-12p40/p70 production by macrophages and dendritic cells, driving a type 1 healer phenotype in cutaneous leishmaniasis.* Eur J Immunol, 2011. **41**(3): p. 706-15.
88. Parihar, S.P., et al., *Protein kinase C-delta (PKCdelta), a marker of inflammation and tuberculosis disease progression in humans, is important for optimal macrophage killing effector functions and survival in mice.* Mucosal Immunol, 2018. **11**(2): p. 496-511.
89. Yang, Q., et al., *The Role of Tyrosine Phosphorylation of Protein Kinase C Delta in Infection and Inflammation.* Int J Mol Sci, 2019. **20**(6).
90. Steinberg, S.F., *Structural basis of protein kinase C isoform function.* Physiol Rev, 2008. **88**(4): p. 1341-78.
91. Dempsey, E.C., et al., *Protein kinase C isozymes and the regulation of diverse cell responses.* Am J Physiol Lung Cell Mol Physiol, 2000. **279**(3): p. L429-38.
92. Sabri, A. and S.F. Steinberg, *Protein kinase C isoform-selective signals that lead to cardiac hypertrophy and the progression of heart failure.* Mol Cell Biochem, 2003. **251**(1-2): p. 97-101.
93. Gallegos, L.L. and A.C. Newton, *Spatiotemporal dynamics of lipid signaling: protein kinase C as a paradigm.* IUBMB Life, 2008. **60**(12): p. 782-9.
94. Mellor, H. and P.J. Parker, *The extended protein kinase C superfamily.* Biochem J, 1998. **332 (Pt 2)**: p. 281-92.

95. Stempka, L., et al., *Phosphorylation of protein kinase Cdelta (PKCdelta) at threonine 505 is not a prerequisite for enzymatic activity. Expression of rat PKCdelta and an alanine 505 mutant in bacteria in a functional form.* J Biol Chem, 1997. **272**(10): p. 6805-11.
96. Jackson, D.N. and D.A. Foster, *The enigmatic protein kinase Cdelta: complex roles in cell proliferation and survival.* FASEB J, 2004. **18**(6): p. 627-36.
97. Sawai, H., et al., *Ceramide-induced translocation of protein kinase C-delta and -epsilon to the cytosol. Implications in apoptosis.* J Biol Chem, 1997. **272**(4): p. 2452-8.
98. Germano, P., et al., *Phosphorylation of the gamma chain of the high affinity receptor for immunoglobulin E by receptor-associated protein kinase C-delta.* J Biol Chem, 1994. **269**(37): p. 23102-7.
99. Malavez, Y., M.E. Gonzalez-Mejia, and A.I. Doseff, *PRKCD (protein kinase C, delta).* Atlas of genetics and cytogenetics in oncology and haematology, 2011.
100. Fan, C.Y., M. Katsuyama, and C. Yabe-Nishimura, *PKCdelta mediates up-regulation of NOX1, a catalytic subunit of NADPH oxidase, via transactivation of the EGF receptor: possible involvement of PKCdelta in vascular hypertrophy.* Biochem J, 2005. **390**(Pt 3): p. 761-7.
101. Brodie, C. and P.M. Blumberg, *Regulation of cell apoptosis by protein kinase c delta.* Apoptosis, 2003. **8**(1): p. 19-27.
102. Liu, J., et al., *NF-kappaB is required for UV-induced JNK activation via induction of PKCdelta.* Mol Cell, 2006. **21**(4): p. 467-80.
103. Yuan, L.W., J.W. Soh, and I.B. Weinstein, *Inhibition of histone acetyltransferase function of p300 by PKCdelta.* Biochim Biophys Acta, 2002. **1592**(2): p. 205-11.
104. Kwon, M.J., et al., *Role of PKCdelta in IFN-gamma-inducible CIITA gene expression.* Mol Immunol, 2007. **44**(11): p. 2841-9.
105. Yamaguchi, T., Y. Miki, and K. Yoshida, *Protein kinase C delta activates IkappaB-kinase alpha to induce the p53 tumor suppressor in response to oxidative stress.* Cell Signal, 2007. **19**(10): p. 2088-97.
106. Tapia, J.A., R.T. Jensen, and L.J. Garcia-Marin, *Rottlerin inhibits stimulated enzymatic secretion and several intracellular signaling transduction pathways in pancreatic acinar cells by a non-PKC-delta-dependent mechanism.* Biochim Biophys Acta, 2006. **1763**(1): p. 25-38.
107. Contreras, X., et al., *Protein kinase C-delta regulates HIV-1 replication at an early post-entry step in macrophages.* Retrovirology, 2012. **9**: p. 37.
108. Wang, Y. and J.F. Oram, *Unsaturated fatty acids phosphorylate and destabilize ABCA1 through a protein kinase C delta pathway.* J Lipid Res, 2007. **48**(5): p. 1062-8.
109. Loegering, D.J. and M.R. Lennartz, *Protein kinase C and toll-like receptor signaling.* Enzyme Res, 2011. **2011**: p. 537821.
110. Kilpatrick, L.E., et al., *Protection against sepsis-induced lung injury by selective inhibition of protein kinase C-delta (delta-PKC).* J Leukoc Biol, 2011. **89**(1): p. 3-10.
111. Strasser, D., et al., *Syk kinase-coupled C-type lectin receptors engage protein kinase C-delta to elicit Card9 adaptor-mediated innate immunity.* Immunity, 2012. **36**(1): p. 32-42.
112. Tabula Muris, C., et al., *Single-cell transcriptomics of 20 mouse organs creates a Tabula Muris.* Nature, 2018. **562**(7727): p. 367-372.
113. Inoue, M., et al., *Studies on a cyclic nucleotide-independent protein kinase and its proenzyme in mammalian tissues. II. Proenzyme and its activation by calcium-dependent protease from rat brain.* J Biol Chem, 1977. **252**(21): p. 7610-6.
114. Nishizuka, Y., *Intracellular signaling by hydrolysis of phospholipids and activation of protein kinase C.* Science, 1992. **258**(5082): p. 607-14.
115. Denning, M.F., et al., *Activation of the epidermal growth factor receptor signal transduction pathway stimulates tyrosine phosphorylation of protein kinase C delta.* J Biol Chem, 1996. **271**(10): p. 5325-31.
116. Page, K., et al., *Regulation of airway smooth muscle cyclin D1 transcription by protein kinase C-delta.* Am J Respir Cell Mol Biol, 2002. **27**(2): p. 204-13.

117. De Servi, B., et al., *Impact of PKCdelta on estrogen receptor localization and activity in breast cancer cells.* Oncogene, 2005. **24**(31): p. 4946-55.
118. Mecklenbrauker, I., et al., *Protein kinase Cdelta controls self-antigen-induced B-cell tolerance.* Nature, 2002. **416**(6883): p. 860-5.
119. Miyamoto, A., et al., *Increased proliferation of B cells and auto-immunity in mice lacking protein kinase Cdelta.* Nature, 2002. **416**(6883): p. 865-9.
120. Neehus, A.L., et al., *Impaired respiratory burst contributes to infections in PKCdelta-deficient patients.* J Exp Med, 2021. **218**(9).
121. Gorelik, G., et al., *T cell PKCdelta kinase inactivation induces lupus-like autoimmunity in mice.* Clin Immunol, 2015. **158**(2): p. 193-203.
122. Leitges, M., et al., *Exacerbated vein graft arteriosclerosis in protein kinase Cdelta-null mice.* J Clin Invest, 2001. **108**(10): p. 1505-12.
123. Niino, Y.S., et al., *PKCdelta deficiency inhibits fetal development and is associated with heart elastic fiber hyperplasia and lung inflammation in adult PKCdelta knockout mice.* PLoS One, 2021. **16**(7): p. e0253912.
124. Majewski, M., et al., *Protein kinase C delta stimulates antigen presentation by Class II MHC in murine dendritic cells.* Int Immunol, 2007. **19**(6): p. 719-32.
125. Pingel, S., Z.E. Wang, and R.M. Locksley, *Distribution of protein kinase C isoforms after infection of macrophages with Leishmania major.* Infect Immun, 1998. **66**(4): p. 1795-9.
126. Li, S., et al., *Conditional Knockout of PKC-delta in Osteoclasts Favors Bone Mass Accrual in Males Due to Decreased Osteoclast Function.* Front Cell Dev Biol, 2020. **8**: p. 450.
127. Bezy, O., et al., *PKCdelta regulates hepatic insulin sensitivity and hepatosteatosis in mice and humans.* J Clin Invest, 2011. **121**(6): p. 2504-17.
128. Li, M., et al., *Role of PKCdelta in Insulin Sensitivity and Skeletal Muscle Metabolism.* Diabetes, 2015. **64**(12): p. 4023-32.
129. Clausen, B.E., et al., *Conditional gene targeting in macrophages and granulocytes using LysMcre mice.* Transgenic Res, 1999. **8**(4): p. 265-77.
130. Mohrs, M., et al., *Differences between IL-4- and IL-4 receptor alpha-deficient mice in chronic leishmaniasis reveal a protective role for IL-13 receptor signaling.* J Immunol, 1999. **162**(12): p. 7302-8.
131. Herbert, D.R., et al., *Alternative macrophage activation is essential for survival during schistosomiasis and downmodulates T helper 1 responses and immunopathology.* Immunity, 2004. **20**(5): p. 623-35.
132. Roy, S., et al., *Redefining the transcriptional regulatory dynamics of classically and alternatively activated macrophages by deepCAGE transcriptomics.* Nucleic Acids Res, 2015. **43**(14): p. 6969-82.
133. Shi, J., et al., *Cre Driver Mice Targeting Macrophages.* Methods Mol Biol, 2018. **1784**: p. 263-275.
134. Davies, L.C., et al., *Distinct bone marrow-derived and tissue-resident macrophage lineages proliferate at key stages during inflammation.* Nat Commun, 2013. **4**: p. 1886.
135. Lewis, S.M., A. Williams, and S.C. Eisenbarth, *Structure and function of the immune system in the spleen.* Sci Immunol, 2019. **4**(33).
136. Liu, Z., et al., *Fate Mapping via Ms4a3-Expression History Traces Monocyte-Derived Cells.* Cell, 2019. **178**(6): p. 1509-1525 e19.
137. Kuehn, H.S., et al., *Loss-of-function of the protein kinase C delta (PKCdelta) causes a B-cell lymphoproliferative syndrome in humans.* Blood, 2013. **121**(16): p. 3117-25.
138. Thomas, B.E., et al., *Psycho-Socio-Economic Issues Challenging Multidrug Resistant Tuberculosis Patients: A Systematic Review.* PLoS One, 2016. **11**(1): p. e0147397.
139. Young, C., G. Walzl, and N. Du Plessis, *Therapeutic host-directed strategies to improve outcome in tuberculosis.* Mucosal Immunol, 2020. **13**(2): p. 190-204.

140. Sakai, S., K.D. Mayer-Barber, and D.L. Barber, *Defining features of protective CD4 T cell responses to Mycobacterium tuberculosis.* Curr Opin Immunol, 2014. **29**: p. 137-42.
141. Zeng, G., G. Zhang, and X. Chen, *Th1 cytokines, true functional signatures for protective immunity against TB?* Cell Mol Immunol, 2018. **15**(3): p. 206-215.
142. van Crevel, R., T.H. Ottenhoff, and J.W. van der Meer, *Innate immunity to Mycobacterium tuberculosis.* Clin Microbiol Rev, 2002. **15**(2): p. 294-309.
143. Cadena, A.M., J.L. Flynn, and S.M. Fortune, *The Importance of First Impressions: Early Events in Mycobacterium tuberculosis Infection Influence Outcome.* mBio, 2016. **7**(2): p. e00342-16.
144. Berrington, W.R. and T.R. Hawn, *Mycobacterium tuberculosis, macrophages, and the innate immune response: does common variation matter?* Immunol Rev, 2007. **219**: p. 167-86.
145. Rajaram, M.V., et al., *Macrophage immunoregulatory pathways in tuberculosis.* Semin Immunol, 2014. **26**(6): p. 471-85.
146. Winslow, G.M., et al., *Early T-cell responses in tuberculosis immunity.* Immunol Rev, 2008. **225**: p. 284-99.
147. Tian, T., et al., *In vivo depletion of CD11c+ cells delays the CD4+ T cell response to Mycobacterium tuberculosis and exacerbates the outcome of infection.* J Immunol, 2005. **175**(5): p. 3268-72.
148. Boer, M.C., et al., *KLRG1 and PD-1 expression are increased on T-cells following tuberculosis-treatment and identify cells with different proliferative capacities in BCG-vaccinated adults.* Tuberculosis (Edinb), 2016. **97**: p. 163-71.
149. Wang, R., et al., *Persistent Mycobacterium tuberculosis infection in mice requires PerM for successful cell division.* Elife, 2019. **8**.
150. Dorhoi, A. and S.H. Kaufmann, *Versatile myeloid cell subsets contribute to tuberculosis-associated inflammation.* Eur J Immunol, 2015. **45**(8): p. 2191-202.
151. Huang, L., et al., *Growth of Mycobacterium tuberculosis in vivo segregates with host macrophage metabolism and ontogeny.* J Exp Med, 2018. **215**(4): p. 1135-1152.
152. Ganchua, S.K.C., et al., *Lymph nodes-The neglected battlefield in tuberculosis.* PLoS Pathog, 2020. **16**(8): p. e1008632.
153. Mishra, A., et al., *GM-CSF Dependent Differential Control of Mycobacterium tuberculosis Infection in Human and Mouse Macrophages: Is Macrophage Source of GM-CSF Critical to Tuberculosis Immunity?* Front Immunol, 2020. **11**: p. 1599.
154. Liu, X., et al., *IL-2 Restores T-Cell Dysfunction Induced by Persistent Mycobacterium tuberculosis Antigen Stimulation.* Front Immunol, 2019. **10**: p. 2350.
155. Beamer, G.L., et al., *Interleukin-10 promotes Mycobacterium tuberculosis disease progression in CBA/J mice.* J Immunol, 2008. **181**(8): p. 5545-50.
156. Kumar, R. and S. Subbian, *Immune Correlates of Non-Necrotic and Necrotic Granulomas in Pulmonary Tuberculosis: A Pilot Study.* Journal of Respiration, 2021. **1**(4): p. 248-259.
157. Marakalala, M.J., et al., *Inflammatory signaling in human tuberculosis granulomas is spatially organized.* Nat Med, 2016. **22**(5): p. 531-8.
158. de Martino, M., et al., *Immune Response to Mycobacterium tuberculosis: A Narrative Review.* Front Pediatr, 2019. **7**: p. 350.
159. Mishra, B.B., et al., *Nitric oxide prevents a pathogen-permissive granulocytic inflammation during tuberculosis.* Nat Microbiol, 2017. **2**: p. 17072.
160. Kroon, E.E., et al., *Neutrophils: Innate Effectors of TB Resistance?* Front Immunol, 2018. **9**: p. 2637.
161. Mishra, B.B., et al., *Nitric oxide controls the immunopathology of tuberculosis by inhibiting NLRP3 inflammasome-dependent processing of IL-1beta.* Nat Immunol, 2013. **14**(1): p. 52-60.
162. Liegeois, M., et al., *The interstitial macrophage: A long-neglected piece in the puzzle of lung immunity.* Cell Immunol, 2018. **330**: p. 91-96.
163. Szeliga, J., et al., *Granulocyte-macrophage colony stimulating factor-mediated innate responses in tuberculosis.* Tuberculosis (Edinb), 2008. **88**(1): p. 7-20.

164. Gonzalez-Juarrero, M., et al., *Disruption of granulocyte macrophage-colony stimulating factor production in the lungs severely affects the ability of mice to control Mycobacterium tuberculosis infection.* J Leukoc Biol, 2005. **77**(6): p. 914-22.
165. Shibata, Y., et al., *GM-CSF regulates alveolar macrophage differentiation and innate immunity in the lung through PU.1.* Immunity, 2001. **15**(4): p. 557-67.
166. Ahmad, F., et al., *Macrophage: A Cell With Many Faces and Functions in Tuberculosis.* Front Immunol, 2022. **13**: p. 747799.
167. Nunes-Alves, C., et al., *In search of a new paradigm for protective immunity to TB.* Nat Rev Microbiol, 2014. **12**(4): p. 289-99.
168. Queval, C.J., R. Brosch, and R. Simeone, *The Macrophage: A Disputed Fortress in the Battle against Mycobacterium tuberculosis.* Front Microbiol, 2017. **8**: p. 2284.
169. Zhai, W., et al., *The Immune Escape Mechanisms of Mycobacterium Tuberculosis.* Int J Mol Sci, 2019. **20**(2).
170. Baros-Steyl, S.S., et al., *Phosphoproteomics reveals new insights into the role of PknG during the persistence of pathogenic mycobacteria in host macrophages.* bioRxiv, 2021.
171. Tram, T.T.B., et al., *Variations in Antimicrobial Activities of Human Monocyte-Derived Macrophage and Their Associations With Tuberculosis Clinical Manifestations.* Front Cell Infect Microbiol, 2020. **10**: p. 586101.
172. Matta, S.K. and D. Kumar, *Hypoxia and classical activation limits Mycobacterium tuberculosis survival by Akt-dependent glycolytic shift in macrophages.* Cell Death Discov, 2016. **2**: p. 16022.
173. Herb, M. and M. Schramm, *Functions of ROS in Macrophages and Antimicrobial Immunity.* Antioxidants (Basel), 2021. **10**(2).
174. Miller, B.H., et al., *Mycobacteria inhibit nitric oxide synthase recruitment to phagosomes during macrophage infection.* Infect Immun, 2004. **72**(5): p. 2872-8.
175. Lee, J., M. Hartman, and H. Kornfeld, *Macrophage apoptosis in tuberculosis.* Yonsei Med J, 2009. **50**(1): p. 1-11.
176. Kato, K., et al., *Caspase-mediated protein kinase C-delta cleavage is necessary for apoptosis of vascular smooth muscle cells.* Am J Physiol Heart Circ Physiol, 2009. **297**(6): p. H2253-61.
177. Domingo-Gonzalez, R., et al., *Cytokines and Chemokines in Mycobacterium tuberculosis Infection.* Microbiol Spectr, 2016. **4**(5).
178. Appelberg, R., et al., *Role of interleukin-6 in the induction of protective T cells during mycobacterial infections in mice.* Immunology, 1994. **82**(3): p. 361-4.
179. Ladel, C.H., et al., *Lethal tuberculosis in interleukin-6-deficient mutant mice.* Infect Immun, 1997. **65**(11): p. 4843-9.
180. Latz, E., T.S. Xiao, and A. Stutz, *Activation and regulation of the inflammasomes.* Nat Rev Immunol, 2013. **13**(6): p. 397-411.
181. Sollberger, G., et al., *Caspase-1: the inflammasome and beyond.* Innate Immun, 2014. **20**(2): p. 115-25.
182. Briken, V., S.E. Ahlbrand, and S. Shah, *Mycobacterium tuberculosis and the host cell inflammasome: a complex relationship.* Front Cell Infect Microbiol, 2013. **3**: p. 62.
183. Ruhl, S. and P. Broz, *Caspase-11 activates a canonical NLRP3 inflammasome by promoting K(+) efflux.* Eur J Immunol, 2015. **45**(10): p. 2927-36.
184. Saiga, H., et al., *Critical role of AIM2 in Mycobacterium tuberculosis infection.* Int Immunol, 2012. **24**(10): p. 637-44.
185. Stoffels, M., et al., *ATP-Induced IL-1beta Specific Secretion: True Under Stringent Conditions.* Front Immunol, 2015. **6**: p. 54.
186. Mezzasoma, L., C. Antognelli, and V.N. Talesa, *Atrial natriuretic peptide down-regulates LPS/ATP-mediated IL-1beta release by inhibiting NF-kB, NLRP3 inflammasome and caspase-1 activation in THP-1 cells.* Immunol Res, 2016. **64**(1): p. 303-12.

187. Rastogi, S., et al., *Mycobacterium tuberculosis inhibits the NLRP3 inflammasome activation via its phosphokinase PknF.* PLoS Pathog, 2021. **17**(7): p. e1009712.
188. Vrieling, F., et al., *Analyzing the impact of Mycobacterium tuberculosis infection on primary human macrophages by combined exploratory and targeted metabolomics.* Sci Rep, 2020. **10**(1): p. 7085.
189. Mishra, A., et al., *Human Macrophages Exhibit GM-CSF Dependent Restriction of Mycobacterium tuberculosis Infection via Regulating Their Self-Survival, Differentiation and Metabolism.* Front Immunol, 2022. **13**: p. 859116.
190. Murray, P.J. and T.A. Wynn, *Obstacles and opportunities for understanding macrophage polarization.* J Leukoc Biol, 2011. **89**(4): p. 557-63.
191. Carrasco Pro, S., et al., *Global landscape of mouse and human cytokine transcriptional regulation.* Nucleic Acids Res, 2018. **46**(18): p. 9321-9337.
192. Venkateshiah, S.B. and A.C. Mehta, *Role of flexible bronchoscopy in the diagnosis of pulmonary tuberculosis in immunocompetent individuals.* Journal of Bronchology & Interventional Pulmonology, 2003. **10**(4): p. 300-308.
193. Dawany, N., et al., *Identification of a 251 gene expression signature that can accurately detect M. tuberculosis in patients with and without HIV co-infection.* PLoS One, 2014. **9**(2): p. e89925.
194. Vanderboom, P.M., et al., *Proteomic Signature of Host Response to SARS-CoV-2 Infection in the Nasopharynx.* Mol Cell Proteomics, 2021. **20**: p. 100134.
195. Wang, H., et al., *PPE38 of Mycobacterium marinum triggers the cross-talk of multiple pathways involved in the host response, as revealed by subcellular quantitative proteomics.* J Proteome Res, 2013. **12**(5): p. 2055-66.
196. Rohde, K., et al., *Mycobacterium tuberculosis and the environment within the phagosome.* Immunol Rev, 2007. **219**: p. 37-54.
197. Dan Dunn, J., et al., *Reactive oxygen species and mitochondria: A nexus of cellular homeostasis.* Redox Biol, 2015. **6**: p. 472-485.
198. Ehrt, S. and D. Schnappinger, *Mycobacterial survival strategies in the phagosome: defence against host stresses.* Cell Microbiol, 2009. **11**(8): p. 1170-8.
199. Podinovskaia, M., et al., *Infection of macrophages with Mycobacterium tuberculosis induces global modifications to phagosomal function.* Cell Microbiol, 2013. **15**(6): p. 843-59.
200. Mayer-Barber, K.D. and C.M. Sassetti, *Type I Interferon and Interleukin-1 Driven Inflammatory Pathways as Targets for HDT in Tuberculosis*, in *Advances in Host-Directed Therapies Against Tuberculosis*. 2021, Springer. p. 219-232.
201. Zhang, G., et al., *Allele-specific induction of IL-1beta expression by C/EBPbeta and PU.1 contributes to increased tuberculosis susceptibility.* PLoS Pathog, 2014. **10**(10): p. e1004426.
202. Rastogi, S. and V. Briken, *Interaction of Mycobacteria With Host Cell Inflammasomes.* Front Immunol, 2022. **13**: p. 791136.
203. Subbarao, S., et al., *Genetic and pharmacological inhibition of inflammasomes reduces the survival of Mycobacterium tuberculosis strains in macrophages.* Sci Rep, 2020. **10**(1): p. 3709.
204. Palsson-McDermott, E.M. and L.A. O'Neill, *The Warburg effect then and now: from cancer to inflammatory diseases.* Bioessays, 2013. **35**(11): p. 965-73.
205. Iyer, S.S., et al., *Necrotic cells trigger a sterile inflammatory response through the Nlrp3 inflammasome.* Proc Natl Acad Sci U S A, 2009. **106**(48): p. 20388-93.
206. Bours, M.J., et al., *P2 receptors and extracellular ATP: a novel homeostatic pathway in inflammation.* Front Biosci (Schol Ed), 2011. **3**(4): p. 1443-56.
207. Mills, E.L., et al., *Succinate Dehydrogenase Supports Metabolic Repurposing of Mitochondria to Drive Inflammatory Macrophages.* Cell, 2016. **167**(2): p. 457-470 e13.
208. Jordao, L., et al., *On the killing of mycobacteria by macrophages.* Cell Microbiol, 2008. **10**(2): p. 529-48.